REGIONAL DIAGENESIS OF MISSISSIPPIAN STRATA

OF

THE SOUTHERN MID-CONTINENT, USA

By

SAHAR MOHAMMADI DEHCHESHMEHI

Bachelor of Science in Geology
Azad University, Khorasgan Branch- Isfahan
Isfahan (Esfahan) - Iran
2002

Master of Science in Geology- Sedimentary Petrology and Sedimentology
Azad University, Science and Research Branch-Tehran
Tehran- Iran
2009

Submitted to the Faculty of the Arts and Science
Graduate College of the Arts and Science
Oklahoma State University
in partial fulfillment of
the requirements for
the Degree of Geology
DOCTOR OF PHILOSOPHY
December, 2016

REGIONAL DIAGENESIS OF MISSISSIPPIAN

STRATA OF THE SOUTHERN MID-CONTINENT, USA

Dissertation Approved:

Jay M. Gregg, Ph.D., Chair

Dissertation Adviser

Michael G. Grammer, Ph.D.

James O. Puckette, Ph.D.

Kevin L. Shelton, Ph.D.

Jeffery L. White, Ph.D.

ACKNOWLEDGEMENTS

First and foremost, I would like to express my deepest gratitude to my committee chair and advisor, Dr. Jay Gregg for his insight, assistance, continuous support, and constant encouragement throughout my research. I have learned so much from him at Oklahoma State University and I would not be the geologist I am today without his guidance. I thank my committee members: Dr. James Puckette, Dr. Michael Grammer, and Dr. Kevin Shelton for their contributions and support towards my work. I genuinely thank my external Committee member Dr. Jeffery White for supporting me and taking part in this exciting research. I would like to thank Dr. Martin Appold from University of Missouri-Rolla for teaching me FL analysis. I would like to thank Dr. Marry Hileman, although she did not contribute to my research directly, her experience and insight helped me to improve the quality of my research. I also would like to thank Drs. Robert Goldstein, Gordon MacLeod, and Abbas Seyedolali for valuable suggestions and encouragement during this study.

This research was supported by the Oklahoma State University Industry Consortium on the Reservoir Distribution and Characterization of the Mid-Continent Mississippian Carbonates—A Major Unconventional Resource Play (American Energy Partners, Chaparral Energy, Chesapeake Energy, Devon Energy, Longfellow Energy, Marathon Oil, Maverick Brothers, Newfield Exploration, SM Energy, Samson Energy, Sinopec (Tiptop), Redfork Energy, Trey Resources, and Unit Petroleum).

I am also deeply grateful to a handful of close friends and colleagues, in particular Solmaz Bastani, Ibukun Bode Omoleye, Jingyao Meng, Liang Xue, and Andrew Katumwehe and other graduate fellows for standing by me throughout the sinuous doctoral path and for being a motivation to strive to be better. They have made my time here at Oklahoma State University very enjoyable, and I am thankful I had the opportunity to work alongside such intelligent, kind people. I cannot find words to express my gratitude to Mickey Gregg who supported me along the way and was always there for me.

Last but not least, to my family for all their encouragement, support, and love throughout the duration of graduate studies:

از عشق خالصانه، گذشت، صبوری، و حمایتتان در این راه سپاسگذارم.

Especial thanks to my lovely sister Maryam Mohammadi, for her support and care.

Sahar Mohammadi Dehcheshmehi

Name: SAHAR MOHAMMADI DEHCHESHMEHI

Date of Degree: DECEMBER, 2016

Title of Study: REGIONAL DIAGENESIS OF MISSISSIPPIAN STRATA OF THE SOUTHERN MID-CONTINENT, USA

Major Field: GEOLOGY

Abstract: Mississippian carbonates are one of the most complex and largest resource plays on the southern Midcontinent. This study involves petrographic, geochemical, and fluid inclusion analysis of fracture, breccia, vug, and inter- and intragrain porosity filling dolomite, calcite, and authigenic quartz cements on Mississippian carbonates from the Cherokee-Ozark platform area of Northern Oklahoma, SE Kansas, SW Missouri, and NW Arkansas to north-central Oklahoma. Open space filling calcite, quartz, and dolomite cements were observed in Mississippian rocks throughout the study area. These include early and late calcite cements and saddle dolomite cements precipitated by seawater, mixed meteoric and seawater, and late (burial) diagenetic fluids. Carbon and oxygen isotope values for calcite, dolomite, and quartz cements in the whole studied region are consistent with three types of diagenetic fluids: seawater; seawater modified by meteoric water; and evolved basinal water. Low $\delta^{13}C$ values of some of the calcite and dolomite cements indicate diagenesis under conditions of microbial sulfate reduction, in the case of early cements or thermochemical sulfate reduction associated with later petroleum migration. Analysis of fluid inclusions in late calcite, dolomite, and quartz cements in the study area indicates the presence of both dilute and high salinity end-member fluids (salinities range from 0 to 25 equivalent weight % NaCl). Homogenization temperatures (T_h) of fluid inclusions range from 50° to 175°C. The salinities and temperatures of these included fluids are consistent with a saline basinal fluid variably displacing and mixing with a dilute fluid of meteoric or mixed seawater/meteoric origin. Petroleum inclusions were observed in the late diagenetic calcite and dolomite cements indicating that precipitation of these cements was concurrent with petroleum migration. Calculated equilibrium $\delta^{18}O_{water}$ values (VSMOW) for fluids that precipitated open space filling calcite and dolomite cements are variable in study area as a whole, and do not reflect a single end-member water. There is more overlap in calculated $\delta^{18}O_{water}$ values for carbonate cement and host carbonate in most areas of north-central Oklahoma than in the Cherokee-Ozark platform area. This could represent mixing between resident and non-resident fluids, dominated by resident fluids in equilibrium with the host limestone.

PUBLICATION DISSERTATION OPTION

This dissertation has been structured in three sections. An outline is presented here of the dissertation and introduces the scientific questions that were investigated in this research. This section also lists the three manuscripts resulting from this dissertation that are in various stages of the publication process.

Paper I: Influence of late diagenetic fluids on Mississippian carbonate rocks on the Cherokee-Ozark Platform, NE Oklahoma, NW Arkansas, SW Missouri, and SE Kansas: *in* Grammer, G. M., Gregg J. M., Puckette, J. O., Jaiswal, P., Pranter, M., Mazzullo, S. J., and Goldstein, R. H., eds., Mississippian Reservoirs of the Mid-Continent, U.S.A: AAPG Memoir, accepted for publication.

Paper II: Diagenesis of Mississippian carbonate rocks in north-central Oklahoma, USA: *in* Grammer, G. M., Gregg J. M., Puckette, J. O., Jaiswal, P., Pranter, M., Mazzullo, S. J., and Goldstein, R. H., eds., Mississippian Reservoirs of the Mid-Continent, U.S.A: AAPG Memoir, in editorial review.

Paper III: Comparison of fluid inclusion data in Mississippian carbonates and vitrinite reflectance data in underlying Devonian Woodford Shale, Oklahoma, USA
Research presented in this section contributes significantly to:
Evidence of fault/fracture “hydrothermal” reservoirs in the southern midcontinent Mississippian Carbonates *in* Grammer, G. M., Gregg J. M., Puckette, J. O., Jaiswal, P., Pranter, M., Mazzullo, S. J., and Goldstein, R. H., eds., Mississippian Reservoirs of the Mid-Continent, U.S.A: AAPG Memoir, in editorial review.

SUMMARY OF PROBLEM

The Mississippian Limestone of the southern Mid-continent of the United States contains major conventional and unconventional hydrocarbon reservoirs. The Mississippian carbonate sequence consists of limestones, cherts, and dolomites (Montgomery et al., 2000; Mazzullo and Wilhite, 2011) and are one of the most complex unconventional resource plays in North America. These rocks also host the Tri-State Mississippi Valley-type (MVT) Zn-Pb district as well as several smaller mineral deposits and sulfide mineral occurrences (Mohammadi, et al., in press). The Tri-State MVT district is believed to have been formed by the migration of basinal brines, that were generated in deep sedimentary basins, whose chemistry was altered by interactions with basement rocks (Garven et al., 1993; Garven, 1995; Leach et al., 2005). Few detailed subsurface diagenetic studies of the Mississippian carbonates of the southern Midcontinent exist, although some studies have been undertaken in outcrops of the Ozark Mountain region of Missouri and Arkansas (Shoeia, 2012; Unrast, 2012).

Previous studies of the Mississippian carbonates consist largely of stratigraphy and facies analysis (Johnson, 1994; Peace, 1994; Montgomery et al., 2000; Mazzullo and Wilhite, 2011; Shoeia, 2012; Unrast, 2012) and sedimentology and diagenesis of associated cherts (Montgomery et al., 1998; Rogers, 2001; Mazzullo et al., 2009; Zhao, 2011). However, little is understood concerning the effects of late diagenetic fluids on the Mississippian carbonates, despite the known effects of similar diagenetic alteration on

other carbonate reservoirs (Tucker and Wright, 1990). This lack of understanding adversely affects petroleum exploration in the Mississippian carbonates.

Among the more important diagenetic events, and possibly the least understood, are those associated with basinal fluid migration through Mississippian strata. These fluids likely are related to those that formed the Tri-State Mississippi Valley-type (MVT) mineral district located at the junction of Kansas, Missouri, and Oklahoma (Hagni, 1976). The basinal fluids likely originated from evaporated seawater that may have interacted with siliciclastic sediments and, in some cases, crystalline basement rocks (Shelton et al., 2009; Gregg and Shelton, 2012). In the Tri-State district, basinal fluids likely were focused along faults (Appold and Nunn, 2005) and ores were emplaced at temperatures of 60° to 250°C (Gregg and Shelton, 2012). The Tri-State mineralization is genetically associated with petroleum migration (Fowler, 1933) and evidence of sulfide mineralization in carbonate rocks has been observed from northern Arkansas to western Kansas (Leach, 1975; Coveney and Goebel, 1983; Gregg and Shelton, 2012).

FUNDAMENTAL QUESTIONS ADDRESSED

The principal hypotheses that are addressed by this study are: (1) Mississippian carbonates of the southern Midcontinent were significantly affected by regional basinal fluids and (2) Basinal fluids substantially altered the characteristics of carbonate petroleum reservoirs of the Mississippian carbonates.

The fundamental questions that are answered by this research are:

1) What the relationship is between carbonate cementation and other diagenetic events?

2) When did diagenetic/basinal fluids migrate through the Mississippian rocks?
3) What is the relative timing of migration of different fluids?
4) What are the source of the diagenetic fluids?
5) Did the same diagenetic fluids move through the faults and fractures in the region?
6) How did fluid movements relate to regional tectonic history, specifically the Ouachita Orogeny?
7) Were resident fluids in the Mississippian rocks displaced by and/or did they mix with non-resident basinal fluids?

   When did petroleum migration occur relative to other diagenetic events in the Mississippian rocks?

REFERENCES

Appold, M. S., and J. A. Nunn, 2005, Hydrology of the Western Arkoma basin and Ozark platform during the Ouachita orogeny: implications for Mississippi Valley-type ore Formation in the Tri-State Zn-Pb strict: Geofluids, v. 5, p. 308-325.

Coveney, R. M, and E. D. Goebel, 1983, New fluid-inclusion homogenization temperatures for sphalerite from minor occurrences in the Mid-Continent area, International Conference on Mississippian Valley Type Lead-Zinc deposits proceeding volume. p. 234-256.

Fowler, G. M., 1933, Oil and oil structures in Oklahoma-Kansas zinc-lead mining field: AAPG Bulletin v. 17, p. 1430-1445.

Garven, G., S. Ge, M. A. Person, and D. A. Sverjensky, 1993, Genesis of stratabound ore deposits in the midcontinent basins of North America. 1. The role of regional groundwater flow: American Journal of Science, v. 293, p. 497-568.

Garven, G., 1995, Continental-scale groundwater flow and geologic processes: Annu. Rev. Earth Planet. Sci., 23, p. 89-117.

Gregg, J. M., and K. L. Shelton, 2012, Mississippi Valley-type mineralization and ore deposits in the Cambro-Ordovician Great American Carbonate Bank, *in* Derby, J. and Fritz, R., eds., The Great American Carbonate Bank a Volume in Honor of James Lee Wilson: American Association of Petroleum Geologists Memoir 98, p. 163-186.

Hagni, R. D., 1976, Tri-State ore deposits: The character of their host rocks and their genesis, in Wolf, K. H., Handbook of strata-bound and stratiform ore deposits: Amsterdam, Elsevier Scientific Publishing Company, p. 457-494.

Johnson, R. A., 1994, Distribution and architecture of subunconformity carbonate reservoirs: Lower Meramecian (Mississippian) subcrop trend, western Kansas, in J. C. Dolson, ed., Unconformity-related hydrocarbons in sedimentary sequences: Denver, Colorado, Rocky Mountain Association of Geologists, p. 231–244.

Leach, D. L., R. C. Nelson, and D. Williams, 1975, Fluid inclusion studies in the northern Arkansas zinc district: Economic Geology, v. 70, p. 1084-1091.

Leach, D. L., D. F. Sangster, K. D. Kelley, R. R. Large, G. Garven, C. Allen, J. Gutzmer, and S. Walters, 2005, Sediment-hosted lead-zinc deposits: A global perspective, in J. W. Hedenquist, J. F. H. Thompson, R. J. Goldfarb, and J. P. Richards, eds., Economic Geology one hundredth anniversary volume 1905–2005: Littleton, Colorado, Economic Geology Publishing, p. 561–607.

Mazzullo, S. J., B. W. Wilhite, and I. W. Woolsey, 2009, Petroleum reservoirs within a spiculite-dominated depositional sequence: Cowley Formation (Mississippian: Lower Carboniferous), south-central Kansas: AAPG Bulletin, v. 93, p. 1649-1689.

Mazzullo, S. J., B. W. Wilhite, and D. R. Boardman, 2011, Lithostratigraphic architecture of the Mississippian Reeds Spring Formation (Middle Osagean) in southwest Missouri, northwest Arkansas, and northeast Oklahoma: Outcrop analog of subsurface petroleum reservoirs: Shale Shaker, March/April, p. 254-269.

Mohammadi, S., J. M. Gregg, K. L. Shelton, M. S. Appold, and J. O. Puckette, (in press), Influence of late diagenetic fluids on Mississippian carbonate rocks on the Cherokee –

Ozark Platform, NE Oklahoma, NW Arkansas, SW Missouri, and SE Kansas: *in* Grammer, G. M., Gregg J. M., Puckette, J. O., Jaiswal, P., Pranter, M., Mazzullo, S. J., and Goldstein, R. H., eds., Mississippian reservoirs of the mid-continent, U.S.A: American Association of Petroleum Geologists Memoir.

Montgomery, S. L., J. C. Mullarkey, M. W. Longman, W. M. Colleary, and J. P., Rogers, 1998, Mississippian "chat" reservoirs, South Kansas: Low-Resistivity pay in a complex chert reservoir: AAPG Bulletin, v. 82, p. 187-205.

Montgomery, S. L., E. K. Franseen, S. Bhattacharya, P. Gerlach, A. Byrnes, W. Guy, and T. R. Carr, 2000, Schaben Field, Kansas: Improving performance in a Mississippian shallow-shelf carbonate: AAPG Bulletin, v. 84, p. 1069-1086.

Peace, H. W., 1994, Mississippian facies relationships eastern Anadarko Basin, Oklahoma: Shale Shaker, September/October, p. 193-202.

Rogers, S. M., 2001, Deposition and diagenesis of Mississippian chat reservoirs, north-central Oklahoma: AAPG Bulletin, v. 85, p. 115-129.

Shelton, K. L., J. M. Gregg, and A. W. Johnson, 2009, Replacement dolomites and ore sulfides as recorders of multiple fluids and fluid sources in the southeast Missouri Mississippi Valley-Type District: Halogen-$^{87}Sr/^{86}Sr$-$\delta^{18}O$-$\delta^{34}S$ systematics in the Bonneterre Dolomite: Economic Geology, v. 104, p. 733-748.

Shoeia, O. K., 2012, High resolution stratigraphy of Lower Mississippian strata near Jane, Missouri: Unpublished M.S. Thesis, Oklahoma State University, p. 254.

Thompson, T. L., 1986, Paleozoic succession in Missouri, part 4 Mississippian System: Missouri Dept. Natural Resources, Report of Investigations No. 70, 182 p.

Tucker, M.E. and V.P. Wright, 1990, Carbonate Sedimentology, Blackwell, New York, p. 482.

Unrast, M. A., 2012, Composition of Mississippian carbonate mounds in the Ozark region, North America and Ireland: M.S. thesis, Oklahoma State University, 120 p.

Zhao, M., 2011, Petrologic and petrophysical characteristics: Mississippian chert, Oklahoma: Unpublished M.S. Thesis, Oklahoma State University, p. 75.

TABLE OF CONTENTS

LIST OF TABLES

PAPER I

Table Page

LIST OF TABLES
PAPER II

Table Page

LIST OF FIGURES

PAPER I

Figure Page

LIST OF FIGURES

PAPER II

Figure Page

LIST OF FIGURES

PAPER III

Figure Page

PAPER I

Influence of late diagenetic fluids on Mississippian carbonate rocks on the Cherokee-Ozark Platform, NE Oklahoma, NW Arkansas, SW Missouri, and SE Kansas

2.0. ABSTRACT

Petrographic, geochemical, and fluid inclusion analysis of dolomite and calcite cements has been conducted on Mississippian carbonates collected from the surface and subsurface of the southern mid-continent of the U.S. (Oklahoma, Missouri, Kansas and Arkansas). Fracture and vug, intergrain, and intragrain porosity are filled with calcite, authigenic quartz, and dolomite cements. Primary limestone porosity is filled partially by early marine and meteoric calcite cements. Equant (blocky) calcite cements were precipitated under seawater or mixed meteoric-seawater conditions in the phreatic zone and in the deep phreatic zone under late (burial) diagenetic conditions. Fracture- and breccia-filling saddle dolomite cements that were observed are late diagenetic and are likely related to the nearby Tri-State Mississippi Valley-type (MVT) mineral district. Carbon and oxygen isotope values of dolomite cements range from $\delta^{18}O_{(VPDB)}$ = -9.5 to -2.7‰ and $\delta^{13}C_{(VPDB)}$ = -4.0 to -0.4‰. Values for calcite cements range from $\delta^{18}O_{(VPDB)}$ = -11.6 to -1.9‰ and $\delta^{13}C_{(VPDB)}$ = -12.2 to +4.6‰. These values are consistent

with three types of diagenetic fluids: seawater; seawater modified by meteoric water; and evolved basinal water. Analysis of fluid inclusions in late calcite, dolomite, and quartz cements indicates the presence of both dilute and high salinity end-member fluids. Homogenization temperatures (T_h) of fluid inclusions range from 57° to 170°C and salinities range from 0 to 25 equivalent weight % NaCl. Fluid inclusion T_h values and salinities are consistent with a saline basinal fluid variably diluted by fluids of meteoric or mixed seawater/meteoric origin. Petroleum inclusions were observed in late diagenetic calcite and dolomite cements. The late diagenetic cements filled porosity that remained after early diagenetic cementation indicating that some original porosity in the Mississippian carbonate rocks remained open during petroleum migration. Elevated fluid inclusion T_h values over a broad region, not just in the Tri-State mineral district, imply that the regional thermal maturity of rocks may be higher than believed previously.

This study indicates that the Mississippian carbonate resource play on the southern mid-continent has a very complex diagenetic history, continuing long after early diagenetic cementation. Possibly the most important diagenetic events affecting these rocks occurred during burial and basinal fluid migration through these strata.

2.1. INTRODUCTION

Mississippian carbonate rocks on the southern mid-continent of North America comprise an important unconventional petroleum play (Milam, 2013) (Figure 1). These rocks also host the world-class Tri-State Mississippi Valley-type (MVT) Zn-Pb district as well as several smaller mineral deposits and sulfide mineral occurrences. The occurrence of MVT mineralization in these Mississippian carbonate rocks suggests that they were

affected by pervasive regional basinal fluids associated with sulfide mineralization (Gregg and Shelton, 2012).

This study applies petrography, fluid inclusion microthermometry, and isotope geochemistry to examine the effects of late diagenetic fluids and identify the composition and source(s) of these fluids regionally in Mississippian rocks in the Cherokee and Ozark Platform region (northeastern Oklahoma, northwestern Arkansas, southeastern Kansas and southwestern Missouri). Of particular interest is the effect of late diagenetic fluids on the evolution of porosity and the thermal history of the region as it relates to petroleum migration.

2.1.1. GEOLOGICAL BACKGROUND

Mississippian carbonate rocks were deposited in parts of Colorado, Nebraska, Kansas, Oklahoma, Arkansas, Missouri, Iowa, and Illinois across the ancient Burlington Shelf (Lane, 1978; Gutschick and Sandberg, 1983). Mississippian rocks in the study area (Figure 1) were deposited in a ramp/shelf system that trended along an approximate northeast-southwest strike and that deepened to the south into the Arkoma basin (Figure 2). This system is bounded by the Ozark uplift on the east and by the Transcontinental Arch (Nemaha Uplift) to the north and northwest. Shallower water (shelf) depositional settings occurred in the northern part of the study area and deepened toward the south into the Arkoma Basin (Wilhite et al., 2011).

Mississippian strata in the study area are separated into four stages based on lithologic, biostratigraphic, and electric log characteristics (Figure 3). In ascending stratigraphic order these are: Kinderhookian; Osagean; Meramecian; and Chesterian

(Jordan and Rowland, 1959). In northern Oklahoma, Mississippian carbonates are mainly Kinderhookian, Osagean and Meramecian. In the study area, Kinderhookian units represent a transgressive sequence (Handford, 1989; Shelby, 1986; Mazzullo et al., 2011) that contains the Bachelor, Compton, Northview, and Pierson Formations (Unrast, 2012). At the base of the section, the Bachelor Formation is comprised of a light colored sandstone and greenish shale, which is overlain by the Compton Limestone consisting of thinly bedded mudstones and containing biohermal mud mounds (Anglin, 1966; Huffman, 1958; Unrast, 2012). The Northview Shale is composed of light green, soft limy shale and marl; the Pierson Formation is a grey, thinly bedded, crinoidal wackestone to packstone and also contains individual biohermal mounds as well as mound complexes (Anglin, 1966; Unrast, 2012). Osagean units consist of interbedded light and dark-colored, dolomitic and argillaceous, cherty limestone (Jordan and Rowland, 1959). Lower Meramecian age rocks cropping out in the Tri-State MVT district are characterized by chert beds (McKnight and Fischer, 1970), whereas in northern Oklahoma these beds are predominantly limestone (Huffman, 1958). Chesterian rocks are largely absent in northeastern Oklahoma as a result of erosion prior to Pennsylvanian deposition (Jordan and Rowland, 1959).

The Mississippian limestone section has been described as an overall 2nd order sequence made up of a series of higher frequency, 3rd and 4th order sequences that occurred in response to eustatic sea level change. This stratigraphic hierarchy is thought to play a significant role in the quality and vertical heterogeneity of the Mississippian reservoir (LeBlanc, 2014). In the study area, regressive, skeletal (dominantly crinoidal) grainstones exhibit abundant syntaxial cement, which occludes much of the pore space.

This cement has been interpreted to be of early diagenetic origin (Morris, et al., 2013). Packstones deposited during transgressions typically contain little void-filling cement and display varying degrees of silicification and dissolution, making them better reservoir rocks (Price, 2014). Mazzullo et al. (2009) documented the main diagenetic events in the Cowley Formation in south-central Kansas, including at least three generations of silicification, several periods of porosity-creating dissolution, and minor dolomitization. In the Compton and Pierson Formations within the present study area, Morris et al. (2013) recognized early marine radiaxial calcite cementation, meteoric dissolution, and void-filling equant calcite cementation that they attributed to meteoric diagenesis, followed by minor dolomitization (see also Unrast, 2012).

The presence of the Tri-State MVT district (Figure 1) has largely been ignored by petroleum geologists working on the southern mid-continent. This world class mineral district covers an area of about 5000 km^2 (1900 mi^2) on the western flank of the Ozark Uplift in southwestern Missouri, southeastern Kansas, and northeastern Oklahoma (Hagni and Grawe, 1964; Hagni, 1982). Within the Tri-State MVT district, exposed sedimentary rocks are Mississippian and Pennsylvanian age and subsurface rocks range from Precambrian through Devonian age as determined by drilling (Hagni, 1976). Evidence of sulfide mineralization throughout the Carboniferous strata extends eastward into northern Arkansas and westward into Kansas (Leach et al., 1975; Coveney and Goebel, 1983; Gregg and Shelton, 2012). The ore deposits in the Tri-State MVT district are strata-bound and are hosted almost entirely by the cherty limestones of the Burlington-Keokuk Formation (Figure 3) (Hagni, 1982). The most abundant ore and gangue minerals in the district are sphalerite, galena, chalcopyrite, pyrite, marcasite, calcite, dolomite, and quartz

(jasperoid) (Hagni and Grawe, 1964). Tri-State Zn-Pb mineralization has been linked to petroleum migration across the region (Fowler, 1933; Wei, 1975; Ragan et. al, 1996; Gregg and Shelton, 2012). The ores and gangue minerals are believed to have been precipitated by saline basinal fluids emanating from the Arkoma Basin during the Alleghanian-Ouachita Orogeny (Late Pennsylvanian to Permian) at temperatures from 50° to 200°C (Leach, 1994; Appold and Nunn, 2005).

2.2. METHODS

Samples used in this study were collected from outcrops and core in Oklahoma, Missouri, Kansas, and Arkansas. Subsurface core was sampled at the Missouri Geological Survey core repository in Rolla, MO, the Oklahoma Geological Survey core repository in Norman, OK, and the Kansas Geological Survey in Lawrence, KS. Other core samples used in this study were donated by industry members of the OSU Mississippian Consortium.

Petrographic analysis was conducted on 146 thin sections with particular attention given to void-filling dolomite and calcite cements. Cathodoluminescence (CL) petrography was carried out using a CITL MK5-1 cathodoluminescence system mounted on an Olympus-BX51 microscope equipped with 4X, 10X, and 40X long focal distance objective lenses, and a "Q Imaging" 5-megapixel, cooled, low-light, digital camera system.

Carbon and oxygen isotope compositions were determined for dolomite and calcite samples using Thermo-Finnigan Delta Plus gas-source mass spectrometers at the stable isotope laboratories of Oklahoma State University and the University of Missouri. The

$\delta^{13}C$ and $\delta^{18}O$ values (relative to the VPDB standard) have standard errors of less than ±0.05‰, based on replicate measurements of the NBS-19 calcite reference standard, and have been corrected for reaction with 103% phosphoric acid at 70°C (Rosenbaum and Sheppard, 1986). Ratios of $^{87}Sr/^{86}Sr$ were determined using a TIMS at the University of Kansas Radiogenic Isotope Laboratory and have errors of ±0.000014 at a 95 percent confidence interval.

Fluid inclusion microthermometric measurements were made using a Linkam THMSG 600 heating and cooling stage mounted on an Olympus BX41 microscope equipped with 40X and 100X long focal distance objective lenses. Homogenization (T_h) and last ice melting (T_m) temperatures have errors of ±1.0°C and ±0.3°C, respectively, based on analysis of synthetic fluid inclusions (Shelton and Orville, 1980). The inclusions analyzed in this study were aqueous, two-phase, primary and secondary inclusions, using the terminology of Roedder (1984). Salinities were calculated from T_m measurements using equations from Bodnar (1992).

2.3. RESULTS

2.3.1. PETROGRAPHY

For the purpose of describing the limestone lithologies and diagenetic features encountered in this study, it is convenient to divide the study area into four regions, A, B, C, and D, as shown in Figure 1.

Region A includes samples from the Tri-State MVT district. They include several core and mine samples from the Joplin area of southwest Missouri including the mines at Neck City (Jasper Co.), and Granby (Newton Co.). Samples from the Picher Field (a sub-

district of the Tri-State MVT district) of southeastern Kansas and northeastern Oklahoma include mines near Treece and Baxter Springs (Cherokee Co.), Kansas, and Picher (Ottawa Co.), Oklahoma. Because mining activity in the Tri-State district ceased in 1967, most of the mine samples were collected from tailings dumps, so accurate locations within mines are unknown. Several samples were donated for this study from private mineral collections and labels indicate only the mine name. All of the mine samples in the Tri-State district likely are from the upper part of the Burlington-Keokuk Formation (Figure 3), which hosted most of the mineralization in this district (Hagni, 1976). Tri-State samples consist of chert breccias cemented by mineralized jasperoid containing dolomite, calcite, sphalerite, and galena filling open spaces ranging from mm to dm scale.

In addition to mine samples, one core (PM-21 from Cherokee County, KS) was sampled, which penetrated Osagean-Meramecian strata (Figure 3). This core consists of three units, in ascending order: (1) chert-free, grain-supported limestone and dolomite overlain by argillaceous, micritic, cherty dolomite; (2) interbedded argillaceous wackestone and brecciated chert; and (3) echinoderm-rich, bioclastic wackestone-packstone (as described by Young, 2010). Replacement dolomite crystals observed in this core have planar-e to s texture (Sibley and Gregg, 1987) and range in size from approximately 0.05 to 0.1 mm. Solution-enlarged fractures ranging from ~1 mm to several cm in this core are filled by coarse crystalline (cm size) calcite and saddle dolomite cement.

Two cores from Carterville (Jasper Co.), MO were sampled from the Burlington-Keokuk Formation. The lithology here is mostly cherty and muddy limestone, with calcite-filled fractures ranging from 1 to 5 mm in width.

Region B samples (Figure 1) are from two cores, the Blackbird 4-33 and the Perryman 2 oil wells, in Osage Co., Oklahoma. The rocks encountered in the Blackbird well include 84.7 m (278 ft) [959.2 to 1043.9 m (3147 to 3425 ft) core interval] of the Reeds Spring Formation (Osage) based on sponge spicule facies (Darwin Boardman, personal communication). Lithologies sampled in the Blackbird core include argillaceous and siliceous mudstone with scattered fossils and intragrain, vug, and fracture porosity. Intragrain and vug porosity is filled by calcite cement (Figure 4C & D). Fracture porosity includes ptygmatic fractures and solution-widened fractures ranging from 1 to 3 cm (0.4 to 1.2 in) and is filled by calcite, and quartz cements (Figures 6C and 7). The Perryman 2 core includes 12.7 m (41.7 ft) of chert breccia and partially dolomitized limestone. The exact stratigraphic position of the cored section within the Mississippian is not known. Lithologies in the Perryman 2 core include chert breccia in the upper 6.3 m (20.7 ft) and chert breccia and partly dolomitized lime mudstones dominating the lower 6.4 m (21 ft). No carbonate cements were observed in the Perryman 2 core.

Region C samples (Figure 1) include outcrop and core samples taken along the Seneca Fault system in Mayes, Wagoner, and Delaware Co., OK. Samples from Mayes County were collected from a quarry near Pryor, OK and include large fracture- and breccia-filling calcite and dolomite ranging from mm to cm scale near the top of the Burlington-Keokuk Formation (Figure 3). Core samples from the Hall 2-13 well in Wagoner County, OK include 15 m [200.5 to 215.6 m (657.8 to 707.3 ft) core interval] of the Fayetteville Formation (Figure 3) and are comprised of skeletal packstone containing fractures ranging from 0.5 to 1.0 cm (0.2 to 0.4 in) filled by calcite and quartz cement.

Samples from Delaware Co., OK were collected from a crinoidal mound in the Pierson Formation along Spavinaw Creek.

Region D (Figure 1) includes outcrops of the Compton, Pierson, and Reeds Spring Formations in Benton and Boone Co., AR, and McDonald and Stone Co., MO. (Figure 3). The sedimentology and petrology of the units in this region were described in detail by Unrast (2012) and Morris et al. (2013). The samples collected are comprised of skeletal grainstones and packstones containing porosity-filling calcite, and cherty mudstones. We selected samples that preferentially contain fractures and solution-widened fractures ranging in size from 0.5 mm to 1.0 cm (0.2 to 0.4 in), filled by calcite cement.

2.3.2. CEMENT PARAGENESIS

Radiaxial fibrous and bladed calcite cements were observed in stromatactis-like cavities in Lower Mississippian biohermal mud mounds in southern Missouri and northern Arkansas by Unrast (2013) and Morris et al. (2013). Similar fibrous and bladed calcite cements were observed in grainstones of the current study (Figure 4A). Intergrain-filling, bladed calcite cement was observed that nucleated on non-crinoid skeletal fragments in Mississippian grainstones in region ‘D’ of this study (Figure 4A & B). Similar bladed calcite cement was observed as intragrain -fillings in rugose corals observed in region ‘B’ (Osage Co., OK) (Figure 4C & D). Syntaxial calcite cements typically nucleated on crinoids (Figure 4E & F). Bladed and syntaxial calcites are followed by blocky (equant) calcite cement that typically fills remaining intergrain and intragrain porosity (Figure 4).

Strong compositional zoning was deduced by CL microscopy in all inter- and intra-grain calcite cements and vug-filling cements. Unrast (2013) studied the CL cement stratigraphy in Mississippian limestones associated with mud mound build-ups and divided calcite cements into 5 stages, the first of which consists of non-ferroan fibrous to bladed calcite followed by four distinct stages of non-ferroan equant calcite. Stage 1 cements are non-CL to mottled CL; stage 2 are non-CL; stage 3 are bright yellow CL; stage 4 are alternating dull orange to brown CL, and stage 5 are dull orange-brown CL with no internal zoning (Unrast, 2013). These patterns of CL zonation generally were observed in the study, although some of the stages are absent depending on the sample locality. For instance, intragrain, porosity-filling calcite cement observed in a rugose coral sample from Region B (Figure 1) contains only stages 1, 3, 4, and 5 cement (Figure 4D), whereas intergrain porosity-filling cement from region D contains all of the CL stages (Figure 5).

Calcite and, infrequently, quartz cement filling fractures, solution-widened channels, and breccias (Figures 6 and 7) was observed throughout the study area. Calcite cement-filled ptygmatic fractures in cherty mudstone occur in Region B in Osage Co., OK (Figure 6C). Quartz and calcite cement were observed in fracture porosity from Wagoner Co., OK (Region C, Figure 1) and in fracture, solution-widened channel, and breccia porosity (Figure 7) from Osage Co., OK (Region B, Figure 1).

The CL characteristics of fracture-filling, equant calcite cement differ among the four regions studied. For example, calcite cement filling fractures in samples from Mayes Co., OK (Region C) and core samples from Jasper Co., MO (Region A) display yellow CL with no internal zoning. Equant calcite cement that fills solution-widened channels in

mine samples from the Tri-State MVT district (Region A) and core samples from Osage Co., OK (Region B) and Benton Co. AR (Region D) display alternating bright to dull CL zoning (Figure 6 A&B). Authigenic quartz crystals associated with calcite cement filling fractures from Wagoner Co., OK (Region C) and Osage Co., OK (Region B) are non-CL.

Replacement dolomite is uncommon in the study area. Typically, dolomite occurs as scattered rhombic crystals replacing mudstone or carbonate mud matrix in packstone and wackestone (Figure 8A, B). An exception to this observation is the PM-21 core from Cherokee County, KS (Region A), which displays both matrix-replacing dolomite and fracture-filling saddle dolomite (Figure 8C, D).

Open-space-filling saddle dolomite cement was observed in Mayes Co., OK (Region C, Figure 1) and throughout the Tri-State district (Region A, Figure 1). Figure 8 (E & F) shows an example of saddle dolomite cement from the Picher Field, Admiralty Mine (#3 Shaft), OK. The compositional stratigraphy of this dolomite cement, as revealed by CL, is typical of the study area and includes up to 4 stages of cement growth: bright yellow-orange CL followed by a thin dull gray zone (stage 1); red-orange and thin non-CL zone (stage 2); dark red-orange and thick non-CL (stage 3); orange grading to yellow CL zones (stage 4) (Figure 8E, F). It is important to note that all four stages are not always present in all of the dolomite samples studied throughout the district.

2.3.3. FLUID INCLUSION MICROTHERMOMETRY

Two-phase, aqueous fluid inclusions (liquid and vapor) were observed in open-space-filling cements throughout the study area. This includes intergrain and intragrain blocky (equant) calcite cement and fracture- and breccia-filling calcite, dolomite and quartz

cements (Figure 9A, B, C, D). Measured inclusions range from 2 to 30 μm in their longest dimension. Smaller two-phase inclusions were observed in some dolomite cements, but were not measured due to poor optical resolution. Single-phase (liquid only) petroleum inclusions were observed in calcite cements from the Tri-State district (Region A). (These include samples from the Admiralty Mine (OK), Anna Beaver Mine (OK), Wood Chuck Mine (OK), Neck City Mine (MO), Treece (KS), and one sample without a specific mine location from the Picher Field, OK). Single-phase petroleum inclusions also were observed in fracture-filling calcite cements from Osage Co., OK (Region B) and Benton Co., AR (Region D). Single- and two-phase (liquid and vapor) petroleum inclusions were observed in fracture- and breccia-filling calcite and dolomite cements from Wagoner and Mayes Co., OK (Region C). Petroleum inclusions observed in this study are characterized by a light blue fluorescence under UV light (Figure 9E & F).

Values for T_h and/or T_m were obtained for 240 aqueous fluid inclusions (Table 1). T_h values for all fluid inclusions measured range from approximately 50º to 175ºC and T_m values range from 4.2 to -25.2 (Table 1). A small population of the low salinity inclusions yielded T_m values above 0ºC (Table 1). This likely is caused by metastable, superheated ice that forms due to the failure of a vapor bubble to nucleate on heating (Roedder, 1967). The T_h data for these inclusions is reported in Table 1.

Figure 10A displays the fluid inclusion data as salinity, expressed as equivalent weight % NaCl, calculated from measured T_m values (Bodnar, 1992) plotted against T_h values for calcite, dolomite, and quartz cements from the study area. Only inclusions for which both T_h and T_m values were determined are plotted. These results indicate the presence of both dilute and high salinity end-member fluids (calculated values ranging

from 0 to 25 equivalent weight % NaCl). Ranges of T_h values are similar for both of these end-member salinity populations.

Figure 10B displays the fluid inclusion data with data fields shown from earlier studies in and near the Tri-State mineral district. The individual fluid inclusions in Figure 10B are grouped on the basis of being observed in the same microscope field, being the same type of inclusion (*e.g.* primary or secondary) and having almost the same T_h and T_m values (thus more than one fluid inclusion group can be identified in a single microscope field). Because the groups of fluid inclusions are in close proximity to one another both spatially and temporally they are treated here as fluid inclusion assemblages. Figure 10B shows more clearly the presence of two distinct salinity end members. The fields displaying previously published data (Figure 10B) from in and near the Tri-State Mineral district are consistent with two salinity end members. Data for fluid inclusion assemblages in the four regions of the study area document the presence of the two salinity end members in each region (Figure 11).

2.3.4. ISOTOPE ANALYSIS

2.3.4.1. CARBON AND OXYGEN ISOTOPES

Carbon and oxygen isotope analysis was conducted on carbonate samples from all four regions of the study area (Figure 1) (Table 2). Calcite mud from region D has $\delta^{18}O$ values of -5.6 to -1.4‰ and $\delta^{13}C$ values of 1.9 to 4.3‰. Calcitic crinoid debris from regions C and D has $\delta^{18}O$ values of -2.5 to -1.3‰ and $\delta^{13}C$ values of 2.3 to 4.0‰. These values are similar to those of brachiopods and marine calcite cement from the same areas measured by Morris et al. (2013) (Figure 12).

Intergrain and vug-filling calcite cement and fracture- and breccia-filling calcite cement from regions C and D form two clusters of differing $\delta^{18}O$ values. The first cluster has $\delta^{18}O$ values of -5.0 to -1.9‰ and $\delta^{13}C$ values of 1.6 to 4.6‰. The second cluster, which also contains samples from regions A and B, displays $\delta^{18}O$ values of -9.9 to -6.3‰ and $\delta^{13}C$ values of 0.8 to 3.7‰. Morris et al. (2013) obtained values for intergrain equant calcite cements that are similar to the values obtained for the second cluster observed in this study (Figure 12). Equant (blocky) fracture- and breccia-filling calcite cements, from regions A, B, and C, form a grouping with distinct $\delta^{18}O$ and $\delta^{13}C$ values that range from -11.6 to -6.2‰, and -12.1 to -2.6‰, respectively. This group also contains one value for saddle dolomite cement from Mayes Co. (Figure 12).

Replacement dolomite and saddle dolomite cements in the Tri-State mineral district (region A) have $\delta^{18}O$ and $\delta^{13}C$ values of -9.5 to -5.6‰ and -4.0 to -1.0‰, respectively. Replacement and saddle dolomite cements from Cherokee Co., KS (region A) display $\delta^{18}O$ and $\delta^{13}C$ values ranging from -6.3 to -2.6‰, and -2.0 to 2.3‰, respectively.

2.3.4.2. STRONTIUM ISOTOPES

Ratios of $^{87}Sr/^{86}Sr$ for crinoid debris and associated intergrain equant calcite cement from region D are 0.7081 and 0.7085, respectively (Table 3). Fracture-filling calcite cement from all of the regions displays Sr isotope ratio values ranging from 0.7091 to 0.7112. The values for $^{87}Sr/^{86}Sr$ obtained for intergrain calcite cement and a crinoid grain are 0.7085 and 0.7082, respectively. These ratios and their $\delta^{18}O$ values (~ -3 to -2‰) are consistent with precipitation in equilibrium with the Mississippian seawater (Figure 13, Mii et al., 1999; Bruckschen et al., 1999). The $^{87}Sr/^{86}Sr$ values for the late diagenetic

fracture- and breccia-filling calcite and dolomite cements are more radiogenic, ranging from 0.7091 to 0.7100 and their $\delta^{18}O$ values are low, from ~ -11 to -6‰. One sample of fracture-filling cement in Osage Co., OK has a value of 0.7112 that is anomalously radiogenic, compared to the other values.

2.4. DISCUSSION

2.4.1. PARAGENESIS

A paragenesis of diagenetic events in the study area is shown in Figure 14. Early diagenesis includes stabilization of high-Mg calcite (and possibly aragonite) skeletal grains and micrite to low-Mg calcite. Early fibrous and bladed calcite cements likely were precipitated initially from seawater (Unrast 2012, 2013). Values of $^{87}Sr/^{86}Sr$ and $\delta^{18}O$ (Figure 13, Table 3) indicate that these early diagenetic fabrics are in, or near equilibrium, with Mississippian seawater (Mii et al., 1999; Bruckschen et al., 1999). Carbonate cements precipitated from Early Mississippian seawater likely were high-Mg calcite transitioning to aragonite by Late Mississippian time (Lowenstein et al., 2003). Carbon and oxygen isotope values for calcite mud matrix and crinoid grains (Figure 12) are consistent with precipitation from Mississippian seawater (Mii et al., 1999). Stable isotope values for brachiopods and marine calcite cement obtained by Morris et al. (2013) also are consistent with precipitation from Mississippian seawater (Figure 12).

2.4.1.1. INTRAGRAIN, INTERGRAIN AND VUG-FILLING CALCITE CEMENTS

Unrast (2012, 2013) described 5 distinct compositional zones, visible with CL, from blocky intergrain and vug-filling calcite cements in the study area (Figure 5). This CL

zoning pattern is similar to the 5-zone CL stratigraphy described by Kaufman et al. (1988) for the Burlington-Keokuk Formation in a region extending from the Mississippi Valley of Illinois and Missouri into southwestern Missouri. On the basis of stratigraphy and cross-cutting relationships, they attributed the first three CL zones to mixing of seawater and meteoric water or inundation by meteoric water associated with sea level falls during the Mississippian.

Ritter and Goldstein (2012) also recognized 5 major CL zones in intergrain calcite cements in the Burlington-Keokuk in a region extending from east-central Kansas and west-central Missouri to southeastern Kansas and southwestern Missouri. These CL zones are comparable to those of Unrast (2012, 2013) and Kaufman et al. (1988) (Table 4). Carbon and oxygen isotope values for the first three CL zones of Ritter and Goldstein (2012) were interpreted by them to be consistent with precipitation from fresh phreatic and brackish water prior to deep burial. They observed and analyzed one phase (liquid) fluid inclusions that they interpreted to indicate an entrapment temperature below 50º C. Based on one $^{87}Sr/^{86}Sr$ value (0.7088), which is slightly more radiogenic than Mississippian seawater, Ritter and Goldstein (2012) suggested that this meteoric water interacted with continental-derived argillaceous sediments.

On the basis of crosscutting relationships with MVT mineralization, Kaufman et al. (1988) assigned an Early Permian minimum age for their CL zones 4 and 5, which may correspond in timing with MVT mineralization in the Ozark region (Leach et al. 2001; Gregg and Shelton, 2012). Both Kaufman et al. (1988) and Ritter and Goldstein (2012) suggested that the later CL zones of calcite cements are related to post-Pennsylvanian fluids that may have been associated with either deep circulation of low temperature

meteoric water from the overlying Pennsylvanian strata or warm basinal waters presumably moving up from underlying Cambrian-Ordovician strata.

The $\delta^{18}O$ and $\delta^{13}C$ values of intergrain, intragrain and vug-filling calcite cements obtained in this study (Figure 12) range from -8.2 to -1.9‰ and 1.5 to 4.7‰, respectively. On the basis of low $\delta^{18}O$ values, Morris et al. (2013) interpreted equant intergrain calcite cements to have a meteoric origin. We interpret the equant calcite cements of Morris et al. (2013) to be equivalent to the blocky intergrain calcites of our study. Carbon and oxygen isotope values for the equant calcite cements of Morris et al. (2013) overlap significantly with blocky intergrain cement values of our study (Figure 12) and with carbon and oxygen isotope values obtained by Ritter and Goldstein (2012) for all of the CL stages of calcite cements observed in their study (Figure 12).

The presence of two-phase fluid inclusions in the later stages (CL zones 4 and 5) of intergrain, intragrain and vug-filling calcite cements (Figure 9A &B) observed in our study indicates that these cements likely precipitated from warm (>50º C) fluids. We therefore reinterpret the low $\delta^{18}O$ values of Morris et al. (2013) to indicate precipitation of their equant calcite cement from warm basinal fluids rather than from meteoric waters (Figure 12).

The assignment of CL zone 4 and 5 calcite cements to precipitation from post-Pennsylvanian basinal waters requires that porosity was not totally destroyed during early diagenesis and that considerable porosity remained through the period of petroleum migration. This interpretation also was made by Ritter and Goldstein (2012) for Mississippian rocks north and west of our study area (western Missouri and Eastern

Kansas). Ritter and Goldstein (2012) believed that an average porosity of 24% remained in the Burlington-Keokuk bioclastic limestones into late stage diagenesis.

2.4.1.2. FRACTURE AND BRECCIA-FILLING CALCITE CEMENT

Calcite cement fills fractures and is an open-space breccia filling in all four regions of the study area. Dolomite cements also were observed as a fracture- and breccia-filling in regions A, B, and C (Figure 1). Throughout most of the study area, fracture- and breccia-filling calcite cements display uniformly bright yellow to orange CL. An exception is fracture-filling calcite cement from region D (Benton Co., AR) that displays dull to bright CL zonation (Figure 6 A & B).

Carbon and oxygen isotope values for fracture- and breccia-filling calcite cements in all four regions of the study area are consistent with precipitation from fluids ranging from Mississippian seawater to basinal water (Figure 12). Low $\delta^{13}C$ values for fracture- and breccia-filling calcite cements in the Tri-State mineral district and in Mayes Co., OK along the Seneca Fault system are consistent with oxidation of organic matter associated with petroleum generation (Figure 12) (Machel et al., 1995). These same samples contain petroleum-bearing inclusions (Figure 9E &F).

Significant planar replacement dolomite was observed only in one core from region A (Cherokee Co., KS). Slightly lower $\delta^{18}O$ values for this dolomite are consistent with dolomitization by meteoric and seawater or, more likely, initial dolomitization by seawater with later resetting of the isotopic composition by recrystallization in the presence of warm basinal water (Figure 12). The presence of fracture-filling saddle dolomite in this core supports this latter hypothesis. Planar replacement dolomite may

correspond in timing and have a similar origin as dolomites I & II identified by Banner et al. (1988) and Cander et al. (1988) in the Mississippian Burlington-Keokuk Formation in western Illinois and eastern and central Missouri.

Saddle dolomite cements were observed only in regions A and C of the study area (Figure 1). Hagni and Graw (1964) interpreted saddle dolomite formation in the Tri-State mineral district (Region A) to be associated with the main stages of sphalerite and galena ore precipitation. Similar CL stratigraphy among saddle dolomites in the Tri-State mineral district, Cherokee Co., KS, and along the Seneca Fault (Mayes Co. OK) system in Mayes Co., OK (Figure 8) suggest precipitation by the same or similar fluids.

Low $\delta^{18}O$ (and $\delta^{13}C$) values (Figure 12) for saddle dolomites are consistent with precipitation from basinal brines, as is their close association with sulfide mineralization in the Tri-State district (Hagni and Graw, 1964). Saddle dolomite in the study area likely corresponds in timing with dolomite III identified by Cander et al. (1988) in the Mississippian Burlington-Keokuk Formation in western Illinois and eastern and central Missouri, which also is attributed to a late diagenetic origin. The timing of this dolomite may also correspond to the widely dispersed occurrences of saddle dolomite in Mississippian strata elsewhere in the U.S. mid-continent observed by Goldstein and King (2014) and King and Goldstein (2016).

Authigenic quartz cement was observed associated with fracture- and breccia-filling calcite in Regions B and C. In region B, quartz cement occurs paragenetically earlier than calcite, whereas in region C it is later. All of the quartz cement examined in this study is non-CL. Possible sources of silica for authigenic quartz in the study area are the cherts, tripolites, and spiculites that are ubiquitous in Mississippian strata in the mid-continent

(Mazzullo et al., 2009; Mazzullo et al., 2011). Most of these are thought to be early diagenetic, so the late diagenetic authigenic quartz studied here would represent a remobilization of this silica. Alternatively, silica may have been introduced by basinal fluids originating in the underlying Cambrian-Ordovician section.

2.4.2. ORIGIN AND TIMING OF LATE DIAGENETIC FLUIDS

2.4.2.1. FLUID INCLUSION CONSTRAINTS

Fluid inclusion analysis of calcite, dolomite, and quartz cements in the study area indicate precipitation by at least two end-member fluids. Figure 10 shows two distinct clusters of fluid inclusion data: (1) a high salinity fluid; and (2) a fluid having moderate salinity to no salinity. Previous studies conducted in the Tri-State district (Ragan, 1996; Young, 2010; Wenz et al., 2012) found similar distributions of high and low salinity values (Figure 10B). Both clusters of fluid inclusion data in Figure 10 have similar T_h ranges (approximately 60 to 175º C). Two earlier studies of fluid inclusions in calcite, dolomite, and sphalerite from the Tri-State district (Schmidt, 1962; Wei, 1975) found ranges of T_h values similar to those of our study. These studies did not determine T_m values, so salinities are not available for comparison.

The major difference between the present study and earlier studies is that this study collected fluid inclusion data for Mississippian-hosted carbonates regionally, whereas previous studies were focused in and near the Tri-State MVT district. Figure 11 indicates that similar distributions of T_h values and salinities exist in all four regions of the study area. Taken together with oxygen isotope data, this indicates that the entire Cherokee-

Ozark platform region was affected by the same fluids or fluids of similar temperature and composition during late diagenesis.

2.4.2.2. OXYGEN ISOTOPE COMPOSITIONS OF CEMENT-DEPOSITING WATERS

The $\delta^{18}O$ values of carbonate cements are a function of several factors including, temperature, the original $\delta^{18}O$ value of the cement-depositing fluid, and the extent of fluid-rock interaction along the fluid's flow paths. In order to unravel the history of fluids that precipitated the cements, equilibrium $\delta^{18}O_{water}$ values were calculated. These values may allow us to determine whether the fluids that deposited carbonate cements were in isotopic equilibrium with the local host rock carbonates or instead, reflect non-resident fluids that retained their source-derived oxygen isotope signatures (Shelton et al., 2011). Another possibility is that the $\delta^{18}O_{water}$ values may reflect the presence of both resident and non-resident fluids with the potential of fluid mixing.

Equilibrium $\delta^{18}O_{water}$ values (VSMOW) for fluids that precipitated calcite and dolomite cements were calculated using fractionation equations from O'Neil et al. (1969) for calcite-water and Northrop and Clayton (1966) for dolomite-water (Table 5, Figure 15). Temperatures utilized for the calculations are based on ranges of T_h values for fluid inclusions in the carbonate cements. For comparison, the $\delta^{18}O_{water}$ values in equilibrium with the host limestone were calculated for the same temperatures (O'Neil et al., 1969).

Figure 15 shows calculated $\delta^{18}O$ values for waters in equilibrium with calcite and dolomite cements from various localities (black and blue lines, respectively) and for waters in equilibrium with host limestones (pink lines). An important observation is that

the calculated $\delta^{18}O_{water}$ values for calcite and dolomite cements vary considerably (from -5 to +12‰) and do not define a single end-member water. Neither do they show a correspondence between temperature (inferred depth of burial) and $\delta^{18}O_{water}$ values. This might reflect (1) isotopic differences in the fluid source regions, (2) differences in lithologies encountered along flow paths, or (3) varying water to rock ratios associated with types of fluid flow (i.e. lack of reaction along fault pathways versus extensive reaction during stratigraphically controlled flow).

The $\delta^{18}O_{water}$ values calculated for both calcite and dolomite cements in all four regions of the study area typically differ substantially from calculated $\delta^{18}O_{water}$ values in equilibrium with the host limestone. The variation of $\delta^{18}O_{water}$ values for the carbonate cements compared to those calculated for the host limestone indicates that waters that deposited the cements were not in isotopic equilibrium with the local host rocks (limestone). Their elevated $^{87}Sr/^{86}Sr$ ratios, compared to those of Mississippian limestones, further supports this interpretation (Figure 13).

Overlapping $\delta^{18}O_{water}$ values for carbonate cement and host limestone observed at Osage Co., OK (Region B) indicate that the cement-depositing fluids approached isotopic equilibrium with local carbonate rocks, likely reflecting a large degree of reaction along flow paths at low water/rock ratios. Alternatively, the overlap in values could represent mixing between resident and non-resident fluids, dominated by the resident fluids in equilibrium with the host limestones. The intermediate T_h values of different fluid compositions is consistent with variable mixing throughout the region (Figure 15).

2.4.2.3. CONCEPTUAL MODEL

A regional fluid flow model is shown in Figure 16 in which large volumes of fluid from the underlying aquifer moved up along faults and fractures and mixed with more dilute resident fluids in overlying Mississippian rocks. There is abundant evidence that saline brines, at similar temperatures and salinities to those observed in Mississippian rocks, were ubiquitous in underlying Cambrian and Ordovician strata (Leach et al., 1975; Shelton et al, 1992; Temple, 2016). The likely primary drive for the saline fluids is a regional gravity driven system postulated as a result of the Ouachita Orogeny (Leach 1994; Appold and Garven, 1999; Gregg and Shelton, 2012). Pulses of saline fluids moved upward along faults and fractures into the overlying Mississippian strata and displaced resident lower salinity fluids. During periods between pulses of saline fluids, the resident fluids reasserted themselves. A similar model was proposed by Shelton et al. (2011) for Mississippian age fracture-related dolomitization and sulfide mineralization on the Isle of Man. An alternative hypothesis, that dilute fluids sourced from overlying strata migrated downward through Mississippian strata, possibly driven by thermal buoyancy, is not as well supported by the data. The overlying Pennsylvanian strata are relatively shale-rich and impermeable. Also, if the overlying strata were the source of the dilute fluid it would be expected that inclusions of these fluids would have displayed lower T_h values.

High $^{87}Sr/^{86}Sr$ values of carbonate cements in the Mississippian rocks (Figure 13) suggest interaction of the cement-depositing fluids with continental basement or arkosic sandstone derived from continental basement. Elevated $^{87}Sr/^{86}Sr$ values also could indicate a continental shale source for fluids, but the underlying Woodford Shale is relatively thin or absent throughout most of the study area. Furthermore, previous fluid inclusion and isotope studies of underlying Cambrian carbonates in the Ozark region

indicate that those strata are a potential source of saline brines with high $^{87}Sr/^{86}Sr$ values derived from interaction with underlying basement rocks (Shelton et al., 1992; 2009). These studies and others (e.g. Gregg, 1985; Gregg & Shelton, 1989; Rowan & Leach, 1989; Bethke & Marshak, 1990; Appold & Garven, 1999; Appold & Nunn, 2005) indicate that regional flow of basinal brines and associated mineralization throughout the Cherokee-Ozark Platform region was associated with the Ouachita orogeny and involved flow of fluids through deep Cambrian-Ordovician and basement aquifers.

Goldstein and King (2014) and King and Goldstein (2016), in a study of Cambrian through Mississippian strata in the mid-continent, suggested a three-stage late diagenetic history based on petrographic, fluid inclusion, and isotope data. Their study area is located in southeastern Kansas, partly overlapping with our study area in southwestern Missouri and northeastern Oklahoma. Stage 1 is characterized by authigenic megaquartz and was interpreted to be related to relatively early migration of dilute fluids, prior to regional reflux of Permian brines. This was based on fluid inclusions with relatively low salinities (3 to 6 wt.% NaCl). Stage 2 is characterized by the widespread presence of saddle (baroque) dolomite cements containing high-salinity fluid inclusions (15 to 23 wt% NaCl) and radiogenic Sr isotope values. They attributed this event to advective flow of brines northward out of the Anadarko and Arkoma basins during the Ouachita Orogeny. Stage 3 is less well constrained, but is characterized by late-stage calcite cements. A lack of uniformity in stable and radiogenic isotope values in these cements was interpreted to indicate more localized fluid flow events than during stage 2. They hypothesized that stage 3 was related to reactivation of faults during the Laramide orogeny.

In contrast to the conclusions of Goldstein and King (2014) and King and Goldstein (2016), we documented both saline and dilute fluid inclusions in quartz, saddle dolomite, and calcite cements in Mississippian strata throughout the study area (Figure 10). Our diagenetic paragenesis indicates that late stage calcite and authigenic quartz cements both predate and postdate saddle dolomite cements. Petroleum-rich fluid inclusions were observed in both saddle dolomite and calcite cements. A specific trend of early dilute fluids followed by saline fluids was not observed; rather our data suggest an alternation between the influences of two fluid end members during late diagenesis.

2.4.3. IMPLICATIONS FOR THE MISSISSIPPIAN PETROLEUM SYSTEM ON THE SOUTHERN MID-CONTINENT

Data from our study area indicate the regional importance of hydrothermal fluid flow on Mississippian carbonates in the southern mid-continent. Most of the fracture and breccia porosity and much of the intergrain and vug porosity is filled by carbonate cements that are demonstrably late diagenetic. Some of these contain petroleum inclusions (Figure 9) and two-phase aqueous fluid inclusions (Table 1). These observations indicate that cementation occurred during migration of petroleum in the system.

Porosity and permeability in the Mississippian carbonate rocks in the southern mid-continent likely remained relatively high through early seawater and meteoric diagenesis. Ritter and Goldstein (2012) estimated an original mean porosity of 42% for bioclastic grainstones in Osagean-Meramecian rocks in Kansas and Missouri north of and overlapping with our study area. They estimated that original porosity was reduced to a mean porosity of 18% following initial stages of diagenesis. Late stage cementation

reduced much of the rest of this porosity (Ritter and Goldstein, 2012). This study indicates that similar stages of porosity loss due to early and late diagenesis extended southward and eastward into eastern Oklahoma and western Arkansas. This means that Mississippian lithologies maintained relatively high porosity through early seawater and meteoric diagenesis and well into the period of petroleum migration when late diagenetic cements occluded much of the remaining porosity.

Regional flow of warm basinal fluids may also have perturbed the regional thermal gradient in the mid-continent, including the study area, relative to that which could be attributed to burial alone (Newell, 1997). As was suggested by Goldstein and King (2014) and King and Goldstein (2016), this likely impacted the thermal maturity of the region and enhanced the generation of hydrocarbons in the Mississippian carbonates as well as in underlying and overlying source rocks.

2.5. CONCLUSIONS

Mississippian carbonate rocks in the Cherokee and Ozark platform region were cemented by seawater followed by mixed seawater and meteoric waters during early diagenesis as indicated by petrographic fabrics and carbon, oxygen, and strontium isotope geochemistry. This early cementation partially filled primary intragrain, intergrain, and vug porosity. Remaining primary porosity, as well as late diagenetic fracture and breccia porosity was filled by calcite, dolomite and quartz cements that were precipitated by evolved basinal fluids as indicated by isotope geochemistry and fluid inclusion microthermometry. Two-phase fluid inclusions display T_h values of 50º to 175ºC and salinities of 0 to 25 equivalent wt.% NaCl.

Analysis of fluid inclusion data indicate that two distinct fluids were present in the study area during late diagenesis: a dilute fluid having salinities ranging from 0 to 10 wt.% NaCl equivalent and a saline fluid with salinities ranging from 15 to 25 wt.% NaCl equivalent. Radiogenic Sr isotope values for fracture and breccia filling cements indicate that one of these fluids likely interacted with continental basement. A model is presented where an evolved saline fluid moved up through faults and fractures from underlying Cambrian-Ordovician strata and displaced or mixed with a dilute resident fluid.

Migration of late diagenetic fluids through the study area likely corresponded with the emplacement of sulfides in the Tri-State MVT district, which is related to regional fluid flow events instigated by the Ouachita Orogeny. The basinal fluids were accompanied by petroleum migration as indicated by the presence of petroleum inclusions in some of these cements. The regional flow of warm basinal fluids likely increased the geothermal gradient in the region, affecting the thermal maturity of the rocks. Porosity and permeability of the Mississippian carbonate rocks likely remained relatively high prior to and during migration of these fluids.

2.6. ACKNOWLEDGEMENTS

This study was supported by the Oklahoma State University-Industry Mississippian Consortium and the Boone Pickens School of Geology. We thank all of the companies that supported this Consortium. Also, thanks to the National Association of Black Geoscientists (NABG) for financial support for SM during this study. Thanks are due to Dr. Eliot Atekwana and Dr. Kenneth MacLeod for use of the isotope laboratory facilities at Oklahoma State University and University of Missouri, respectively. Also we would

like to thank Morgan Unrast and Cory Godwin for providing some samples from their independent studies of the Mississippian carbonates. Thanks are due to Francis C. Furman who contributed samples from the Tri-State mineral District for the study. We thank Michael Grammer, Jeffrey White, Gordon MacLeod, and Abbas Seyedolali for their valuable comments and suggestions. Finally, we thank R. D. Hagni and Jeff Lonnee for their concise reviews and G. Michael Grammer for his editorial handling of this manuscript.

2.7. REFERENCES

Anglin, M. E., 1966, The petrography of the bioherms of the St. Joe Limestone of northeastern Oklahoma: Shale Shaker, v. 16, p. 150-164.

Appold, M. S., and G. Garven, 1999, The hydrology of ore formation in the southeast Missouri district: Numerical models of topography-driven fluid flow during the Ouachita orogeny: Economic Geology, v. 94, p. 913-936.

Appold, M. S., and J. A. Nunn, 2005, Hydrology of the Western Arkoma basin and Ozark platform during the Ouachita orogeny: Implications for Mississippi Valley-type ore formation in the Tri-State Zn–Pb district: Geofluids, v. 5, p. 308-325.

Banner, J. L., G. N. Hanson, W. J. Meyers, 1988, Determination of initial Sr isotopic compositions of dolostones from the Burlington-Keokuk Formation (Mississippian): Constraints from cathodoluminescence, glauconite paragenesis and analytical methods: Journal of Sedimentary Petrology, v. 58, no. 4, p. 673-687.

Bethke, C. M., and S. Marshak, 1990, Brine migrations across North America- The plate tectonics of groundwater: Earth and Planetary Sciences, v. 18, p. 287-315.

Bodnar, R. J., 1992, Revised equation and table for determining the freezing point depression of H_2O-NaCl solutions: Geochimica et Cosmochimica Acta, v. 57, p. 683-684.

Bruckschen, P., S. Oesmann, and J. Veizer, 1999, Isotope stratigraphy of the European Carboniferous: Proxy signals for ocean chemistry, climate and tectonics. Chemical Geology, v. 161, p. 127-163.

Cander, H. S., J. Kaufman, L. D. Daniels, and W. J. Meyers, 1988, Regional dolomitization of shelf carbonates in the Burlington-Keokuk Formation (Mississippian), Illinois and Missouri: Contrast from cathodoluminescence zonal stratigraphy, *in* V. Shukla, and P. A. Baker, eds., Sedimentology and geochemistry of dolostones: SEPM Special Publication, 43, p. 129-144.

Coveney, Jr. R. M., and E. D. Goebel, 1983, New fluid inclusion homogenization temperatures for sphalerite from minor occurrences in the mid-continent area, *in* G. Kisvarsanyi, S. K. Grant, W. P. Pratt, and J. W. Koenig, eds., International conference on Mississippi Valley-type lead zinc deposits: Proceedings volume: Rolla, Missouri, University of Missouri-Rolla Press, p. 234-242.

Fowler, G. M., 1933, Oil and oil structures in Oklahoma-Kansas zinc-lead mining field: AAPG Bulletin, v. 17, p. 1436-1445.

Friedman, I., and J. R. ONeil, 1977, Compilation of stable isotope fractionation factors of geochemical interest: USGS Professional Paper, 440-KK, 12 p.

Goldstein, R. H., and B. D. King, 2014, Impact of hydrothermal fluid flow on Mississippian reservoir properties, Southern Midcontinent: Unconventional Resources Technology Conference (URTeC), Denver, Colorado, p. 25-27.

Gregg, J. M., 1985, Regional epigenetic dolomitization in the Bonneterre Dolomite (Cambrian), southeastern Missouri: Geology, v. 13, p. 503-506.

Gregg, J. M., and K. L. Shelton, 1989, Minor and trace element distributions in the Bonneterre Dolomite (Cambrian), southeastern Missouri: Evidence for possible multiple basin fluid sources and pathways during lead-zinc mineralization: Geological Society of America Bulletin, v. 101, p. 221-230.

Gregg, J. M., and K. L. Shelton, 2012, Mississippi Valley-type mineralization and ore deposits in the Cambrian – Ordovician great American carbonate bank, *in* J. R. Derby, R. D. Fritz, S. A. Longacre, W. A. Morgan, and C. A. Sternbach, eds., The great American carbonate bank: The geology and economic resources of the Cambrian – Ordovician Sauk megasequence of Laurentia: AAPG Memoir 98, p. 163-186.

Gutschick, R. C., and C. A. Sandberg, 1983, Mississippian continental margins of the conterminous United States, *in* D. J. Stanley and G. T. Moore, eds., The shelfbreak: Critical interface on continental margins: SEPM Special Publication, 33, p. 79-96.

Hagni, R. D., 1976, Tri-State ore deposits: The character of their host rocks and their genesis, *in* K. H. Wolf, ed., Handbook of strata-bound and stratiform ore deposits: Amsterdam, Elsevier, p. 457-494.

Hagni, R. D., 1982, The influence of original host rock character upon alteration and mineralizalion in the Tri-State District of Missouri, Kansas, and Oklahoma U.S.A., *in* G. C. Amstutz, A. E. Goresy, G. Frenzel, C. Kluth, G. Moh, A. Wauchkuhn, and R. A. Zimmermann, eds., ore genesis: The state of the art: Berlin, Springer-Verlag, p. 99-107.

Hagni, R. D., and O. R. Grawe, 1964, Mineral paragenesis in the Tri-State district Missouri, Kansas, Oklahoma: Economic Geology, v. 59, p. 449-457.

Handford, C. R., 1989, Sequence stratigraphy of Mississippian oolitic limestones in northern Arkansas: AAPG Bulletin, v. 73, p. 1032-1033.

Harris, S. A., 1987, Hydrocarbon accumulation in "Meramec-Osage" (Mississippian) rocks, Sooner Trend, Northwest-Central Oklahoma *in* B. Rascoe, Jr., and N. J. Hyne, eds., Petroleum geology of the mid-continent: Tulsa Geological Society Special Publication 3, p. 74-81.

Huffman, G. G., 1958, Geology of the flanks of the Ozark uplift: Oklahoma Geological Survey Bulletin, v. 77, 281 p.

Jordan, L., and T. L. Rowland, 1959, Mississippian rocks in northern Oklahoma: Tulsa Geological Society Digest, v. 27, p. 124-136.

Kaufman, J., H. S. Cander, L. D. Daniels, and W. J. Meyers, 1988, Calcite cement stratigraphy and cementation history of the Burlington-Keokuk Formation (Mississippian), Illinois and Missouri: Journal of Sedimentary Petrology, v. 58, p. 312-326.

King, B. D., and R. H. Goldstein, 2016, History of hydrothermal fluid flow in the midcontinent, USA: the relationship between inverted thermal structure,

unconformities and porosity distribution: *in* Armitage, P. J., Butcher, A. R., Churchill, J. M., Csoma, A. E., Hollis, C., Lander, R. H., Omma, J. E. &Worden, R. H. (eds.) Reservoir Quality of Clastic and Carbonate Rocks: Analysis, Modelling and Prediction: Geological Society, London, Special Publications, 435 p., http://doi.org/10.1144/SP435.16.

Lane, H. R., 1978, The Burlington Shelf (Mississippian, north-central United States): Geologica et Palaeontologica, v. 12, p. 165-176.

Lane, H. R., and T. L. DeKyser, 1980, Paleogeography of the late Early Mississippian (Tournasian 3) in the central and southwestern United States, *in* T. D. Fouch, and E. R. Magathan, eds., Paleozoic paleogeography of west-central United States: Rocky Mountain Paleogeography Symposium 1, Rocky Mountain Section SEPM, p. 149-162.

Leach, D. L., R. C. Nelson, and D. Williams, 1975, Fluid inclusion studies in the Northern Arkansas zinc district: Economic Geology, v. 70, p. 1084-1091.

Leach, D. L., D. Bradley, M. T. Lewchuk, D. T. A. Symon, G. de Marsily, and J. Brannon, 2001, Mississippi Valley-type lead-zinc deposits through geological time: Implication from recent age-dating research: Mineralium Deposita, v. 36, p. 711-740.

Leach, D. L., 1994, Genesis of the Ozark Mississippi Valley-type metallogenic province, Missouri, Arkansas, Kansas, and Oklahoma, USA. in L. Fontboté and M. Boni, eds., Sediment-Hosted Zn–Pb Ores: Springer-Verlag, Berlin, p. 104-138.

LeBlanc, S. L., 2014, High resolution sequence stratigraphy and reservoir characterization of the "Mississippian limestone" in north-central Oklahoma: M.S. thesis, Oklahoma State University, 449 p.

Lowenstein, T. K., L. A. Hardie, M. N. Timofeeff, and R. V. Demicco, 2003, Secular variation in seawater chemistry and the origin of calcium chloride basinal brines: Geology, v. 31, p. 857-860.

Machel, H. G., H. R. Krouse, and R. Sassen, 1995, Products and distinguishing criteria of bacterial and thermochemical sulfate reduction: Applied Geochemistry, v. 10, p. 373-389.

Mazzullo, S. J., B. W. Wilhite, and I. W. Woolsey, 2009, Petroleum reservoirs within a spiculite-dominated depositional sequence: Cowley Formation (Mississippian: Lower Carboniferous), south-central Kansas: AAPG Bulletin, v. 93, p. 1649-1689.

Mazzullo, S. J., B. W. Wilhite, and D. R. Boardman, 2011, Lithostratigraphic architecture of the Mississippian Reeds Spring Formation (Middle Osagean) in southwest Missouri, northwest Arkansas, and northeast Oklahoma: Outcrop analog of subsurface petroleum reservoirs: Shale Shaker, v. 61, p. 254-269.

Mazzullo, S.J., D. R. Boardman, B. W. Wilhite, C. Godwin, and B. T. Morris, 2013, Revisions of outcrop lithostratigraphic nomenclature in the Lower to Middle Mississippian Subsystem (Kinderhookian to Basal Meramecian Series) along the shelf-edge in southwest Missouri, northwest Arkansas, and northeast Oklahoma: Shale Shaker, v. 63, p. 414-454.

McKnight, E. T., and R. P. Fischer, 1970, Geology and ore deposits of the Picher field, Oklahoma and Kansas: U.S. Geological Survey Professional Paper 588, 165 p.

Mii, H., E. L. Grossman, and T. E. Yancey, 1999, Carboniferous isotope stratigraphies of North America: Implications for Carboniferous paleoceanography and Mississippian glaciation: Geological Society of America Bulletin, v. 111, p. 960-973.

Milam, K., 2013, OSU-Industry consortium eyes Mississippian: AAPG Explorer, v. 34, no. 3, p. 36-39.

Morris, B. T., S. J. Mazzullo, B. W. Wilhite, 2013, Sedimentology, biota, and diagenesis of 'reefs' in Lower Mississippian (Kinderhookian To Basal Osagean: Lower Carboniferous) strata in the St. Joe Group in the western Ozark Area: Shale Shaker, v. 64, p. 194-227.

Newell, K. D., 1997, Comparison of maturation data and fluid inclusion homogenization temperatures to simple thermal model: Implications for thermal history and fluid flow in the Midcontinent: Current Research in Earth Sciences, Kansas Geological Survey Bulletin, v. 240, part 2, p. 13-27.

Northrop, D. A., and R. N. Clayton, 1966, Oxygen-isotope fractionations in systems containing dolomite: Journal of Geology, v. 74, p. 174-196.

O'Neil, J. R., R. N. Clayton, and T. K. Mayeda, 1969, Oxygen isotope fractionation in divalent metal carbonates: Journal of Chemical Physics, v. 51, p. 5547-5558.

Price, B. J., 2014, High resolution sequence stratigraphic architecture and reservoir characterization of the Mississippian Burlington/Keokuk Formation, northwestern Arkansas: M.S thesis, Oklahoma State University. 144 p.

Ragan, V. M., R. M. Coveney, and J. C. Brannon, 1996, Migration paths for fluids and northern limits of the Tri-State District from fluid inclusions and radiogenic isotopes: *in* D. F. Sangster, ed., Carbonate-hosted lead-zinc deposits: Society of Economic Geologists Special Publication 4, p. 419-431.

Ritter, M. E., and R. H. Goldstein, 2012, Diagenetic controls on porosity preservation in lowstand oolithic and crinoidal carbonates, Mississippian, Kansas and Missouri, USA: International Association of Sedimentologists (special publication) 45, p. 379-406.

Roedder, E., 1984, Fluid inclusions: Mineralogical Society of America, Reviews in Mineralogy, v. 12, 644 p.

Roedder, E., 1967, Metastable Superheated Ice in Liquid-Water Inclusions under High Negative Pressure: Science, v. 155, p. 1413-1417.

Rosenbaum, J., and S. M. F. Sheppard, 1986, An isotopic study of siderites, dolomites and ankerites at high temperatures: Geochimica et Cosmochimica Acta, v. 50, p. 1147-1150.

Rowan, E. L., and D. L. Leach, 1989, Constraints from fluid inclusions on sulfide precipitation mechanisms and ore fluid migration in the Viburnum Trend lead district, Missouri: Economic Geology, v. 84, p. 1948-1965.

Schmidt, R. A., 1962, Tempratures of mineral formation in the Miami-Picher District as indicated by liquid inclusions: Economic Geology, v. 57, p. 1-20.

Shelby, P. R., 1986, Depositional history of the St. Joe and Boone Formations in northern Arkansas: Proceedings Arkansas Academy of Science, v. 40, p. 67-71.

Shelton, K. L., and P.M. Orville, 1980, Formation of synthetic fluid inclusions in natural quartz: American Mineralogist, v. 65, p. 1233-1236.

Shelton, K. L., R. M. Bauer, and J. M. Gregg, 1992, Fluid-inclusion studies of regionally extensive epigenetic dolomites, Bonneterre Dolomite (Cambrian), southeast Missouri: Evidence of multiple fluids during dolomitization and lead-zinc mineralization: Geological Society of America Bulletin, v. 104, p. 675-683.

Shelton, K. L., J. M. Gregg, and A. W. Johnson, 2009, Replacement dolomites and ore sulfides as recorders of multiple fluids and fluid sources in the southeast Missouri Mississippi Valley-Type district: Halogen-$^{87}Sr/^{86}Sr$-$\delta^{18}O$-$\delta^{34}S$ systematics in the Bonneterre Dolomite: Economic Geology, v. 104, p. 733-748.

Shelton, K. L., J. M. Beasley, J. M. Gregg, M. S. Appold, S. F. Crowley, J. P. Hendry, and I.D. Somerville, 2011, Evolution of a Carboniferous carbonate-hosted sphalerite breccia deposit, Isle of Man: Mineralium Deposita, v. 46, p. 859-880.

Sibley, D. F., and J. M. Gregg, 1987, Classification of dolomite rock texture: Journal of Sedimentary Petrology, v. 57, p. 967-975.

Temple, B. J., 2016, Petrology and geochemistry of Lower Ordovician and Upper Cambrian (Arbuckle) carbonates, NE Oklahoma and SW Missouri: M.S. thesis, Oklahoma State University, 70 p.

Unrast, M. A., 2012, Composition of Mississippian carbonate mounds in the Ozark region, North America and Ireland: M.S. thesis, Oklahoma State University, 120 p.

Unrast, M. A., 2013, Composition of Mississippian carbonate mounds in the Ozark region, North America: Shale Shaker, v. 63, p. 254-273.

Wei, C. S., 1975, Fluid inclusion geothermometry of Tri-State sphalerite: M.S. thesis, University of Missouri-Rolla, 68 p.

Wenz, Z. J., M. S. Appold, K. L. Shelton, and S. Tesfaye, 2012, Geochemistry of Mississippi Valley-Type mineralizing fluids of the Ozark Plateau: A regional synthesis: American Journal of Science, v. 312, p. 22-80.

Wilhite, B. W., S. J. Mazzullo, B. T. Morris, and D. R. Boardman, 2011, Syndepositional tectonism and its effects on Mississippian (Kinderhookian to Osagean) lithostratigraphic Architecture: Part 1-Based on exposures in the Midcontinent USA, AAPG Search and Discovery Article #30207, 43 p.

Young, E. M., 2010, Controls on reservoir character in carbonate-chert strata, Mississippian (Osagean-Meramecian), southeast Kansas: M.S. thesis, University of Kansas. 198 p.

Table 1. Fluid inclusion microthermometric data for carbonate and authigenic quartz cements.

Sample ID	Location	Assemblage	Mineral	T_h (°C)	T_m (°C)	Calculated salinity (wt.% eq. NaCl)
SMD 2100	Osage Co., OK (#1)	Assemblage 1	Calcite	97	-0.7	1.2
		Assemblage 2	Calcite	112	-0.5	0.8
			Calcite	118	-0.5	0.8
			Calcite	118	-0.5	0.8
		Assemblage 3	Calcite	81	-0.1	0.2
			Calcite	105	-0.1	0.2
			Calcite	84	-1.5	2.6
			Calcite		-0.5	0.9
		Assemblage 4	Calcite	87	2.5	
			Calcite	80	2.5	
			Calcite		0.3	
			Calcite	105		
		Assemblage 5	Calcite	81	3.0	
		Assemblage 6	Calcite	116	0.7	
SMD 2102	Osage Co., OK (#2)	Assemblage 1	Calcite	126	-3.7	6.0
			Calcite	126	-1.8	3.0
			Calcite	125	-3.8	6.1
		Assemblage 2	Calcite	164	-1.9	3.2
			Calcite	149	-1.9	3.2
		Assemblage 3	Calcite	115	-21.0	22.8
			Calcite	118	-19.0	21.7
			Calcite		-19.0	21.7
			Calcite		-15.4	19.0
			Calcite	127		
		Assemblage 4	Calcite	173	-17.5	20.6
			Calcite	168	-15.4	19.0
		Assemblage 5	Calcite	86	-23.0	24.3
		Assemblage 6	Calcite	122	-23.0	24.3

			Calcite	126	-21.2	23.1
		Assemblage 7	Calcite	135	-2.1	3.5
		Assemblage 8	Quartz	126	-21.6	23.4
			Quartz	130	-21.6	23.4
			Quartz	101	-21.6	23.4
			Quartz	130	-21.6	23.4
		Assemblage 9	Quartz	83	-19.6	22.1
			Quartz	87	-19.6	22.1
			Quartz	98	-22.3	23.9
			Quartz	98	-18.6	21.4
			Quartz	98	-17.8	20.8
			Quartz	98	-18.5	21.3
		Assemblage 10	Quartz	122	-2.0	3.4
			Quartz	123	-2.9	4.8
			Quartz	119	-1.4	2.4
			Quartz	113	-1.4	2.4
		Assemblage 11	Quartz	102	-2.3	3.9
			Quartz	102	-2.0	3.4
			Quartz	108	-2.3	3.9
			Quartz	108	-0.4	0.7
SMD 1002	Benton Co., AR	Assemblage 1	Calcite	120	-11.2	15.2
		Assemblage 2	Calcite	132	-19.0	21.7
			Calcite	135	-22.6	24.0
			Calcite		-22.6	24.0
		Assemblage 3	Calcite	125	-20.7	22.8
			Calcite	125	-19.5	22.0
			Calcite	135	-21.0	23.0
			Calcite	139	-21.4	23.3
			Calcite	116	-21.4	23.3
		Assemblage 4	Calcite	149	-2.4	4.0
			Calcite	138	-2.9	4.8
			Calcite	147	-2.9	4.8

		Assemblage 5	Calcite	120	-5.0	7.8
		Assemblage 6	Calcite	101	-19.6	22.1
SMD-P1	Mayes Co., OK (#1)	Assemblage 1	Calcite	200	-18.5	21.3
		Assemblage 2	Calcite	88	-0.4	0.7
		Assemblage 3	Calcite		-19.6	22.1
		Assemblage 4	Calcite		-1.7	2.9
		Assemblage 5	Calcite		1.5	
SMD-P3	Mayes Co., OK (#2)	Assemblage 1	Calcite	112	-8.9	12.7
			Calcite	114	-3.5	5.7
		Assemblage 2	Calcite	104	-3.6	5.8
			Calcite	104	-3.1	5.1
			Calcite	105	-3.1	5.1
			Calcite	105	-4.2	6.7
			Calcite	105	-4.2	6.7
			Calcite	105	-4.2	6.7
		Assemblage 3	Calcite	130	-7.6	11.2
			Calcite	119	-6.6	9.9
			Calcite	128	-7.2	10.7
			Calcite	133		
		Assemblage 4	Calcite	67	0.7	
			Calcite	67	0.7	
			Calcite	67	0.7	
			Calcite	53	0.7	
		Assemblage 5	Calcite	97	-2.0	3.4
			Calcite	74	-3.3	5.4
		Assemblage 6	Calcite	67	-4.5	7.2
			Calcite	88	-1.7	2.9
		Assemblage 7	Calcite	43	-0.7	1.2
			Calcite	74	-0.2	0.3
			Calcite	74	-0.2	0.3
			Calcite	55	-0.2	0.3
		Assemblage 8	Calcite	145	-2.5	4.1

		Assemblage 9	Calcite	80	1.0	
			Calcite	70	1.0	
			Calcite	70	1.0	
			Calcite	70	1.0	
			Calcite	70	1.0	
			Calcite	72	1.0	
			Calcite	97	1.0	
SMD-P5	Mayes Co., OK (#3)	Assemblage 1	Dolomite	62	-8.2	11.9
			Dolomite	75	-13.0	16.9
			Dolomite	65	-13.0	16.9
TSNC1-14	Tri-State, Neck City, MO	Assemblage 1	Calcite	76	-5.5	8.5
			Calcite	84	-4.4	7.0
		Assemblage 2	Calcite	90	-3.3	5.4
		Assemblage 3	Calcite	54	4.2	
			Calcite	54	4.2	
			Calcite	54	4.2	
			Calcite	54	4.2	
			Calcite	54	4.2	
			Calcite	54	4.2	
			Calcite	54	4.2	
			Calcite	54	4.2	
			Calcite	54	4.2	
			Calcite	54	4.2	
			Calcite	54	4.2	
			Calcite	54	4.2	
			Calcite	54	4.2	
			Calcite	54	4.2	
			Calcite	54	4.2	
			Calcite	54	4.2	
			Calcite	54	4.2	
			Calcite	54	4.2	
			Calcite	54	4.2	

			Calcite	54	4.2	
		Assemblage 4	Calcite	59	4.0	
			Calcite	61	4.0	
			Calcite	65		
		Assemblage 5	Calcite	74		
			Calcite	74	0.7	
		Assemblage 6	Calcite	86	0.0	0.0
			Calcite	94	0.0	0.0
			Calcite	90	0.0	0.0
			Calcite	90		
			Calcite	56		
			Calcite	86		
			Calcite	98	0.6	
TSOG2	Tri-State, Old Goat Mine, Treece, KS	Assemblage 1	Calcite	89		
JC5	McDonald Co. MO	Assemblage 1	Calcite	129	1.7	
			Calcite		2.2	
			Calcite		2.2	
			Calcite	140	0.7	
			Calcite		2.2	
		Assemblage 2	Calcite	129	-1.5	2.6
		Assemblage 3	Calcite	158		
		Assemblage 4	Calcite		0.0	0.0
		Assemblage 5	Calcite	112	-21.8	23.6
			Calcite	95	-21.8	23.6
			Calcite	86	-21.8	23.6
			Calcite	112	-21.8	23.6
			Calcite		-21.8	23.6
		Assemblage 6	Calcite	114		
			Calcite	114		
			Calcite	114		
			Calcite	114		
			Calcite	114		

TSA-1	Tri-State, Admiralty Mine (#1)	Assemblage 1	Dolomite	142	-24.3	25.1
		Assemblage 2	Dolomite	103	-15.5	19.0
		Assemblage 3	Dolomite	130	-23.2	24.5
			Dolomite	135	-23.7	24.8
			Dolomite	128	-22.7	24.1
			Dolomite	130	-21.8	23.6
			Dolomite	135	-23.6	24.7
		Assemblage 4	Dolomite	127	-24.0	25.0
			Dolomite	83	-16.5	19.8
			Dolomite		-23.5	24.6
			Dolomite		-18.5	21.3
			Dolomite		-20.3	22.6
TSA-4	Tri-State, Admiralty Mine (#2)	Assemblage 1	Dolomite	111		
			Dolomite	111		
		Assemblage 2	Sphalerite	107		
TSAB1	Tri-State, Anna Beaver Mine, OK	Assemblage 1	Dolomite	102	-24.4	25.2
			Dolomite	116	-20.3	22.6
		Assemblage 2	Dolomite	112	-24.2	25.0
			Dolomite	112	-22.0	23.7
			Dolomite	112	-17.9	20.9
			Dolomite	102	-21.4	23.3
			Dolomite		-23.6	24.7
		Assemblage 3	Dolomite	112	-2.4	4.0
			Dolomite	112	-2.4	4.0
			Dolomite		-3.5	5.7
		Assemblage 4	Dolomite	110	-21.2	23.2
			Dolomite	107	-20	22.4
			Dolomite		-25.2	25.7
			Dolomite		-22.9	24.3
			Dolomite		-22.9	24.3
			Dolomite		-20	22.4
TSPF1	Tri-State, Ottawa Co., OK	Assemblage 1	Calcite	198	-21.7	23.5

		Assemblage 2	Calcite		-6.8	10.2
TSW-1	Tri-State, Wood Chuck Mine, OK	Assemblage 1	Sphalerite	170		
			Sphalerite	178		
TSWB-3-3B	Tri-State, Treece, KS	Assemblage 1	Dolomite	112	-23.3	24.5
			Dolomite		-16.0	19.5
		Assemblage 2	Dolomite	151		
H2-13-663	Wagoner Co., OK (#1)	Assemblage 1	Calcite	109	-18.0	21.0
			Calcite	113	-16.1	19.5
		Assemblage 2	Calcite	114		
			Calcite	117		
			Calcite	101		
			Calcite	101		
			Calcite	112		
		Assemblage 3	Calcite	115		
			Calcite	115		
			Calcite	115		
		Assemblage 4	Calcite	87	0.9	
			Calcite	86		
			Calcite	98	-6.6	10.0
		Assemblage 5	Calcite	85	-7.8	11.5
			Calcite	74	-1.8	3.0
			Calcite	74	-1.8	3.0
		Assemblage 6	Calcite	62	14.1	
			Calcite	62	14.1	
		Assemblage 7	Calcite	151		
		Assemblage 8	Calcite	83		
			Calcite	91		
			Calcite	85		
			Calcite	99		
			Calcite	99		
		Assemblage 9	Calcite	110	-2.3	3.9
			Calcite	110	-2.3	3.9

			Calcite	110	-2.3	3.9
H2-13-675	Wagoner Co., OK (#2)	Assemblage 1	Calcite	99		
			Calcite	103	-15.3	18.9
		Assemblage 2	Calcite	71	1.6	
		Assemblage 3	Calcite	61		
			Calcite	66	-0.1	0.2
			Calcite	66	-0.1	0.2
		Assemblage 4	Quartz	116	-13.1	17.0
			Quartz	92	-11.4	15.4
		Assemblage 5	Quartz	89	-1.4	2.4
			Quartz	89	-1.4	2.4
			Quartz	89	-1.4	2.4
			Quartz	89	-1.4	2.4
			Quartz	89	-1.4	2.4
			Quartz	94	-1.4	2.4
		Assemblage 6	Quartz	153	-3.4	5.6
			Quartz	153	-3.4	5.6
			Quartz	153	-3.4	5.6
			Quartz	153	-3.4	5.6
			Quartz	153	-3.4	5.6
		Assemblage 7	Quartz	172	-3.4	5.6

Table 2. Stable isotope analyses of carbonate cements and host rocks. Clay sized calcite referred to "calcite mud".

Sample	Locality	Mineralogy	$\delta^{13}C‰$ (VPDB)	$\delta^{18}O‰$ (VPDB)	$\delta^{18}O‰$ (VSMOW)
TSAB1	Tri-State-Anna Beaver Mine, OK	Calcite Cement	-4.75	-10.98	19.60
TSAB1	Tri-State-Anna Beaver Mine, OK	Dolomite-Nonplanar	-1.58	-6.68	24.04
TSAB1	Tri-State-Anna Beaver Mine, OK	Dolomite Cement	-1.68	-6.40	24.33
TSAB1	Tri-State-Anna Beaver Mine, OK	Dolomite-Nonplanar	-0.98	-5.61	25.13
TSW-1	Tri-State-Wood Chuck Mine, OK	Dolomite-Nonplanar	-1.55	-7.17	23.53
TSW-2	Tri-State-Wood Chuck Mine, OK	Dolomite-Nonplanar	-2.06	-6.88	23.83
TSA-1	Tri-State, Admiralty Mine, OK	Dolomite-Nonplanar	-1.55	-7.03	23.67
TSA-2	Tri-State, Admiralty Mine, OK	Dolomite-Nonplanar	-1.68	-7.61	23.07
TSA-3	Tri-State, Admiralty Mine, OK	Dolomite Cement	-1.53	-7.72	22.96
TSA-4	Tri-State, Admiralty Mine, OK	Dolomite Cement	-1.48	-7.35	23.35
TSP-1	Tri-State- Premier Mine, OK	Dolomite Cement	-1.34	-6.16	24.57
TSP-2	Tri-State- Premier Mine, OK	Dolomite Cement	-1.86	-7.17	23.52
TSOG-1	Tri-State, Old Goat Mine, Treece, KS	Calcite Cement	-4.35	-10.29	20.31
TSOG-2	Tri-State, Old Goat Mine, Treece, KS	Calcite Cement	-4.53	-10.71	19.88
SMD1002	Benton Co., AR	Calcite Cement	1.76	-8.45	22.21
SMD1008	McDonald Co., MO	Calcite Cement	2.84	-3.11	27.72
SMD2100	Osage Co., Ok	Calcite Cement	2.58	-4.04	26.76
SMD2102	Osage Co., Ok	Calcite Cement	-2.58	-6.21	24.52
SMD2103	Osage Co., Ok	Calcite Cement	0.90	-7.06	23.64
SMD3001	White Rock Co., MO	Calcite Cement	2.78	-8.86	21.78
PM21-608	Cherokee Co., KS	Dolomite Cement	-2.00	-2.66	28.18
PM21-608	Cherokee Co., KS	Dolomite-Planar	-0.42	-3.80	27.00
PM21-600	Cherokee Co., KS	Saddle Dolomite	-1.19	-6.28	24.44
PM21-614	Cherokee Co., KS	Replacement Dolomite	2.02	-5.83	24.91

PM21-618	Cherokee Co., KS	Replacement Dolomite	2.30	-4.46	26.32
A04-1220	Jasper Co., MO	Calcite Cement	1.82	-4.40	26.38
B50-1-85.5	Jasper Co., MO	Calcite Cement	0.79	-9.93	20.68
J5.5	McDonald Co., MO	Calcite Crinoid	2.26	-1.26	29.62
JC2	McDonald Co., MO	Calcite Cement	3.18	-3.84	26.96
JC2	McDonald Co., MO	Calcite Mud	2.66	-4.04	26.75
JC4	McDonald Co., MO	Calcite Cement	2.90	-5.06	25.70
JC4	McDonald Co., MO	Calcite Mud	2.52	-4.06	26.73
JC5	McDonald Co., MO	Calcite Cement	1.94	-8.30	22.36
JC5	McDonald Co., MO	Calcite Mud	3.01	-3.86	26.94
JN2	McDonald Co., MO	Calcite Crinoid	3.56	-2.40	28.45
JS5	McDonald Co., MO	Calcite Crinoid	2.87	-2.11	28.74
SW1	Stone Co., MO	Calcite Crinoid	3.18	-2.29	28.56
SWCU2	Stone Co., MO	Calcite Cement	3.69	-6.64	24.08
SWCU2	Stone Co., MO	Calcite Cement	4.57	-1.90	28.96
SWCU4	Stone Co., MO	Calcite Cement	3.57	-7.24	23.46
SWCU4	Stone Co., MO	Calcite Mud	4.29	-1.91	28.96
SEP2	Delaware Co., OK	Calcite Crinoid	3.39	-1.90	28.96
SEP2	Delaware Co., OK	Calcite Cement	2.65	-2.98	27.85
PAEF2	Benton Co., AR	Calcite Crinoid	3.69	-2.49	28.36
PAEC5	Benton Co., AR	Calcite Cement	1.62	-9.21	21.43
PAEC5	Benton Co., AR	Calcite Crinoid	3.97	-1.68	29.19
PAWCBA2	Benton Co., AR	Calcite Mud	1.90	-5.57	25.18
PAWC2	Benton Co., AR	Calcite Cement	2.44	-4.66	26.11
PAWC4	Benton Co., AR	Calcite Crinoid	3.51	-2.43	28.41
PAWC1	Benton Co., AR	Calcite Mud	3.30	-1.43	29.44
PAWF1	Benton Co., AR	Calcite Crinoid	3.29	-1.84	29.02
PAEC4	Benton Co., AR	Calcite Cement	1.92	-7.28	23.42
PAEC4	Benton Co., AR	Calcite Crinoid	3.10	-3.35	27.47
H2-13-663A	Wagoner Co., OK	Calcite Cement	2.03	-9.24	21.39
H2-13-663B	Wagoner Co., OK	Calcite Cement	1.35	-9.89	20.73
H2-13-675B	Wagoner Co., OK	Calcite Cement	1.86	-9.29	21.34

H2-13-675A	Wagoner Co., OK	Calcite Cement	1.82	-9.25	21.39
H2-13-678	Wagoner Co., OK	Calcite Cement	1.86	-9.39	21.24
SMD-P1	Mayes Co., OK	Calcite Cement	-12.12	-10.83	19.75
SMD-P2	Mayes Co., OK	Calcite Cement	-11.12	-11.03	19.54
SMD-P3	Mayes Co., OK	Calcite Cement	-11.84	-11.42	19.15
SMD-P4	Mayes Co., OK	Calcite Cement	-12.10	-11.35	19.22
SMD-P5-B	Mayes Co., OK	Calcite Cement	-4.33	-11.57	18.99
SMD-P5-A	Mayes Co., OK	Dolomite Cement	-3.98	-9.50	21.12
TSNC1-14	Neck City, MO	Calcite Cement	-3.50	-11.04	19.54
TSWB2-3-B	Tri-State, Treece, KS	Dolomite Cement	-1.93	-8.83	21.82
TSWB2-3-A	Tri-State, Treece, KS	Dolomite Cement	-1.38	-7.73	22.95
TSWB2-3A-B	Tri-State, Treece, KS	Dolomite Cement	-1.24	-8.09	22.58
TSWB2-3A-A	Tri-State, Treece, KS	Dolomite Cement	-1.51	-8.82	21.82

Table 3. Sr isotope and oxygen data (‰) for carbonate components in the study area (see Figure 14).

Sample	**Location**	**lithology**	**$^{87}Sr/^{86}Sr$**	**$\delta^{18}O$ (VPDB)**
TSAB-1-A	Anna Beaver Mine, OK	Breccia Filling Calcite Cement	0.7098	-10.98
TSAB-1-B	Anna Beaver Mine, OK	Breccia Filling Dolomite Cement	0.7091	-6.68
SMD2102	Osage Co., OK	Fracture Filling Calcite Cement	0.7112	-6.21
TSNC-1-14	Neck City, MO	Breccia Filling Calcite Cement	0.7099	-11.04
SMD-P5	Mayes Co., OK	Breccia Filling Dolomite Cement	0.7092	-9.50
SMD-P1	Mayes Co., OK	Fracture Filling Calcite Cement	0.7097	-10.83
TSA-1	Admiralty Mine, OK	Breccia Filling Dolomite Cement	0.7093	-7.03
H2-663	Wagoner Co., OK	Fracture Filling Calcite Cement	0.7092	-9.89
JC5	McDonald Co., MO	Fracture Filling Calcite Cement	0.7100	-8.30
SEP2-A	Delaware Co., OK	Calcite Crinoid Skeletal Grain	0.7082	-1.90
SEP2-B	Delaware Co., OK	Intergrain Calcite Cement	0.7085	-2.98

Table 4. Correlation of cathodoluminescence zones in calcite cements among studies of Mississippian rocks on the mid-continent.

This study	Ritter and Goldstein (2012)	Kaufman et al. (1988)
1	NL1-NL5	II
2	ML6-ML7	III
3	NL7	IV
4	SL8-NL8	V
5	SL9	VI

Table 5. T_h values of fluid inclusions, $\delta^{18}O$ values of carbonate cements and calculated $\delta^{18}O$ values of waters in equilibrium with these cements and their host rocks at the temperatures shown. The equation used for calcite cements is O'Neil, et al. (1969) and that for dolomite cements is Northrop and Clayton (1966). The mean $\delta^{18}O$ values (VSMOW) for the host limestone in the study area is 28.2‰.

Sample	**Location and Host Cement**	**T_h °C**	**$\delta^{18}O_{calcite}$‰ VSMOW**	**$\delta^{18}O_{dolomite}$‰ VSMOW**	**$\delta^{18}O_{cement\text{-}depositing\ water}$‰ VSMOW**
JC5	McDonald Co., MO, Calcite	87 to 140	22.4	-	3.9 to 8.9
SMD2100	Osage Co., OK #1, Calcite	80 to 120	26.8	-	7.3 to 11.8
SMD2102	Osage Co., OK #2, Calcite	115, 135, 149, 173	24.5	-	9.0, 11.0, 11.9, 13.5
TSNC1-14	Neck City, MO, Calcite	54 to 98	19.5	-	-3.2 to 2.3
H2-13-663	Wagoner Co., OK #1, Calcite	84 to 118	21.4	-	2.4 to 5.9
H2-13-675	Wagoner Co., OK #2, Calcite	61 to 71	21.4	-	-0.6 to 0.9
SMD1002	Benton Co., AR, Calcite	116 to 150	22.2	-	6.7 to 9.6
SMD-P1	Mayes Co., OK #1, Calcite	88	19.8	-	1.3
SMD-P3	Mayes Co., OK #2, Calcite	44, 89, 97, 145	19.1	-	-5.5, 0.6, 1.6, 6.1
SMD-P5	Mayes Co., OK #3, Dolomite	63 to 75	-	21.1	-4.9 to -2.9
TSWB2-3	Tri-State, Trecee, KS, Dolomite	113	-	22.6	2.6
TSAB1	Anna Beaver Mine, OK, Dolomite	103 to 116	-	24.3	3.3 to 4.8
TSA-1	Admiralty Mine, OK, Dolomite	111, 128, 142	-	23.7	5.7 to 6.9

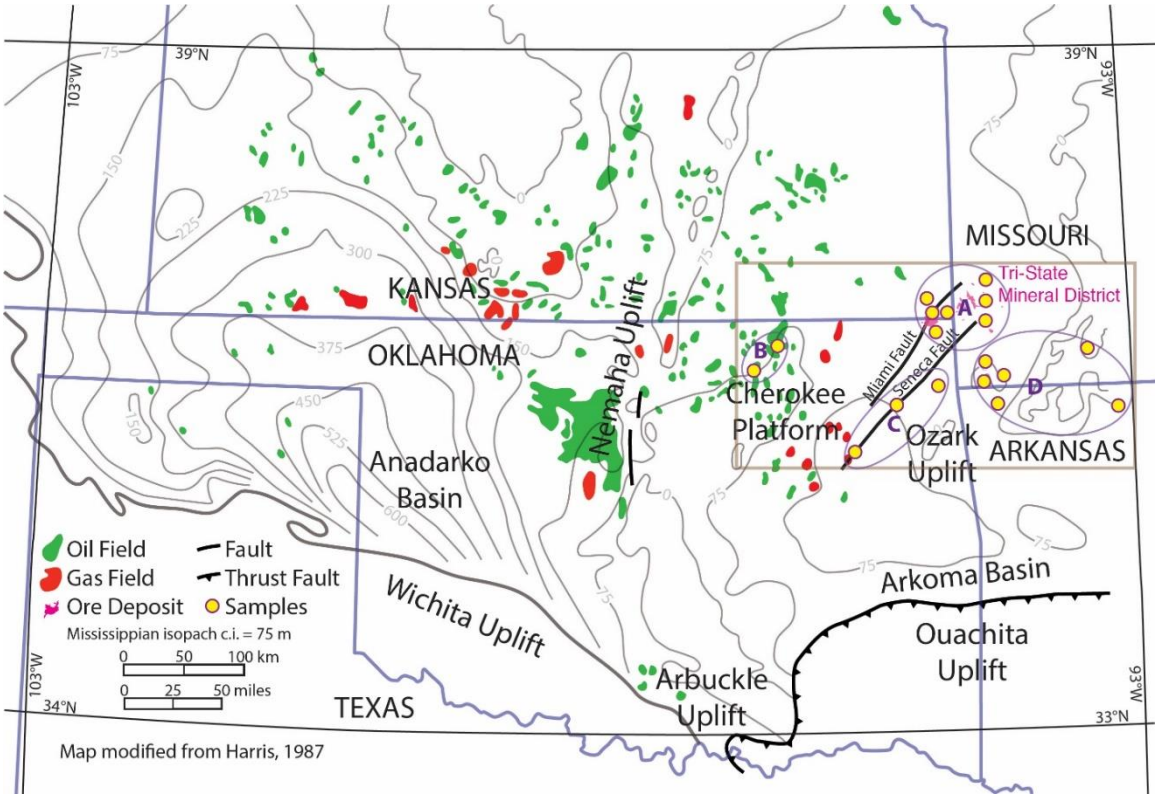

Figure 1. Map of Oklahoma and neighboring states showing the study area (tan rectangle in the east-central portion of the map) and sample localities. Four sampling regions within the study area are shown: 'A' cores in Osage Co. Oklahoma, 'B' surface samples and core in and near the Tri-State MVT mineral district, 'C' core and outcrops on and near the Seneca Trough in Delaware, Wagoner and Mayes counties, northeast Oklahoma, and 'D' core and outcrops in McDonald and Stone counties, southwest Missouri and Benton and Boone counties, northwest Arkansas. Petroleum producing areas and thickness of the Mississippian strata also are shown. Modified from Harris (1987).

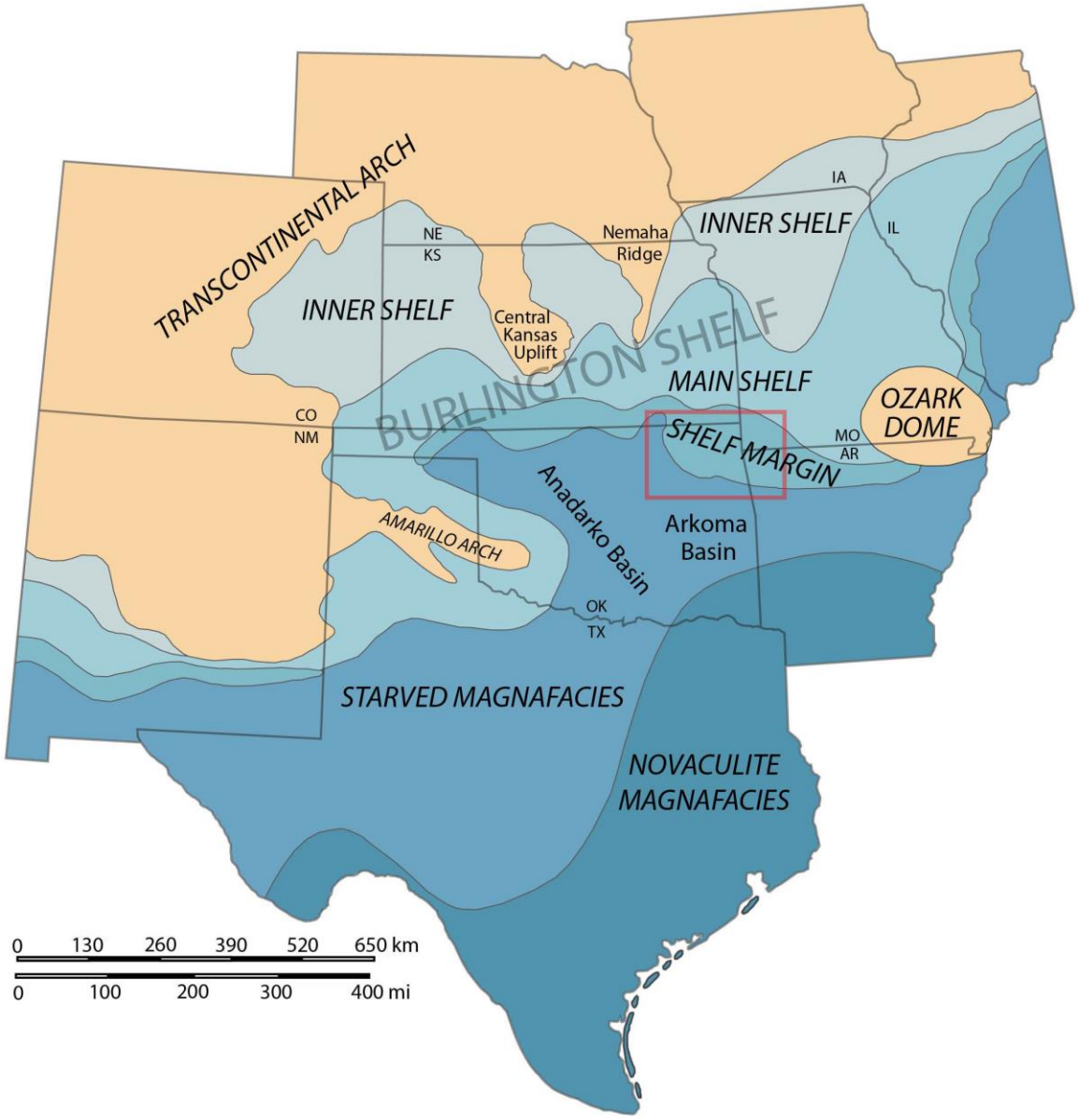

Figure 2. Regional map showing Burlington Shelf depositional systems during early Mississippian time. The study area is outlined by a red rectangle. Modified from Lane and DeKyser (1980).

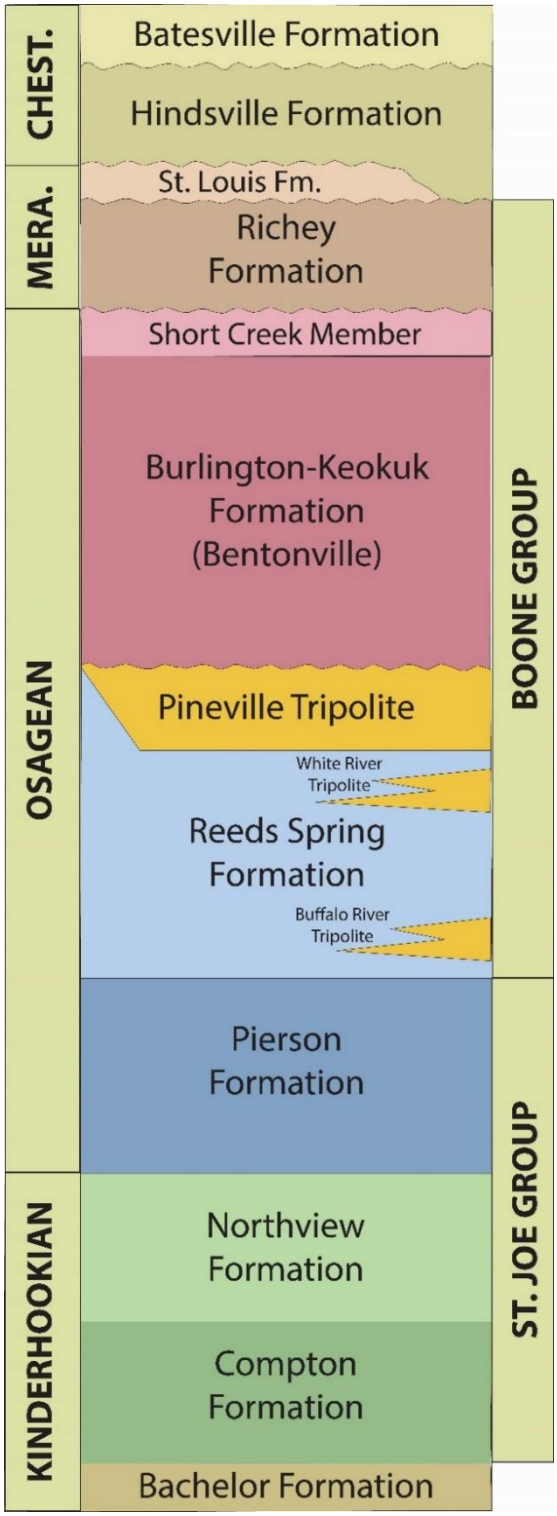

Figure 3. Stratigraphic section for the study area, modified from Mazzullo et al. (2013). MERA = Meramecian; CHEST = Chesterian.

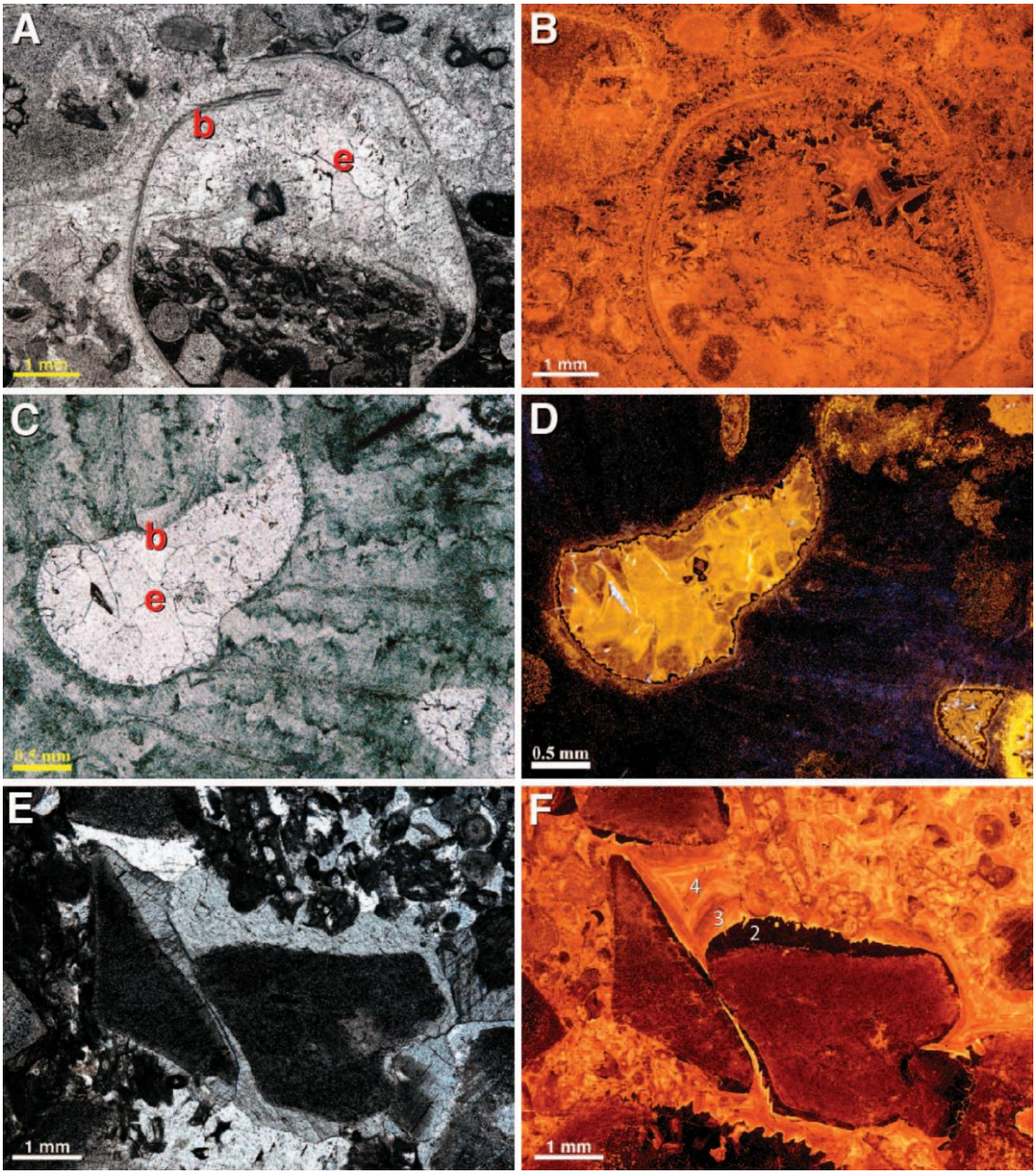

Figure 4. A) Skeletal grainstone from the Pierson Formation, Benton Co. AR. Bladed calcite cement (b) growing on brachiopod shells and equant (blocky) calcite cement (e) filling remaining porosity. Crossed polarized light (XPL). B) Cathodoluminescence (CL) photomicrograph of the same field as (A). Note the apparent compositional zoning of the equant calcite cement. C) Rugose coral, Osage Co., OK, with intragrain porosity filled by bladed and equant calcite cements. Plane polarized light (PPL). D) CL photomicrograph of the same field as (C) showing compositional zoning in the bladed and equant calcite cements. E) Crinoid grainstone from the Pierson Formation, Delaware Co., OK. Porosity is largely filled by syntaxial and equant calcite cement. XPL. F) CL photomicrograph of the same field as (E). Initial syntaxial cement (dark zone 2) extending into banded zones 3 and 4 cement.

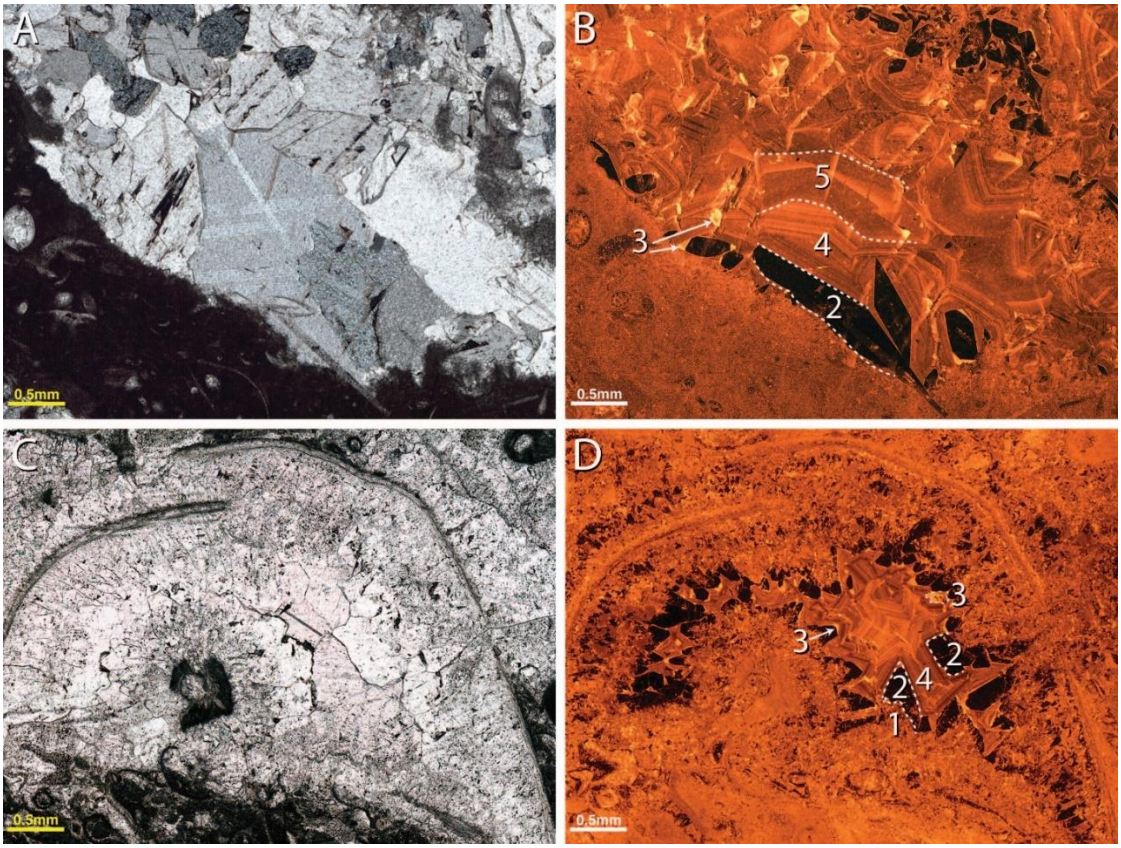

Figure 5. A) Packstone to grainstone with intergrain porosity filled by calcite, McDonald Co., MO. PPL. B) CL photomicrograph of the same field as (A) showing four compositional zones (2, 3, 4, and 5) in the equant calcite cement. C) Grainstone with intragrain porosity filled by calcite, Benton Co., AR. Close-up of field shown in Figure 4A, PPL. D) CL photomicrograph of the same field as (C) showing compositional zoning of the equant calcite cement (zones 1, 2, 3, and 4).

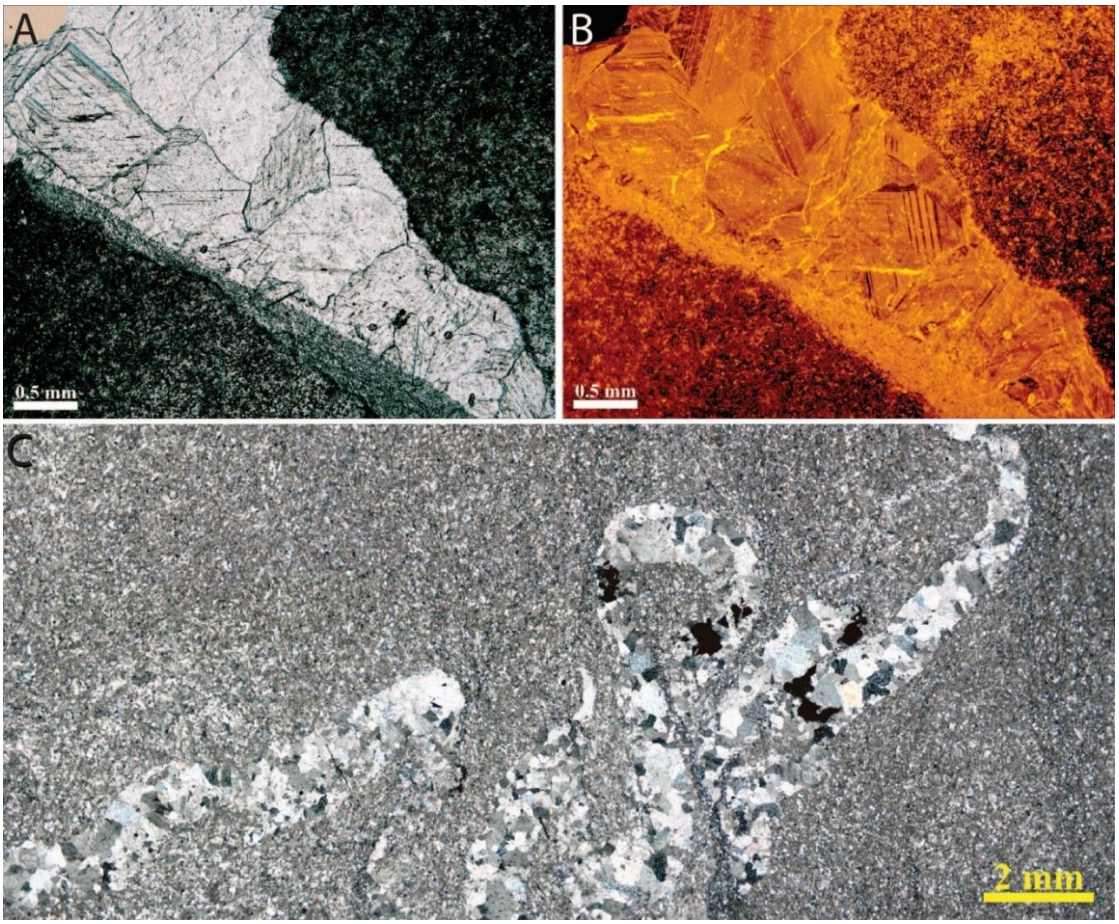

Figure 6. A) Cherty mudstone in the Reeds Spring Formation, Benton Co., AR. Solution-widened fracture (channel) porosity is filled by equant calcite cement. PPL. B) CL photomicrograph of the same field as (A) showing compositional zoning in the equant calcite cement. C) Cherty mudstone, Osage Co. OK, with a ptygmatic fracture filled by equant calcite cement. XPL, composite of nine photomicrographs.

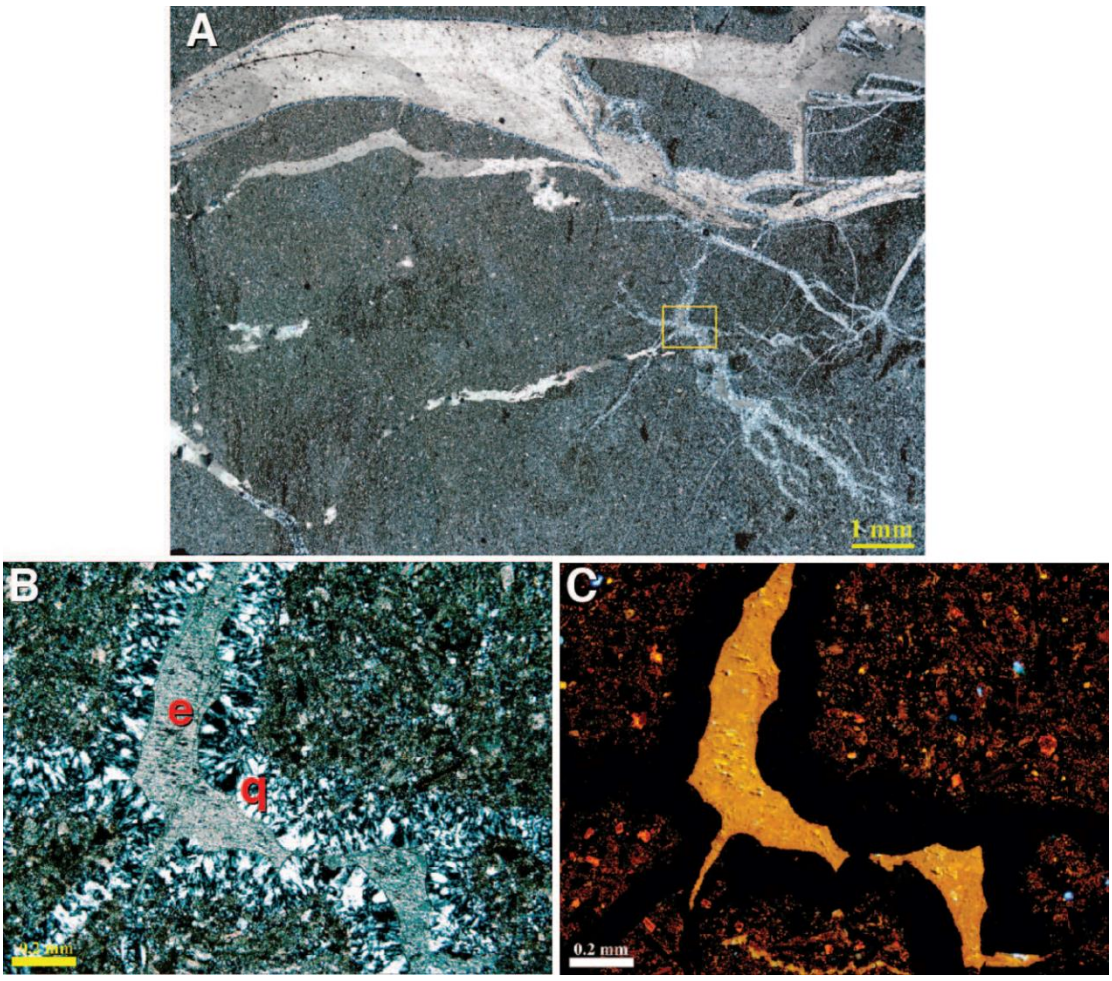

Figure 7. A) Solution-widened fracture (channel) porosity and unmodified breccia porosity, Osage Co., OK are filled by quartz and equant calcite cement. XPL, composite of sixteen photomicrographs. The close-up field is shown by the yellow rectangle. B) Close-up of a solution-widened fracture, shown in (A), filled by quartz (q) and equant calcite (e) cement. XPL. C) CL photomicrograph of the same field as (B). Quartz cement is non-cathodoluminescent and no compositional zoning is apparent in the calcite cement.

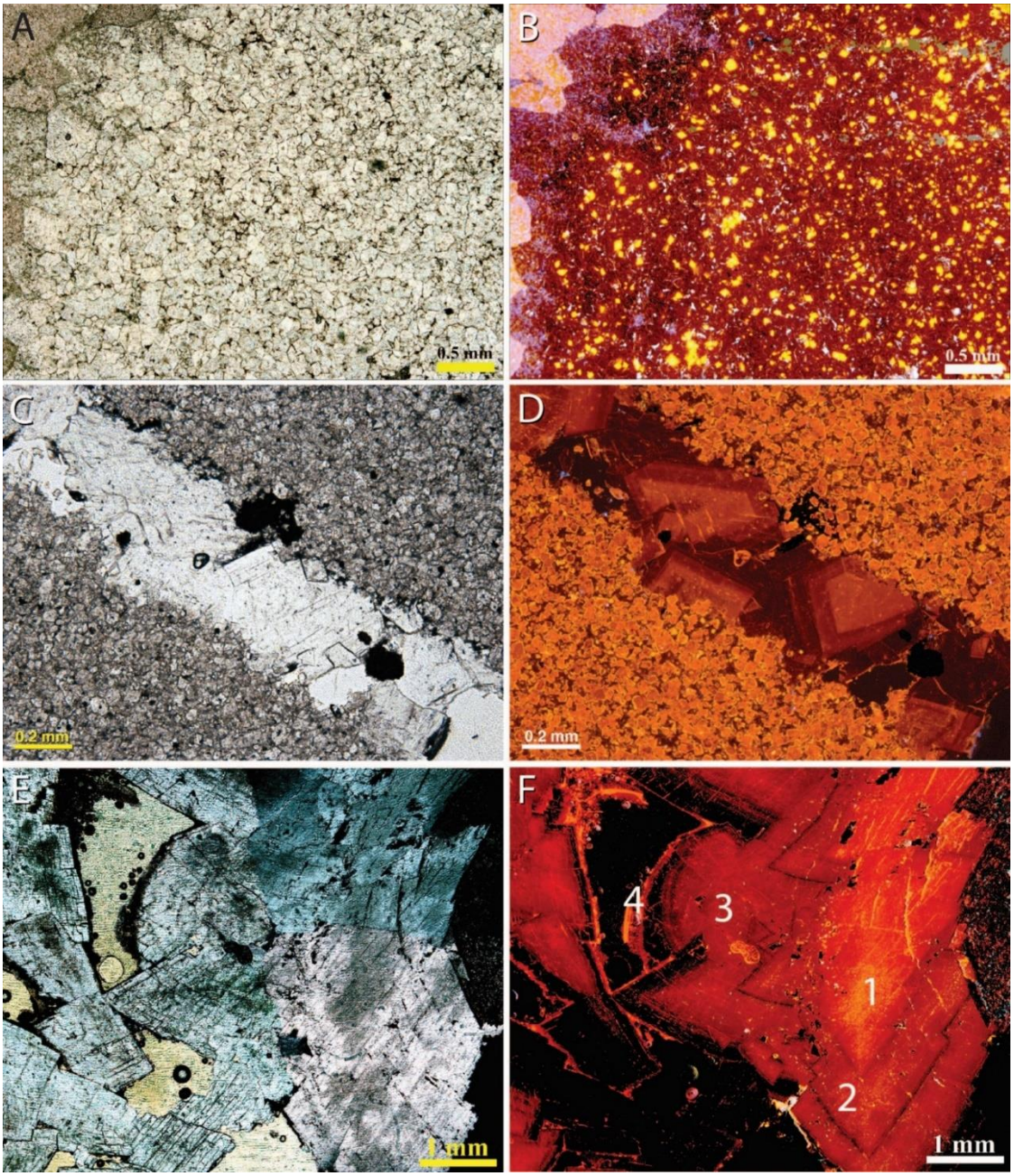

Figure 8. A) Replacement dolomite, Mayes Co., OK. PPL. B) CL photomicrograph of the same field as (A). C) Dolomitized mudstone with a solution-widened fracture filled by saddle dolomite, Cherokee Co., KS. PPL. D) CL photomicrograph of the same field as (C) showing compositional zoning in the dolomite cement. E) Saddle dolomite cement, Tri-State MVT district, Picher-field, Admiralty Mine (#3 Shaft) OK. XPL, composite of four photomicrographs. F) CL photomicrograph of the same field as (E) showing compositional zoning in the dolomite cement.

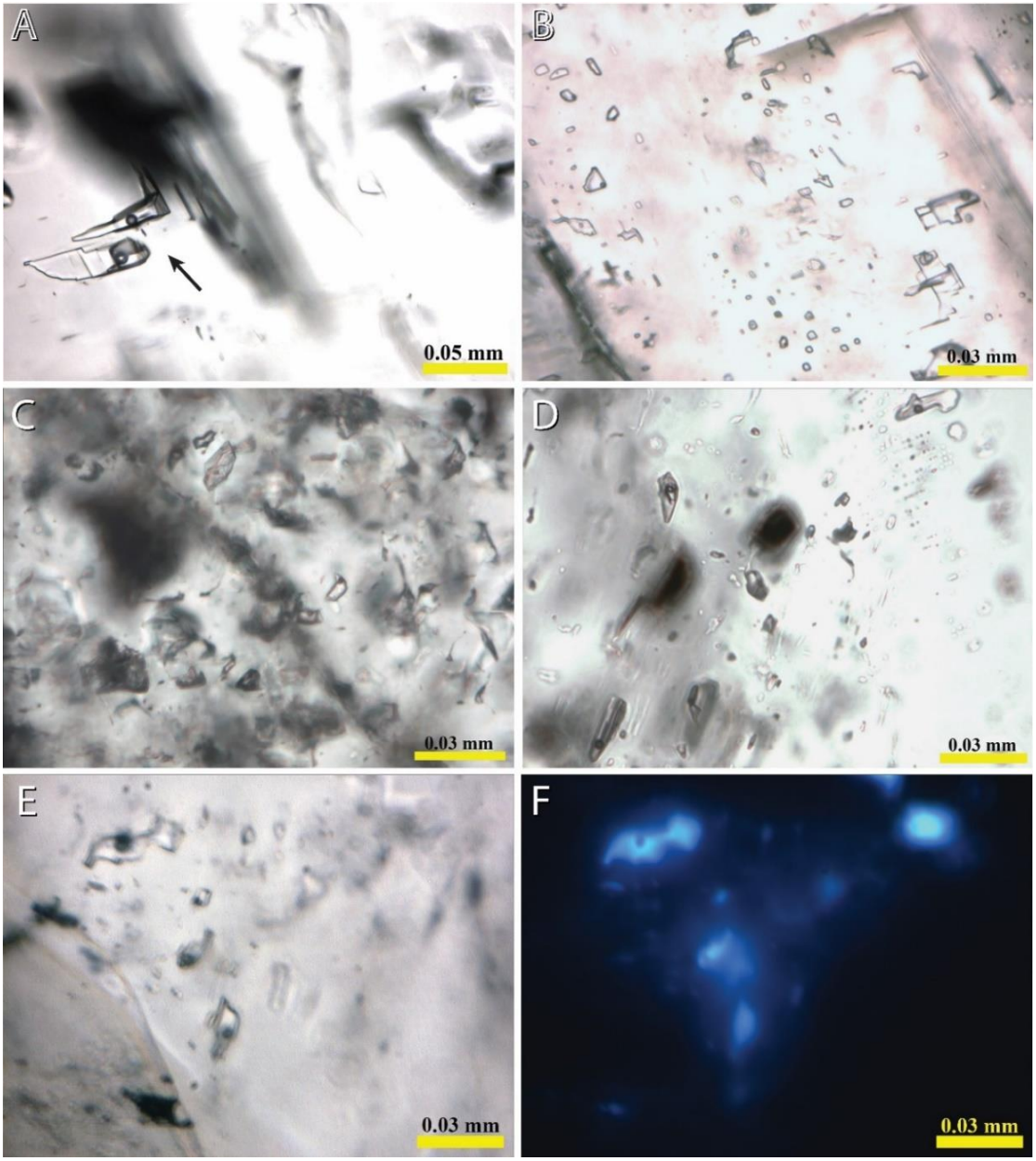

Figure 9. Photomicrographs of fluid inclusions in cements. A) Assemblage of primary two-phase inclusions in open-space-filling calcite cement, Tri-State mineral district, Neck City, MO. B) Secondary inclusions in fracture-filling calcite cement, Mayes Co., OK. C) Primary inclusions in fracture-filling saddle dolomite cement, Mayes Co., OK. D) Primary inclusions in solution-widened fracture-filling quartz cement, Osage Co., OK. E) Assemblage of primary petroleum-bearing inclusions in fracture-filling calcite cement, Wagoner Co., OK. F) Ultraviolet photomicrograph from the same field as (E) showing light-blue fluorescence of petroleum-bearing inclusions.

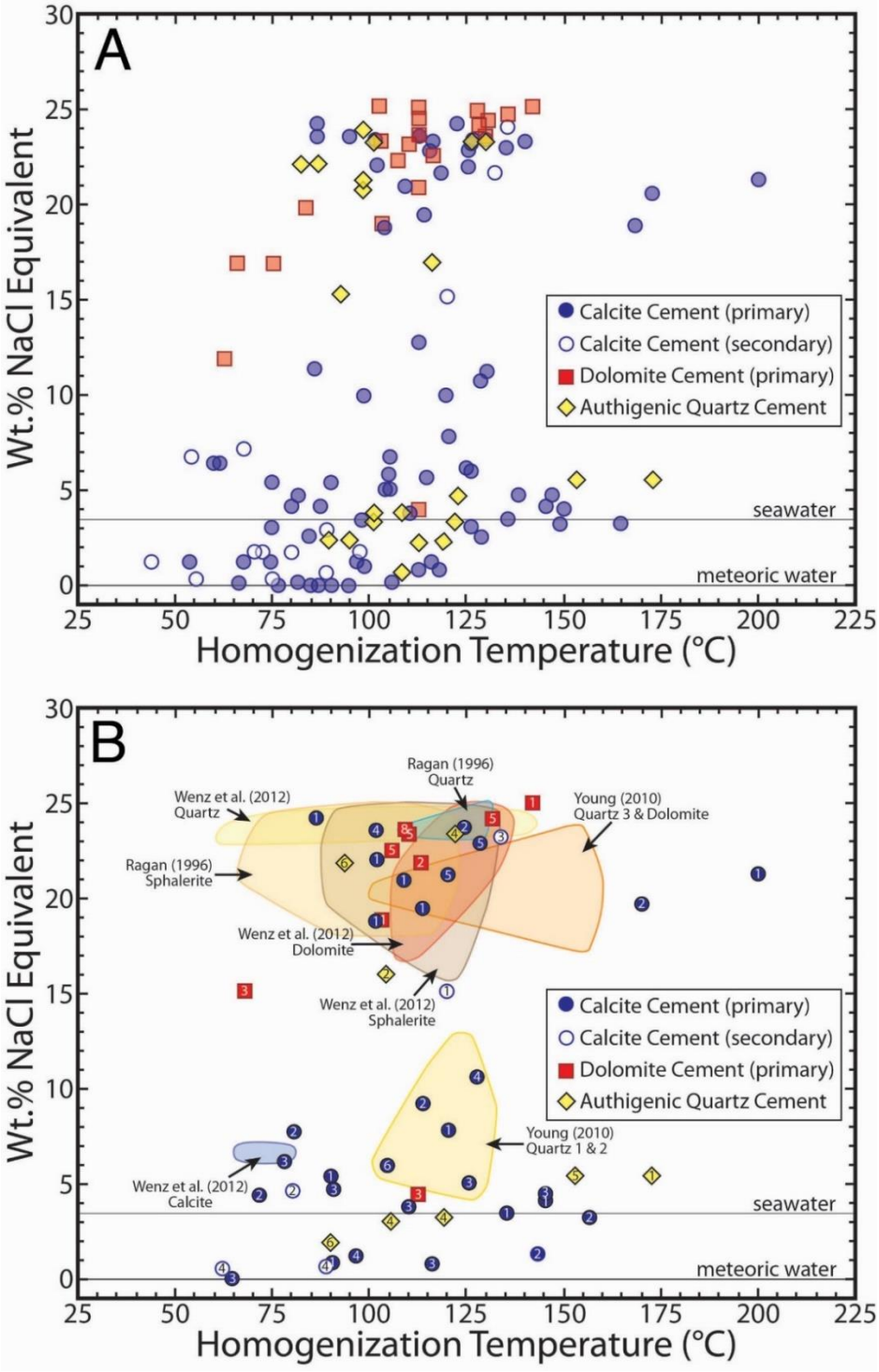

Figure 10. A) Plots of fluid inclusion salinities versus T_h values. B) Fluid inclusion salinities and T_h values grouped as assemblages. The number of individual fluid inclusions for which valid T_h and T_m values were measured are shown on each data point. Data fields are shown for fluid inclusions measurements made in previous studies in and near the Tri-State MVT district.

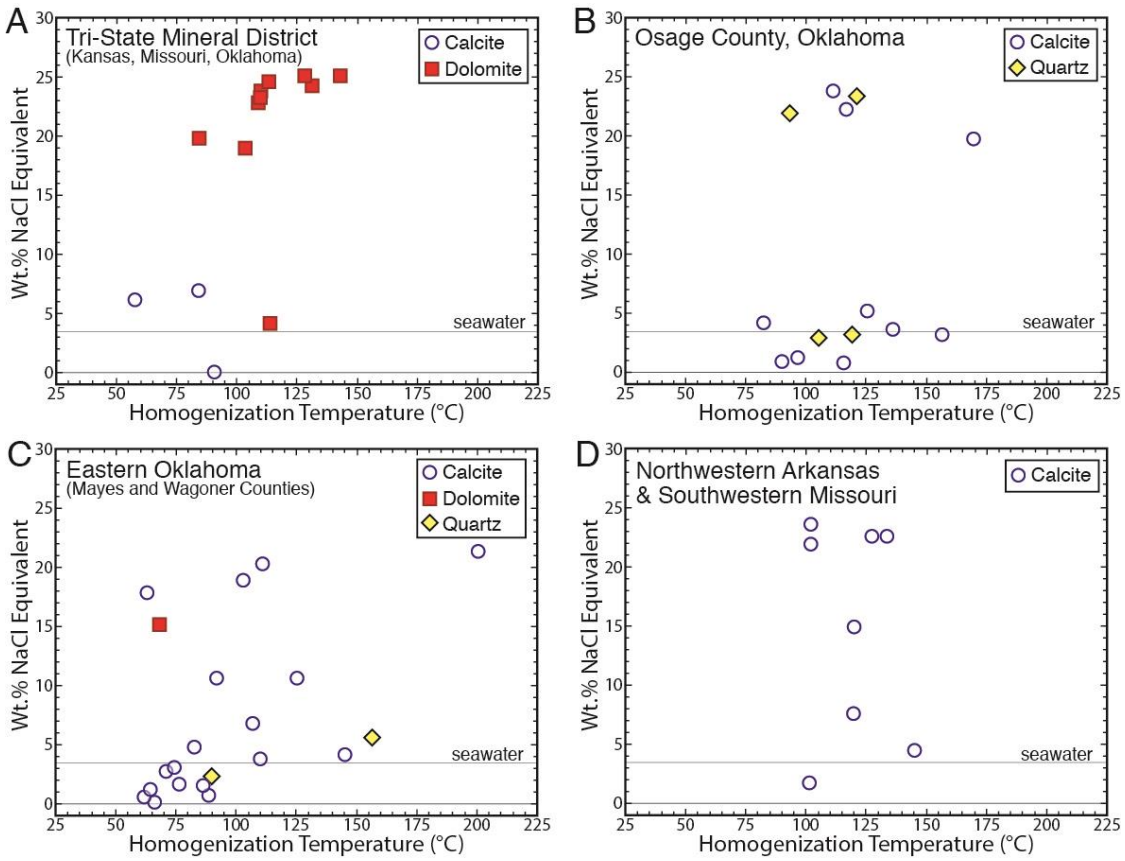

Figure 11. Fluid inclusion assemblages plotted among the four regions in the study area (see Figure 1).

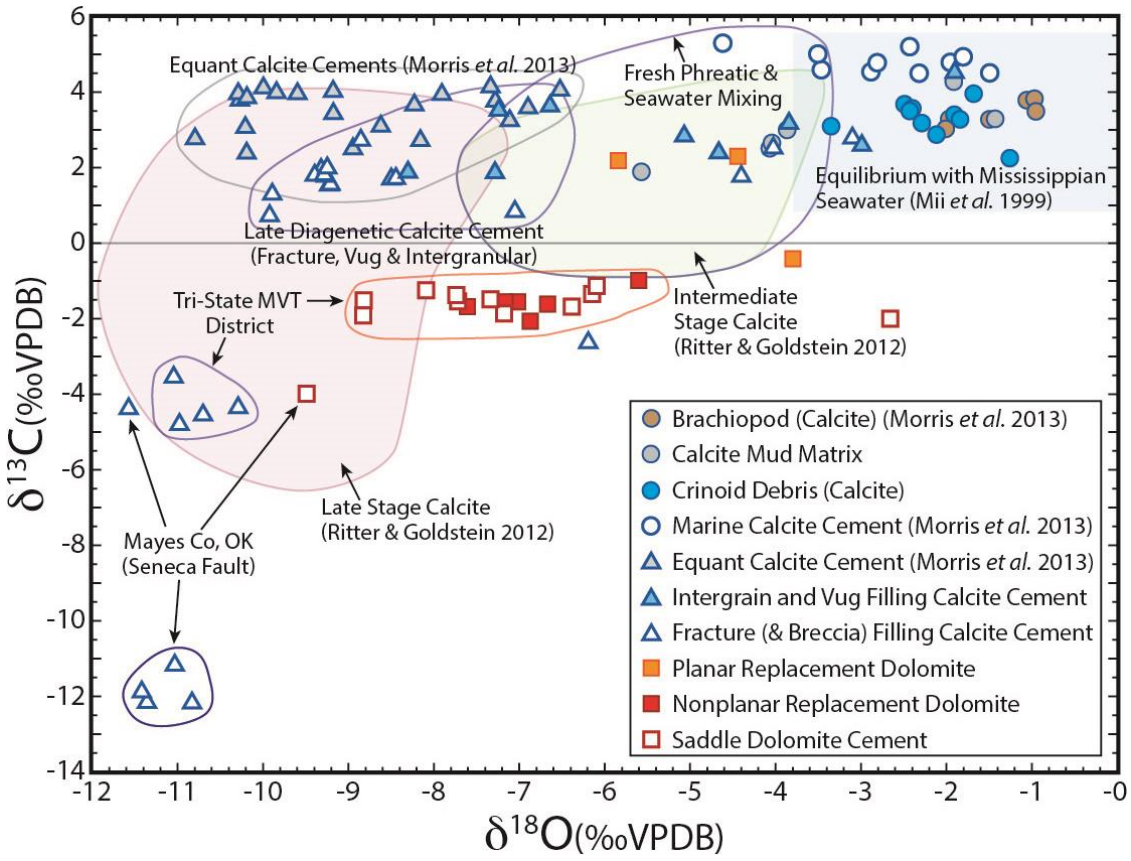

Figure 12. Values of $\delta^{18}O$ and $\delta^{13}C$ (per mil VPDB) for carbonate samples from the study area. The region for calcite in equilibrium with Mississippian seawater (Mii et al., 1999) is shown as well as the regions attributed to fresh phreatic and seawater mixing and late diagenetic calcite. The fields occupied by intermediate stage and late stage calcite cements of Ritter and Goldstein (2012) and equant calcite cements of Morris et al. (2013) are also shown.

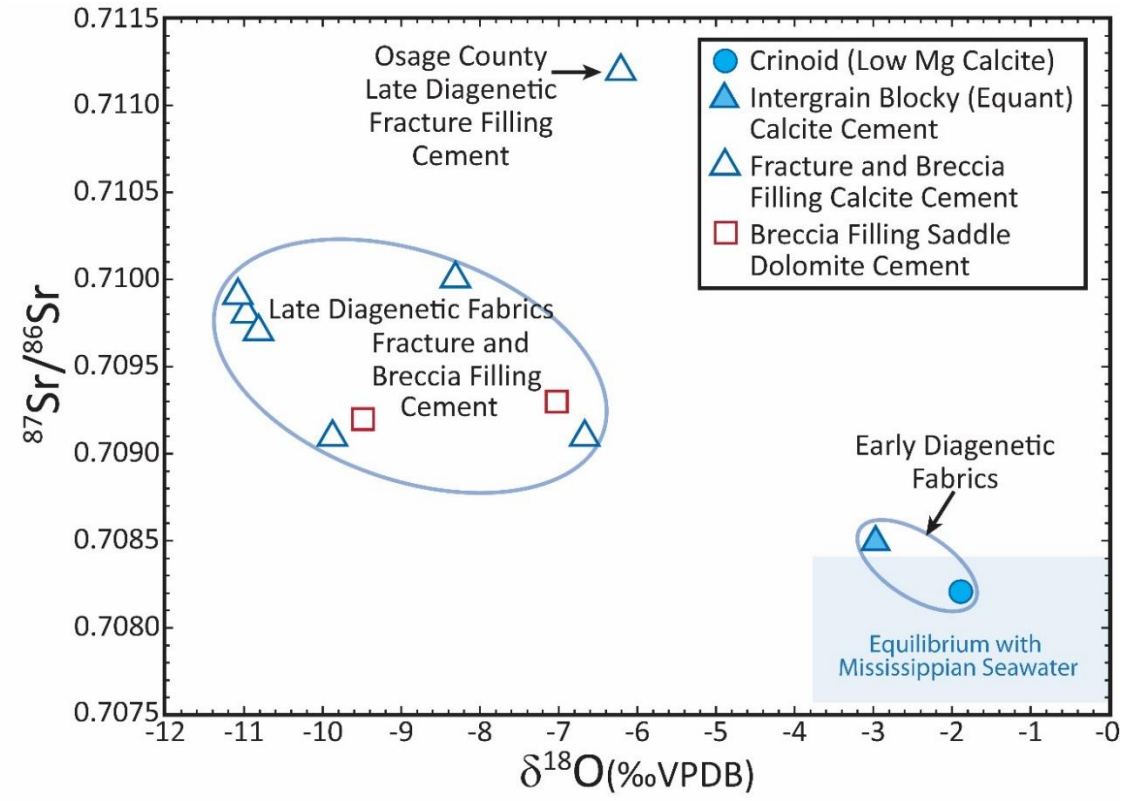

Figure 13. Values of $^{87}Sr/^{86}Sr$ plotted against $\delta^{18}O$ values for carbonate samples of the study area. Limestone in equilibrium with Mississippian seawater is shown as the light blue field (Mii et al., 1999; Bruckschen et al., 1999).

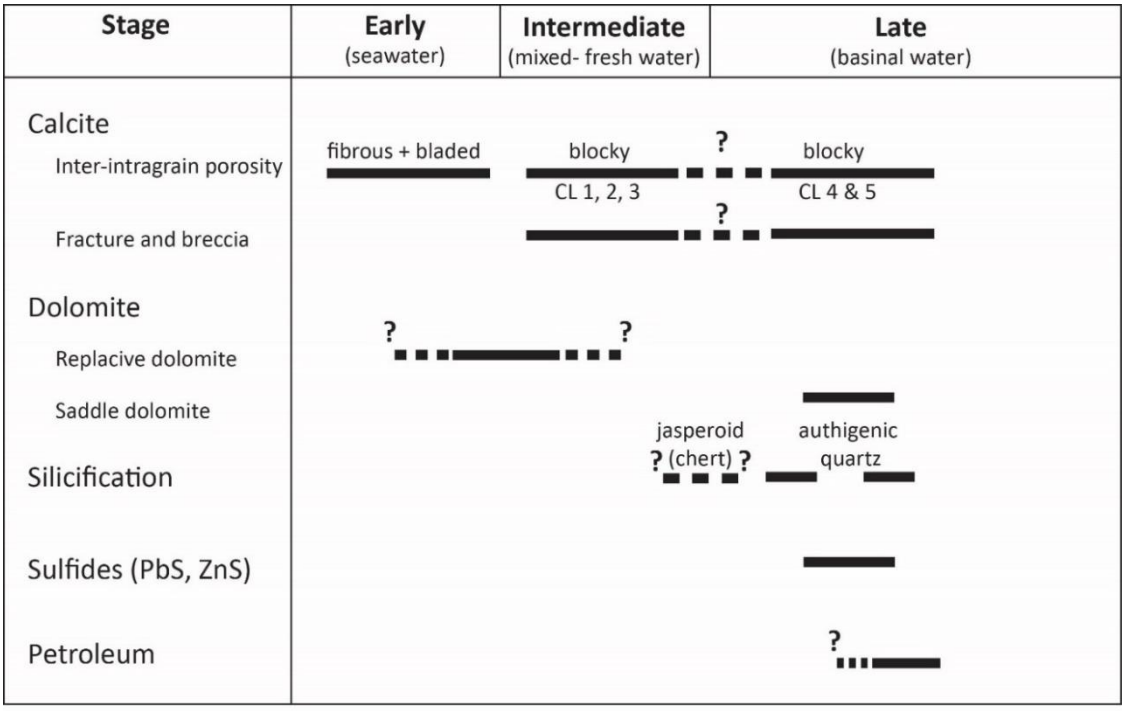

Figure 14. Paragenetic sequence for diagenetic events in the study area. The dashed lines indicate uncertain timing.

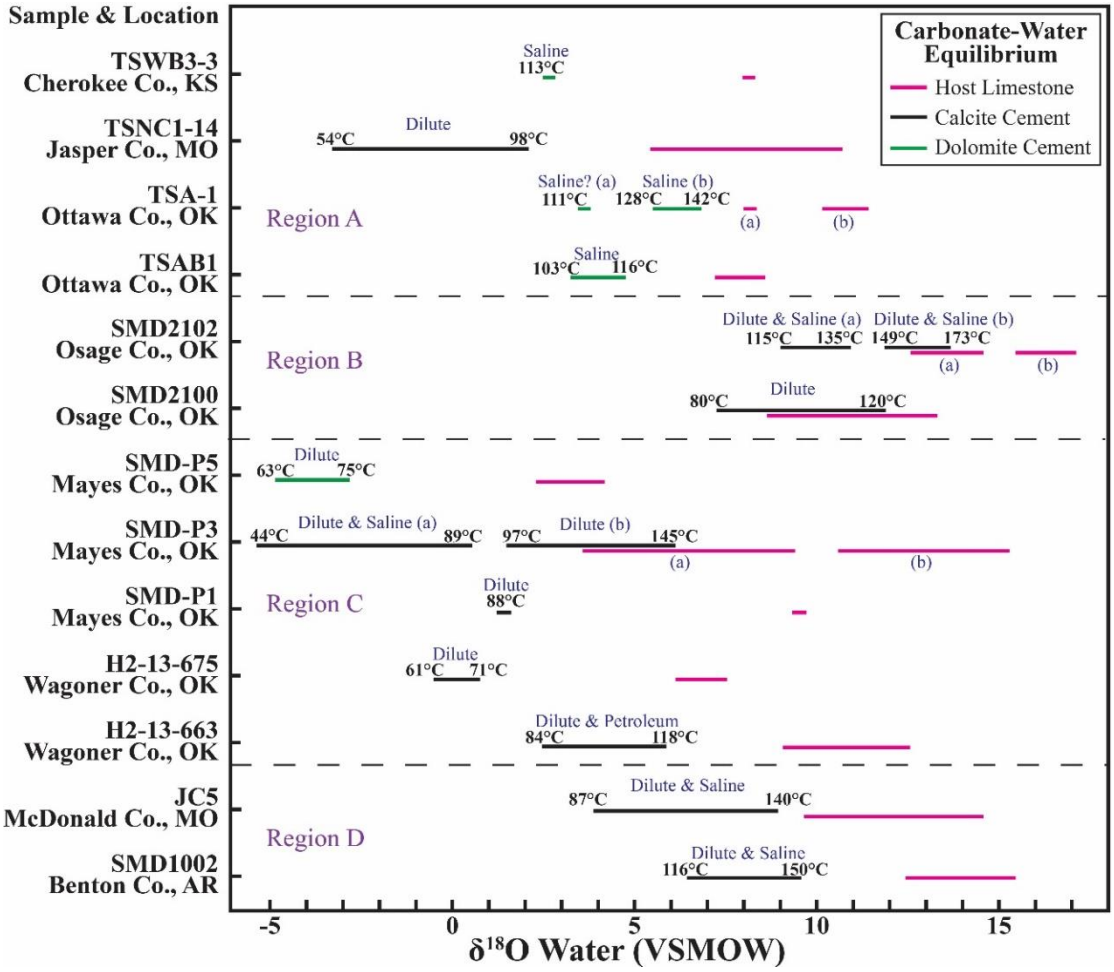

Figure 15. Calculated $\delta^{18}O_{water}$ values in equilibrium with calcite and dolomite cements and host limestones, using temperature ranges determined from fluid inclusions T_h values. Fractionation equations employed are from Friedman and O'Neil (1977) and O'Neil et al. (1969).

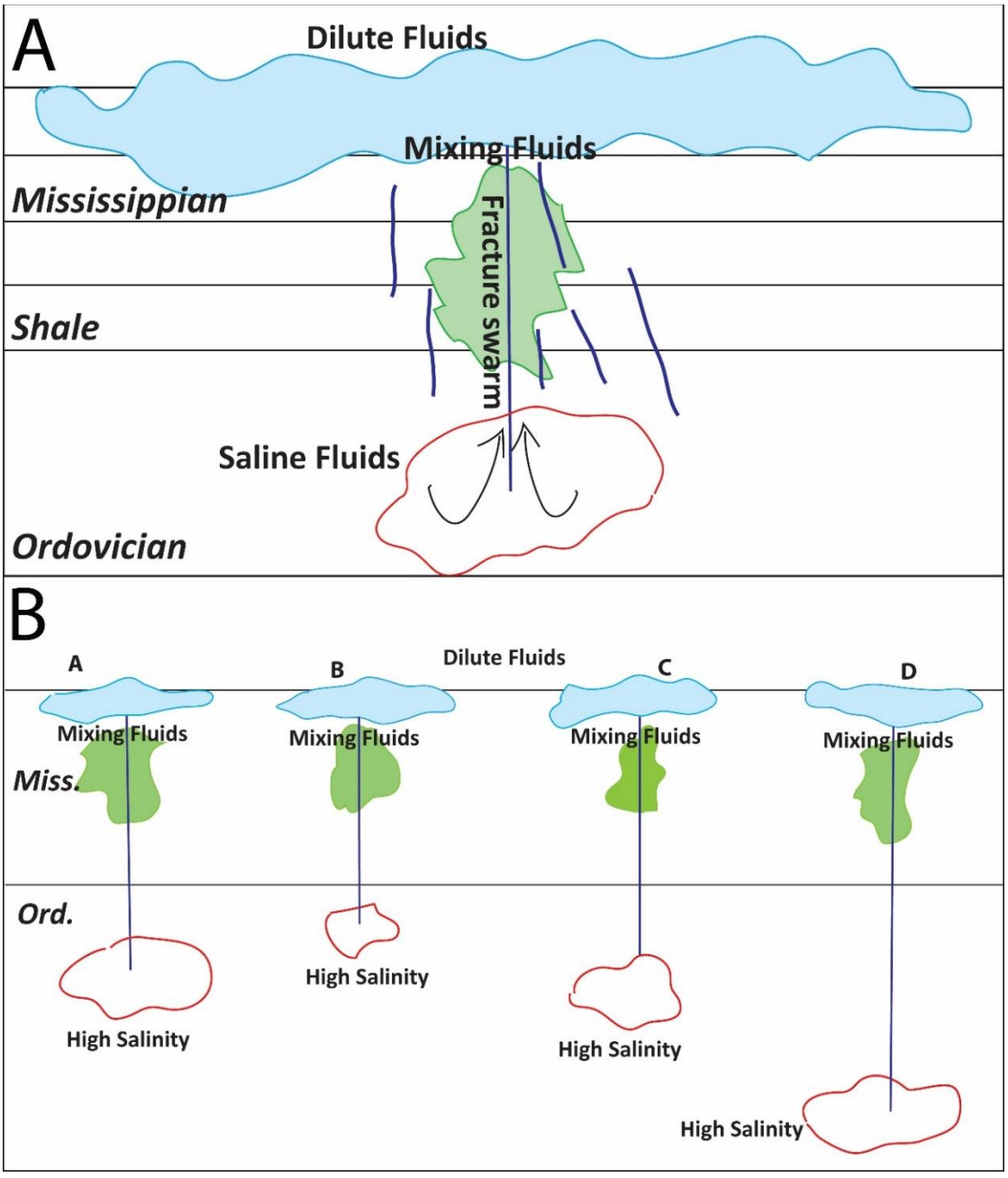

Figure 16. Conceptual model for late diagenetic fluid flow in the southern mid-continent showing: (A) saline fluids from the underlying Ordovician moving up along faults and fractures and mixing with dilute fluids present in the Mississippian strata; B) The fluid migration model applied separately to the four regions in the study area.

PAPER II

DIAGENESIS OF MISSISSIPPIAN CARBONATE ROCKS IN NORTH-CENTRAL OKLAHOMA, USA

3.0. ABSTRACT

Mississippian rocks in north-central Oklahoma were deposited on a ramp/shelf system that trended along an approximate northeast-southwest strike and that deepened to the southeast and southwest into the Arkoma and Anadarko basins. This system is bounded by the Ozark-Uplift on the east and by the Anadarko Basin to the west. Structure in this area is dominated by faulting associated with the Nemaha-Uplift (Transcontinental Arch).

Shallower water (shelf) depositional settings dominate in the northern part of the study area and deepen toward the south into the basins. Sedimentary rocks on the carbonate ramp are dominated by cyclic, partially dolomitized, argillaceous mudstones interbedded with fine-grained wackestones to grainstones. Intergrain pore space is filled by bladed (isopachous) and syntaxial marine cements followed by blocky calcite cements. Carbonates are replaced commonly by chert with intergrain open space filled by fine crystalline quartz (chert) cement. Late diagenetic fracture, breccia, and vug (FBV) porosity are filled by calcite and less commonly, by quartz cement that displays a coarse, blocky habit.

Carbon and oxygen isotope values for limestones are consistent with precipitation from Mississippian seawater and mixed seawater-meteoric water. Early diagenesis was dominated by seawater cementation with likely modification by meteoric water during sea level low-stands. FBV filling calcite and quartz represent a later stage of diagenesis associated with petroleum generation and migration. Stable isotope values for FBV filling calcite cements are consistent with precipitation from evolved basinal waters. Two-phase (liquid plus vapor) aqueous and petroleum inclusions were observed in FBV filling calcite and quartz cements. The two-phase aqueous inclusions have homogenization temperatures ranging from ~48º to 156ºC and have salinities ranging from 0 to 25 equivalent weight % NaCl, reflecting the presence of dilute and saline fluid end-members.

Fault movement and related fracturing in the Mississippian section in north-central Oklahoma is associated with the Ouachita Orogeny during Pennsylvanian-Permian time. This orogenic activity also resulted in regional migration of basinal fluids that contributed to precipitation the late diagentic cements. Calculated equilibrium $\delta^{18}O_{water}$ values (VSMOW) for fluids that precipitated FBV filling calcite cements are variable, ranging from -0.3 to +14.5‰, and do not reflect a single end-member water. Overlapping calculated $\delta^{18}O_{water}$ values for carbonate cement and host limestone in most areas of north-central Oklahoma suggest cement-depositing fluids approached isotopic equilibrium with the host carbonate rocks. Alternatively, the overlapping values could represent mixing between resident and non-resident fluids, dominated by resident fluids in equilibrium with the host limestone.

3.1. INTRODUCTION

Mississippian carbonate rocks in north-central Oklahoma produce petroleum from both conventional and unconventional reservoirs. The conventional plays include the Sooner Trend, which consists of a group of oil fields primarily in Alfalfa, Major, Garfield, and Kingfisher counties in north-central Oklahoma (Figure 1) (Harris, 1975).

The productivity of this trend largely is from fracture-dominated cherty carbonates of Meramacian-Osagean age (Harris, 1975). More recent production has been from horizontal drilling in tight carbonate rocks (Milam, 2013).

There have been few diagenetic studies conducted on Mississippian rocks in north-central Oklahoma and elsewhere in the region. The combined effect of early and late diagenetic events on conventional and unconventional reservoirs in the region is largely unknown. This study investigates petrography, fluid inclusion microthermometry, and isotope geochemistry of these Mississippian rocks, particularly fracture, breccia and vug (FBV) filling carbonate cements, in order to determine the composition and source(s) of the late diagenetic fluids that affected the Mississippian rocks in this region.

The effect of these fluids on porosity evolution, thermal maturity of the organic components of the rocks, and generation and migration of petroleum are addressed here and should be useful in developing future exploration strategies in this region.

3.1.1. GEOLOGICAL BACKGROUND

The study area is located in north-central Oklahoma, straddling the Nemaha Uplift (Figure 1A). The area is bounded by the Ozark uplift on the east, the Arkoma Basin to the southeast, the Anadarko Basin to the west and south, and by the Central Kansas Uplift

and Transcontinental Arch to the north and northwest, respectively (Lane and DeKyser, 1980). During the Early and Middle Mississippian, the midcontinent of the US was relatively inactive in terms of structural deformation and tectonic activity. However, during the Late Mississippian and Early Pennsylvanian, tectonism associated with the Ouachita Orogeny led to the development of structural features around the study area that directly affected the deposition and distribution of Mississippian carbonates. The Nemaha Uplift was superimposed on the earlier Proterozoic Mid-Continent rift, which extends north to the Keweenaw Peninsula (Serpa et al., 1989) and was formed during a regional compressional event that resulted in widespread reverse faulting in Nebraska, Kansas, and Oklahoma (Gay 1999; Gay, 2003a, b) (Figure 1B). It is thought that this activity occurred during Late Mississippian or Early Pennsylvanian time (Gay 1999; Gay, 2003 a, b).

Mississippian rocks were deposited regionally throughout the midcontinent across the ancient Burlington Shelf (Lane, 1978; Gutschick and Sandberg, 1983). In the north-central Oklahoma study area, Mississippian deposition took place on a ramp to distally steepened ramp system extending south and west from north-central Oklahoma into the Anadarko Basin (Mazzullo et al., 2011; LeBlanc, 2014). LeBlanc (2014) suggested that the Nemaha Uplift and associated faults were active during and after deposition in this system and influenced the distribution of depositional facies.

The Mississippian limestone section in the study area (Figure 2) can described as an overall 2nd order sequence comprised of a series of higher frequency, 3rd and 4th order sequences that were deposited as a result of eustatic sea level change. Sequence variability in north-central Oklahoma is thought to play a significant role in the quality

and vertical heterogeneity of the Mississippian reservoirs. However, because of a lack of paleontological control, subsurface correlation of cores examined and assignment of cored intervals to specific stratigraphic units in this region is difficult (LeBlanc, 2014). LeBlanc (2014) studied three cores in Logan Co. (Adkisson 1-33 SWD), and Payne Co. (Elinore 1-18 SWD and Winney 1-8 SWD) (Figure 1B) and identified five repeating facies in the Mississippian section in the study area. In order of interpreted decreasing water depth these facies include: (1) glauconitic sandstone, (2) burrowed calcareous mudstone-wackestone, (3) bioturbated wackestone-packstone, (4) peloidal packstone-grainstone, and (5) skeletal packstone-grainstone. The aerial distribution of these facies strikes in a general northwesterly direction, deepens southwestwardly on the ramp, and is controlled stratigraphically by fourth and fifth order sea level fluctuations (LeBlanc, 2014).

3.2. METHODS

Locations of nine cores from which sample were collected for this research are shown on Figures 1A and B. Petrographic analysis was conducted on 43 thin sections with particular attention given to void-filling calcite and dolomite cements. Cathodoluminescence (CL) petrography was carried out using a CITL MK5-1 cathodoluminescence system mounted on an Olympus-BX51 microscope equipped with 4X, 10X, and 40X long focal distance objective lenses, and a "Q Imaging" 5-megapixel, cooled, low-light, digital camera system.

Fluid inclusion microthermometric measurements were made using a Linkam THMSG 600 heating and cooling stage mounted on an Olympus BX41 microscope

equipped with 40X and 100X long focal distance objective lenses. Homogenization (T_h) and last ice melting (T_m) temperatures have errors of ±1.0°C and ±0.3°C, respectively, based on analysis of synthetic fluid inclusions (Shelton and Orville, 1980). The inclusions analyzed in this study were aqueous, two-phase, primary and secondary inclusions, using the terminology of Roedder (1984). Salinities were calculated from T_m measurements using equations from Bodnar (1992). No corrections were made for pressure as depths of burial at the time of filling are unknown. However, vitrinite reflectance studies of the underlying Woodford Shale (Cardott, 2012) indicate moderate levels of maturity for the study area so that it is unlikely that the rocks were ever deeply buried.

Carbon and oxygen isotope compositions were determined for dolomite and calcite samples using a Thermo-Finnigan Delta Plus gas-source mass spectrometer at the University of Missouri. The $\delta^{13}C$ and $\delta^{18}O$ values (relative to VPDB) have standard errors of less than ±0.05‰, based on replicate measurements of the NBS-19 calcite reference standard, and have been corrected for reaction with 103% phosphoric acid at 70°C (Rosenbaum and Sheppard 1986). Ratios of $^{87}Sr/^{86}Sr$ were determined using a TIMS at the University of Kansas Radiogenic Isotope Laboratory and have errors of ±0.000014 at a 95 percent confidence interval.

3.3. RESULTS

3.3.1. PETROGRAPHY

Limestone lithologies and calcite cements were studied in the cores from Canadian, Osage, Logan, Payne, Blaine, Kingfisher and Woods Counties, Oklahoma (Figure 1B). Leblanc (2014) discussed five repeating facies in shoaling-upward cycles (see previous

discussion). Petrographic description of the lithologies encountered in these repeated cycles follows. Within these facies, lithologies include argillaceous pelletic to siliceous mudstones, containing scattered fossils, and fine-grained packstones and grainstones. Lithologies infrequently are replaced partially by fine to medium crystalline planar dolomite (Mohammadi et al., in editorial review). The Perryman 2 core in Osage Co. (Figure 1B) is comprised largely of chert breccia, and partially dolomitized lime mudstone. It is rare throughout the study area to find inter- and intra-grain porosity that is not completely filled by calcite cement. Vug and breccia porosity are filled by calcite and, less commonly, quartz cement.

Vugs and fractures, including ptygmatic and vertical to sub-vertical solution-enlarged fractures, range in width from ~1 mm to several cm in the cores studied and are filled by coarse crystalline (up to cm size) blocky calcite and, less commonly, quartz crystals (Figure 5). Core samples from Payne and Logan Co., OK contain fractures and vugs ranging in width from 0.2 mm to ~1.0 cm filled by calcite cement. Samples from Blaine Co., OK contain breccia fractures ranging from 0.2 mm to ~2.0 cm filled by calcite and infrequent quartz cements. Core samples from Osage Co. contain up to cm size fractures and open space associated with breccias that are filled by calcite and quartz cement. Calcite-filled FBV were not observed in the Bann 1-14 core in Woods Co., OK. Ptygmatic fractures from 1 to 3 mm wide, were observed in cores from Osage Co., Payne Co., and Kingfisher Co., Blaine Co., and Canadian Co., OK. Frequently, fractures display both vertical and ptygmatic characteristics depending on whether they cut more competent, grain-rich or more compactable, mud-rich lithologies. This transformation may occur across bedding planes of a few centimeters in thickness.

Calcite cement crystals filling FBV porosity frequently display type I twinning (Burkhard, 1993). Those filling ptygmatic fractures frequently display more intense twinning, which is classified here as types I, II, and possibly III using Burkhard (1993) (Figures 3E & F and 4C).

No early diagenetic cements (discussed previously) are associated with FBV open space as was observed in the Cherokee and Ozark Platform areas to the east (Mohammadi et al., in press). In the north-central Oklahoma area, only blocky calcite cements, and less commonly, quartz cements were observed filling FBV open spaces. Breccia-filling quartz crystals from Blaine Co., OK (Figure 3A & B) were precipitated following fracture-filling blocky calcite cements, however quartz crystals partially filling fractures in Osage Co., OK core formed prior to blocky calcite cements. Calcite cement filling vug and breccia porosity typically displays uniform bright orange CL or faintly zoned, bright to dull CL (Figure 3B & D). Quartz cements display no CL response (Figure 3B).

3.3.2. FLUID INCLUSION MICROTHERMOMETRY

Two-phase fluid inclusions (liquid and vapor) were observed in FBV-filling blocky calcite and quartz cements in the study area (Figure 4A & B and Table 1). The small size of many of the fractures and the presence of strain twinning in much of the calcite filling the fractures, especially in ptygmatic fractures, as well as the generally small size of most inclusions (<5μm) made measurement of T_h and T_m values difficult. Values for T_h and/or T_m were obtained for one hundred fifth-one aqueous fluid inclusions (Table 1). T_h values range from 48º to 156ºC and T_m values range from -21.1 to 2.5ºC (Table 1). Figure 5 displays data for fluid inclusions for which both T_h and T_m data were obtained, with

salinity expressed as equivalent weight % NaCl. Fluid inclusion microthermometry defines two distinct end-member salinity populations whose T_h values have similar ranges from 70° to 150°C. Three higher temperature outliers may be due to stretching or necking of the fluid inclusions.

The ranges of T_h values for inclusions in calcite cement filling vertical and ptygmatic fractures, and breccia are similar. The distribution of fluid inclusion data is similar to that obtained from Mississippian cements on the Cherokee-Ozark Platform to the east (Mohammadi et al., in press). Calcite filling vertical fractures and breccia contains both higher and lower salinity inclusions, but ptygmatic fractures appear to contain only lower salinity inclusions (Figure 5).

More lower-salinity inclusions were observed in this study than higher salinity inclusions (Table 1, Figure 5). A population of the lower salinity inclusions yielded T_m values above 0ºC (Table 1). This superheated ice is metastable and formed due to the failure of a vapor bubble to nucleate on heating (Roedder, 1967). In cases where repeated heating and cooling did not eliminate this phenomenon, the T_h data is reported in Table 1, but the inclusions are not plotted on Figure 5.

Two-phase (liquid and vapor) petroleum inclusions were observed in FBV-filling calcite cements in Payne, Blaine, and Kingfisher Counties as indicated by light blue to cream-colored fluorescence under ultraviolet light (Figure 4C & D). Petroleum inclusions in north-central Oklahoma appear to be more abundant than in the Cherokee and Ozark Platform area (Mohammadi et al., in press), and their more cream-colored fluorescence contrasts with a more light blue color of inclusions from the Cherokee-Ozark platform area.

3.3.3. ISOTOPE GEOCHEMISTRY

The results of carbon and oxygen isotope analysis are shown in Figure 6 and Table 2. Calcite micrite matrix has $\delta^{18}O$ values of -7.6 to -1.0‰ and $\delta^{13}C$ values of -3.5 to 2.3‰. The $\delta^{18}O$ and $\delta^{13}C$ values for planar dolomite replacing limestone range from -2.8 to 1.6‰ and -1.7 to 0.5‰, respectively. Values for $\delta^{18}O$ and $\delta^{13}C$ of calcite skeletal debris and early diagenetic cement in grainstones and packstones range from -3.4 to 2.7‰ and -5.3 to -0.0‰, respectively (Mohammadi et al., in editorial review).

Vertical fractures, ptygmatic fractures and breccia-filling calcite cements have $\delta^{18}O$ values that range from -9.2 to -2.4‰ and $\delta^{13}C$ values ranging from -7.1 to 2.4‰. The data are distributed into two distinct clusters based on $\delta^{13}C$ values. The first cluster, comprised of most of the data for vertical fractures, breccia and about half of the ptygmatic calcite values, displays $\delta^{18}O$ values ranging from -9.2 to -4.4‰ and $\delta^{13}C$ values of -1.2 to 2.8‰. The second cluster, comprised mainly of calcite-filled ptygmatic fractures, has $\delta^{18}O$ values of -4.0 to -7.0‰ and $\delta^{13}C$ values of -7.1 to -2.3‰ (Figure 6).

Ratios of $^{87}Sr/^{86}Sr$ for carbonates in the study area are listed in Table 3 and plotted against $\delta^{18}O$ and $\delta^{13}C$ values in Figure 7. The $^{87}Sr/^{86}Sr$ values for calcite micrite in the study area range from 0.70778 to 0.70821 and a single dolomite value (Mohammadi et al., in editorial review) has a value of 0.70782. Calcite cements filling vertical, ptygmatic, breccia, and solution-widened fractures have values from 0.70780 to 0.70820. Four samples of fracture-filling calcite cement from Osage Co., OK have higher $^{87}Sr/^{86}Sr$ values, from 0.71023 to 0.71124; these samples also have lower $\delta^{13}C$ values, from -2.3 to -4.1‰ (Figure 7B).

3.4. DISCUSSION

3.4.1. EARLY DIAGENESIS

Early diagenesis of Mississippian carbonates in the north-central Oklahoma study area (Figure 1) are characterized by marine cementation and partial dolomitization. Mixed skeletal debris and calcite cements comprising fine grained grainstones and packstones, and calcite mud matrix display carbon, oxygen (Figure 6), and strontium isotope (Figure 7) values that are consistent with equilibration with Mississippian seawater (Mii et al., 1999; Bruckschen et al., 1999) modified by meteoric water (Figure 6) (Mohammadi et al., in editorial review). Depleted $\delta^{13}C$ values of some of the host limestone mud matrix and skeletal grainstone are interpreted as evidence for microbial sulfate reduction (Hudson, 1977) or oxidation of organic matter (Oehlert and Swart, 2014) during early stages of burial diagenesis. Dolomite rhombs, partially replacing mudstones, display an increase in $\delta^{18}O$ value of 1 to 3 per mil. as compared to values for calcite in equilibrium with seawater (Figure 6). Mohammadi et al. (in editorial review) observed that these values are consistent with precipitation of dolomite from Mississippian seawater given the difference in the dolomite fractionation factor (Land, 1980).

3.4.2. LATE DIAGENESIS

Blocky calcite and infrequent quartz cements filling fracture, breccia, and vug (FBV) porosity are interpreted as late diagenetic cements in the north-central Oklahoma study area. No evidence of early marine and shallow phreatic cements, as discussed above, was observed in the FBV porosity. Therefore, these features likely postdate the early cements.

An example of late diagenetic cement filling intergrain and intragrain porosity in Osage County (Blackbird 4-33 core, Figure 1B) is discussed in Mohammadi et al. (in press).

Uniform to faintly zoned CL of FBV-filling blocky calcite cements (Figure 3B & D) indicate preservation of subtle changes in water chemistry, suggesting a late diagenetic origin. This contrasts with sharp CL contacts, observed in the early diagenetic cements that are interpreted as abrupt changes associated with fluctuation between marine and meteoric waters (Banner et al., 1988; Mohammadi et al., in editorial review). The CL signature of the FBV-filling cements corresponds to what was observed in late diagenetic cements in the Cherokee-Ozark Platform region to the east of the present study area (Mohammadi et al., in press) suggesting a similar origin. Authigenic quartz cement is observed infrequently; it precipitated both prior and subsequent to stages of calcite cementation.

Several lines of geochemical evidence attest to a late diagenetic origin of FBV-filling calcite cements. Elevated T_h values of primary fluid inclusions in calcite cements filling FBV open spaces (Figure 3A & B) indicate that these cements were precipitate by warm fluids (About 70° to 175°C) during later stages of diagenesis. Salinity and temperature of the fluids in the north-central Oklahoma study area are similar to those of the Cherokee-Ozark Platform study area to the east (Mohammadi et al., in press). Both saline and dilute aqueous fluids, as well as abundant petroleum inclusions were observed (Figure 3A & B). The trapping of petroleum inclusions is consistent with a late diagenetic origin of these calcite cements.

Relatively low $\delta^{18}O$ values (about -4.5 to -7.5‰, Figure 6) obtained for FBV-filling calcite cements suggest precipitation from meteoric water or, more likely, precipitation

by late diagenetic basinal water, considering the fluid inclusion evidence discussed previously. Some of the cements display both lower $\delta^{18}O$ and lower $\delta^{13}C$ values that are consistent with oxidation of organic carbon, possible concomitant with sulfate reduction associated with petroleum generation (Figure 6) (Machel et al., 1995). High $^{87}Sr/^{86}Sr$ values (> 0.710) for fracture-filling calcite cement in Osage County (Figure 1B and Figure 7) may indicate fluid interaction with continental basement or sedimentary rocks derived from basement, such as arkose or shales.

3.4.2.1. RELATION OF FRACTURING TO CEMENTATION

Fractures in the study area formed initially as vertical to subvertical fractures and frequently underwent solution widening prior to cementation and deformation into ptygmatic veins during sediment compaction. Vertical fractures were observed transforming to ptygmatic veins (Figure 3E & F) over a scale of a few centimeters depending on the lithology of the surrounding rock. More grain-rich beds are less compactable and typically host vertical fractures, whereas more argillaceous beds are more compactable and tend to host ptygmatically deformed veins.

Cementation of ptygmatic veins likely occurred when they formed initially as vertical fractures and they deformed subsequently with compaction. Straining of calcite crystals during compaction is shown by strong twinning of calcite cement in the ptygmatic veins compared to weaker twinning of calcite cement in adjacent vertical fractures. Strong twinning [type II and III twins as defined by Burkhard (1993) and Ferrill et al. (2004)] of the calcite crystals observed in ptygmatic veins likely occurred due to strain introduced during compaction. Less intense type I twinning is common in cements filling vertical

and sub-vertical fractures and type I twinning is less common in vugs and breccia filling calcite cements. There is no evidence, though, that calcite cement in ptygmatic fractures underwent recrystallization, which would have eliminated strain induced features such as twinning. At least some primary aqueous and petroleum inclusions survived deformation (Figure 4C & D). If calcite cement filling ptygmatic fractures had undergone dissolution-recrystallization during compaction and deformation, any fluid inclusions present initially would have been destroyed. However, only low-salinity, aqueous fluids were observed in calcite cement filling ptygmatic fractures. This does not necessarily mean that only dilute fluids precipitated calcite filling ptygmatic fractures, as saline aqueous inclusions were observed in associated vertical fractures. It is possible that saline inclusions, though present, were not observed. Successful measurement of T_m values in ptygmatic fractures was infrequent because strong twinning made observations difficult. More likely, higher salinity inclusions, formed prior to deformation, may have been destroyed during deformation. Abundant petroleum inclusions were observed in calcite cement filling ptygmatic fractures using UV fluorescence (Figure 4C & D), as they were in late diagenetic calcite cements filling vertical and subvertical fractures. Carbon, oxygen, and Sr isotope geochemistry of ptygmatic fracture filling calcite overlaps with calcite filling other FVB porosity (Figures 6 & 7).

3.4.2.2. TIMING OF FRACTURING AND CEMENTATION

The most intensive period of fracturing of Mississippian rocks in north-central Oklahoma likely accompanied fault movement along the Nemaha-Uplift during the Ouachita Orogeny to the south and the main Appalachian Orogeny to the east (Figure 1).

The timing of this fault movement was Pennsylvanian continuing into the Permian (Gay, 2003a). Late diagenetic solution widening and cementation in FBV open space likely occurred contemporaneous with or soon after fracture formation, otherwise the fractures would have closed with continuing compaction. Fluid inclusion and isotope studies on underlying Cambrian and Ordovician carbonates in the Ozark region indicate that those strata are a potential source of saline brines (Shelton et al., 1992; 2009; Temple, 2016). The consensus of opinion concerning fluid flow on the southern Midcontinent (e.g. Gregg, 1985; Gregg & Shelton, 1989; Leach & Rowan, 1986; Bethke & Marshak, 1990; Appold & Garven, 1999; Appold & Nunn, 2005; Gregg and Shelton, 2012) is that regional flow of basinal brines was associated with the Pennsylvanian-Permian Ouachita Orogeny and involved fluid movement northward, through deep Cambrian-Ordovician and basement aquifers. The large number of petroleum inclusions associated with aqueous inclusions, observed in all late diagenetic cements in this study, indicates that cementation occurred during generation and migration of petroleum, which likely was derived from the underlying Woodford Shale (Cardott, 2012).

3.4.3. ORIGIN OF LATE DIAGENETIC FLUIDS

Figure 8 and Table 4 show calculated $\delta^{18}O_{water}$ values for FBV-filling calcite cements in north-central Oklahoma. The $\delta^{18}O$ values (standard mean ocean water, SMOW) for waters that precipitated calcite cement and waters in equilibrium with host limestone were calculated using the equation of O'Neil et al. (1969) for calcite-water fractionation, utilizing measured isotope values and temperatures based on T_h values of fluid inclusions. Values were calculated to determine whether the fluids depositing calcite

cement are in isotopic equilibrium with host rock limestone at the temperatures of cement deposition or, instead, reflect the influence of non-resident fluids that retained their source-derived oxygen isotope compositions (see Shelton et al., 2011).

Overlapping $\delta^{18}O_{water}$ values for carbonate cements and host limestone in Osage Co., Payne Co., and Blaine Co., OK (Figure 8) indicate that cement-depositing fluids in these areas approached isotopic equilibrium with local carbonate rocks. The overlap of values in these cases may represent equilibration of non-resident fluids with the hosting carbonate and/or mixing between resident and non-resident fluids, in a system dominated by the resident fluids in equilibrium with the host limestone. This is in contrast with values from some areas in north-central Oklahoma (e.g. Canadian and Osage counties, Figure 8) and most values calculated for calcite and dolomite cements in the Cherokee-Ozark platform area to the east of the north-central Oklahoma study area. In those areas, the $\delta^{18}O_{water}$ values calculated for calcite cement-depositing waters reflect non-resident fluids that did not equilibrate isotopically with the host limestone (Mohammadi et al. in press).

Carbonate lithologies of Mississippian rocks in the Cherokee-Ozark Platform area are mostly grainstone, packstone and wackstone. Late diagnetic calcite cements frequently were observed as filling intergrain porosity in these rocks, as well as filling fractures and breccia (Mohammadi et al., in editorial review). In contrast, late diagenetic cements were observed only as fracture, breccia and infrequent vug-filling cements in the north-central Oklahoma study area, because the lithologies observed in the present study area are composed largely of wackstone and mudstones (deeper water facies) and their low amounts of intergrain porosity are filled dominantly by early marine cements. This may

have had the effect of limiting the total fluid flux in the Mississippian of north-central Oklahoma, creating a more rock-dominated system than that which existed in the Cherokee-Ozark Platform region.

There also is a much thicker intervening section between the Ordovician and Mississippian sections in north central Oklahoma than in the Cherokee-Ozark platform region consisting largely of the Devonian Woodford Shale and underlying Silurian carbonates. Reaction with these rocks may have affected the composition of the ascending fluids during their migration along the faults. The thick shale section underlying the Mississippian in north-central Oklahoma likely affected fluids moving upward from the underlying Ordovician by contributing additional saline fluids along with petroleum.

Low $^{87}Sr/^{86}Sr$ values of FBV-filling cement (Figure 7) suggest either a Mississippian source for fluids or a system dominated isotopically by the hosting Mississippian carbonate rocks. An exception is calcite cement from Osage County, OK which has higher $^{87}Sr/^{86}Sr$ values (> 0.710, Figure 7). This apparent anomaly may indicate: (1) Fluid with a basement strontium isotope signature that moved along faults with limited interaction with host lithologies or mixing with resident fluids, or (2) similar fault-controlled fluids that interacted with subjacent shale with a continental basement strontium isotope signature. We favor the latter interpretation because the fracture-filling calcite veins with high $^{87}Sr/^{86}Sr$ values also have the lowest $\delta^{13}C$ values (-2.3 to -4.1‰) measured in our study, which may reflect oxidation of organic matter derived from shale source rocks (Figure 7B).

3.5. CONCLUSIONS

Late diagenetic calcite and quartz cement was observed filling fractures, breccias, and vugs (FBV) in Mississippian limestones in north-central Oklahoma. High T_h values (70° to 175°C) of fluid inclusions and lower $\delta^{18}O$ values (-9.2 to -4‰) of calcite cements indicate that they were precipitated by warm basinal fluids during later stages of diagenesis. Low $\delta^{13}C$ values of some calcite cements indicate a component of oxidized organic carbon, possibly concomitant with sulfate reduction associated with petroleum migration. Fluid inclusion microthermometry of FBV-filling calcite and quartz cements indicates two distinct end-members fluids based on salinity, a dilute to moderately saline (0 to 6 Wt.% NaCl) fluid and a high salinity fluid (18 to 25 Wt.% NaCl).

Formation of fractures in the Mississippian section in north-central Oklahoma likely is related to fault movement along the Nemaha ridge instigated by Ouachita tectonism during the Pennsylvanian and extending into the Permian. This timing corresponds with regional flow of saline basinal fluids associated with the orogenic activity. These fluids ascended along faults and contributed to precipitation of FBV-filling cements. Calculated $\delta^{18}O_{water}$ values indicate that fluids precipitating fracture- and breccia-filling cements in some areas approached isotopic equilibrium with the host carbonate rocks. In other areas, however, cement-depositing fluids have oxygen isotope signatures that reflect non-resident fluids whose flow was restricted to fault/fracture pathways, which did not permit isotopic equilibration with the host limestone. In particular, fracture-filling calcite veins from Osage County, with high $^{87}Sr/^{86}Sr$ (> 0.710) and low $\delta^{13}C$ values (-2.3 to -4.1‰), reflect fluids that retained isotopic characteristics that were derived through interaction with subjacent shale source rocks.

3.6. ACKNOWLEDGEMENTS

This study was supported by the Oklahoma State University-Industry Mississippian Consortium and the Boone Pickens School of Geology. We thank all of the companies that that supported this Consortium. Also, thanks to the National Association of Black Geoscientists (NABG) for financial support for SM and AAPG for partial support for TAE during this study. We thank G. Michael Grammer, Jeffrey White, Martin Appold, Robert Goldstein, Gordon MacLeod, and Abbas Seyedolali for their valuable comments and suggestions.

3.7. REFERENCES

Appold, M. S., and G. Garven, 1999, The hydrology of ore formation in the southeast Missouri district: Numerical models of topography-driven fluid flow during the Ouachita orogeny: Economic Geology, v. 94, p. 913-936.

Appold, M. S., and J. A. Nunn, 2005, Hydrology of the western Arkoma basin and Ozark platform during the Ouachita orogeny: Implications for Mississippi Valley-type ore formation in the Tri-State Zn–Pb district: Geofluids, v. 5, p. 308-325.

Banner, J. L., G. N. Hanson, and W. J. Meyers, 1988, Determination of initial Sr isotopic compositions of dolostones from the Burlington-Keokuk Formation (Mississippian): Constraints from cathodoluminescence, glauconite paragenesis and analytical methods: Journal of Sedimentary Petrology, v. 58, no. 4, p. 673-687.

Bethke, C. M., and S. Marshak, 1990, Brine migrations across North America - The plate tectonics of groundwater: Earth and Planetary Sciences, v. 18, p. 287-315.

Bodnar, R. J., 1992, Revised equation and table for determining the freezing point depression of H_2O-NaCl solutions: Geochimica et Cosmochimica Acta, v. 57, p. 683-684.

Bruckschen, P., S. Oesmann, and J. Veizer, 1999, Isotope stratigraphy of the European Carboniferous: Proxy signals for ocean chemistry, climate and tectonics. Chemical Geology, v. 161, p. 127-163.

Burkhard, M., 1993, Calcite twins, their geometry, appearance and significance as stress-strain markers and indicators of tectonic regime: A review: Journal of Structural Geology, v. 15, n. 3-5, p. 351-368.

Cardott, B. J., 2012, Thermal maturity of Woodford Shale gas and oil plays, Oklahoma, USA: International Journal of Coal Geology, v. 103, p. 109-119.

Darold, A. P., and A. A. Holland , 2015, Preliminary Oklahoma optimal fault orientations: Oklahoma Geological Survey Open-File Report, OF4-2015.

Ferrill, D., A. P. Morris, M. A. Evans, M. Burkhard, R. H. Groshong, and C. M. Onasch, 2004, Calcite twin morphology: A low-temperature deformation geothermometer: Journal of Structural Geology, v. 26, p. 1521-1529.

Gay, S. P. Jr., 1999, Strike-Slip, Compressional Thrust-Fold Nature of the Nemaha System in Eastern Kansas and Oklahoma: American Association of Petroleum Geologists (AAPG) Midcontinent Section Meeting, p.39-49.

Gay, S. P. Jr., 2003a, The Nemaha Trend – A system of compressional thrust-fold, strike-slip structural features in Kansas and Oklahoma, Part 1: Shale Shaker: v. 54, p. 9-17.

Gay, S. P. Jr., 2003b, The Nemaha Trend – A system of compressional thrust-fold, strike-slip structural features in Kansas and Oklahoma, Part 2: Shale Shaker, v. 54, p. 39-49.

Gregg J. M., 1985, Regional epigenetic dolomitization in the Bonneterre Dolomite (Cambrian), southeastern Missouri: Geology, v. 13, p. 503-506.

Gregg J. M., and K. L. Shelton, 1989, Minor and trace element distributions in the Bonneterre Dolomite (Cambrian), southeastern Missouri: Evidence for possible multiple basin fluid sources and pathways during lead-zinc mineralization: Geological Society of America Bulletin, v. 101, p. 221-230.

Gregg, J. M., and K. L. Shelton, 2012, Mississippi Valley-type mineralization and ore deposits in the Cambrian – Ordovician great American carbonate bank, *in* J. R. Derby, R. D. Fritz, S. A. Longacre, W. A. Morgan, and C. A. Sternbach, eds., The great American carbonate bank: The geology and economic resources of the Cambrian – Ordovician Sauk megasequence of Laurentia: AAPG Memoir 98, p. 163-186.

Gutschick, R. C., and C. A. Sandberg, 1983, Mississippian continental margins of the conterminous United States, *in* D. J. Stanley and G. T. Moore, eds., The shelfbreak: Critical interface on continental margins: SEPM Special Publication, 33, p. 79-96.

Harris, S. A., 1975, Hydrocarbon accumulation in "Meramec-Osage" (Mississippian) rocks, Sooner Trend, Northwest-Central Oklahoma: AAPG Bulletin, n. 4, v.59, p. 633-664.

Harris, S. A., 1987, Hydrocarbon accumulation in "Meramec-Osage" (Mississippian) rocks, Sooner Trend, Northwest-Central Oklahoma *in* B. Rascoe, Jr., and N. J. Hyne, eds., Petroleum geology of the mid-continent: Tulsa Geological Society Special Publication 3, p. 74-81.

Hudson, J. D., 1977, Stable isotope and limestone lithification: Fl geol. Soc. Lond., v. 133, pp. 637-660.

Land, L. S., 1980, The isotopic and trace element geochemistry of dolomite: The state of the art: SEPM Special Publication, n. 28, p. 87-110.

Lane, H. R., 1978, The Burlington Shelf (Mississippian, north-central United States): Geologica et Palaeontologica, v. 12, p. 165-176.

Lane, H. R., and T. L. DeKyser, 1980, Paleogeography of the late Early Mississippian (Tournasian 3) in the central and southwestern United States, *in* T. D. Fouch, and E. R. Magathan, eds., Paleozoic paleogeography of west-central United States: Rocky Mountain Paleogeography Symposium 1, Rocky Mountain Section SEPM, p. 149-162.

Leach, D. L., and E. L. Rowan, 1986, Genetic link between Ouachita foldbelt tectonism and the Mississippi Valley-type lead-zinc deposits of the Ozark, Geology, v. 14, p. 931-935.

LeBlanc, S. L., 2014, High resolution sequence stratigraphy and reservoir characterization of the "Mississippian limestone" in north-central Oklahoma: M.S. thesis, Oklahoma State University, 449 p.

Machel, H. G., H. R. Krouse, and R. Sassen, 1995, Products and distinguishing criteria of bacterial and thermochemical sulfate reduction: Applied Geochemistry, v. 10, p. 373-389.

Mazzullo, S. J., B. W. Wilhite, and D. R. Boardman, 2011, Lithostratigraphic architecture of the Mississippian Reeds Spring Formation (Middle Osagean) in southwest Missouri, northwest Arkansas, and northeast Oklahoma: Outcrop analog of subsurface petroleum reservoirs: Shale Shaker, v. 61, p. 254-269.

Mazzullo, S.J., D. R. Boardman, B. W. Wilhite, C. Godwin, and B. T. Morris, 2013, Revisions of outcrop lithostratigraphic nomenclature in the Lower to Middle Mississippian Subsystem (Kinderhookian to Basal Meramecian Series) along the shelf-edge in southwest Missouri, northwest Arkansas, and northeast Oklahoma: Shale Shaker, v. 63, p. 414-454.

Mii, H., E. L. Grossman, and T. E. Yancey, 1999, Carboniferous isotope stratigraphies of North America: Implications for Carboniferous paleoceanography and Mississippian glaciation: Geological Society of America Bulletin, v. 111, p. 960-973.

Milam, K., 2013, OSU-Industry consortium eyes Mississippian: AAPG Explorer, v. 34, no. 3, p. 36-39.

Mohammadi, S., J. M. Gregg, K. L. Shelton, M. S. Appold, and J. O. Puckette, (in press), Influence of late diagenetic fluids on Mississippian carbonate rocks on the Cherokee – Ozark Platform, NE Oklahoma, NW Arkansas, SW Missouri, and SE Kansas: *in* Grammer, G. M., Gregg J. M., Puckette, J. O., Jaiswal, P., Pranter, M.,

Mazzullo, S. J., and Goldstein, R. H., eds., Mississippian reservoirs of the mid-continent, U.S.A: American Association of Petroleum Geologists Memoir.

Mohammadi, S., T. A. Ewald, J. M. Gregg, and K. L. Shelton, (in editorial review), Diagenesis of Mississippian carbonate rocks in north-central Oklahoma, USA: *in* Grammer, G. M., Gregg J. M., Puckette, J. O., Jaiswal, P., Pranter, M., Mazzullo, S. J., and Goldstein, R. H., eds., Mississippian reservoirs of the mid-continent, U.S.A: American Association of Petroleum Geologists Memoir.

Oehlert, A. M., and P. K. Swart, 2014, Interpreting carbonate and organic carbon isotope covariance in the sedimentary record: Nature Communications, 7 p. DOI: 10.1038/ncomms5672.

O'Neil, J. R., R. N. Clayton, and T. K. Mayeda, 1969, Oxygen isotope fractionation in divalent metal carbonates: Journal of Chemical Physics, v. 51, p. 5547-5558.

Roedder, E., 1984, Fluid inclusions: Mineralogical Society of America, Reviews in Mineralogy, v. 12, 644 p.

Roedder, E., 1967, Metastable superheated ice in liquid-water inclusions under high negative pressure: Science, v. 155, p. 1413-1417.

Rosenbaum, J., and S. M. F. Sheppard, 1986, An isotopic study of siderites, dolomites and ankerites at high temperatures: Geochimica et Cosmochimica Acta, v. 50, p. 1147-1150.

Serpa, L., T. Setzer, and L. Brown, 1989, COCORP seismic-reflection profiling in northeastern Kansas: Kansas Geological Survey, Bulletin 226, p. 165-176.

Shelton, K. L., and P.M. Orville, 1980, Formation of synthetic fluid inclusions in natural quartz: American Mineralogist, v. 65, p. 1233-1236.

Shelton, K. L., R. M. Bauer, and J. M. Gregg, 1992, Fluid-inclusion studies of regionally extensive epigenetic dolomites, Bonneterre Dolomite (Cambrian), southeast Missouri: Evidence of multiple fluids during dolomitization and lead-zinc mineralization: Geological Society of America Bulletin, v. 104, p. 675-683.

Shelton, K. L., J. M. Gregg, and A. W. Johnson, 2009, Replacement dolomites and ore sulfides as recorders of multiple fluids and fluid sources in the southeast Missouri Mississippi Valley-Type district: Halogen-$^{87}Sr/^{86}Sr$-$\delta^{18}O$-$\delta^{34}S$ systematics in the Bonneterre Dolomite: Economic Geology, v. 104, p. 733-748.

Shelton, K. L., J. M. Beasley, J. M. Gregg, M. S. Appold, S. F. Crowley, J. P. Hendry, and I. D. Somerville, 2011, Evolution of a Carboniferous carbonate-hosted sphalerite breccia deposit, Isle of Man: Mineralium Deposita, v. 46, p. 859-880.

Temple, B. J., 2016, Petrology and geochemistry of Lower Ordovician and Upper Cambrian (Arbuckle) carbonates, NE Oklahoma and SW Missouri: M.S. thesis, Oklahoma State University, 70 p.

Wang, Y., T. Thompson, and G. M. Grammer (this volume), Fracture characterization and prediction in the "Mississippian Limestone", central and northeastern Oklahoma: *in* Grammer, G. M., Gregg J. M., Puckette, J. O., Jaiswal, P., Pranter, M., Mazzullo, S. J., and Goldstein, R. H., eds., Mississippian reservoirs of the mid-continent, U.S.A: American Association of Petroleum Geologists Memoir, in editorial review.

Table 1. Fluid inclusion microthermometric data for fluid inclusions in carbonate cements. (Vertical = vertical fracture, Breccia = breccia fracture, Shear = shear zone, Solution = solution-enlarged fracture, Ptygmatic = ptygmatic fracture).

Sample ID	Location	Open space type	Assemblage	Mineral	T_h (°C)	T_m (°C)	Calculated salinity (wt.% eq. NaCl)	Type
GS-9699	Blaine Co., OK (#1)	Breccia	Assemblage 1	Calcite	142	-1.9	3.2	Primary
				Calcite	142	-1.9	3.2	
				Calcite	131	-2.5	4.2	
				Calcite	131			
				Calcite	131	-2.5	4.2	
			Assemblage 2	Calcite	138	-1.9	3.2	Primary
				Calcite	141	-1.9	3.2	
				Calcite	141	-2.7	4.5	
				Calcite	140			
				Calcite	141	-1.3	2.2	
				Calcite	141			
				Calcite	141			
				Calcite	141	-1.3	2.2	
				Calcite	141			
			Assemblage 3	Quartz	128	11.7	15.7	Primary
				Quartz	128	-0.7	1.2	
				Quartz	96	0.7	1.2	
				Quartz	64	3.2	5.3	

				Quartz	104	3.6	5.9	
				Quartz	104			
GS-9698	Blaine Co., OK (#2)	Breccia	Assemblage 1	Calcite	87	-2.6	4.3	Primary
			Assemblage 2	Calcite	117			
				Calcite		-2.5	4.2	
			Assemblage 3	Calcite	110	-2.4	4.0	Secondary
			Assemblage 4	Calcite	106	-18.8	21.5	Secondary
			Assemblage 5	Calcite	115			Secondary
				Calcite	115	-0.3	0.5	
				Calcite	101			
				Calcite	101			
				Calcite	101			
CA-1-99336-B	Canadian Co., OK	Vertical/shear	Assemblage 1	Calcite	141			Primary
			Assemblage 2	Calcite	105	-1.1	1.9	Primary
			Assemblage 3	Calcite	48			Primary
				Calcite	48			
				Calcite	48			
				Calcite	48			
				Calcite	48			
				Calcite	48			
				Calcite	48			
				Calcite	48			

				Calcite	48			
				Calcite	48			
				Calcite	48			
				Calcite	48			
				Calcite	48			
			Assemblage 4	Calcite	111			Primary
				Calcite	111			
				Calcite	148			
AM-8371	Kingfisher Co., OK	Ptygmatic	Assemblage 1	Calcite	130	-2.5	4.2	Primary
SMD-2222	Logan Co., OK (#1)	Solution/vertical	Assemblage 1	Calcite	140	-2.2	3.7	Primary
SMD 2100	Osage Co., OK (#1)	Ptygmatic	Assemblage 1	Calcite	97	-0.7	1.2	Primary
			Assemblage 2	Calcite	112	-0.5	0.8	Primary
				Calcite	118	-0.5	0.8	
				Calcite	118	-0.5	0.8	
			Assemblage 3	Calcite	81	-0.1	0.2	Primary
				Calcite	105	-0.1	0.2	
				Calcite	84	-1.5	2.6	
				Calcite		-0.5	0.9	
			Assemblage 4	Calcite	87	2.5		Primary
				Calcite	80	2.5		
				Calcite		0.3		
				Calcite	105			

			Assemblage 5	Calcite	81	3.0		Primary
			Assemblage 6	Calcite	116	0.7		Primary
SMD 2102	Osage Co., OK (#2)	Solution/vertical	Assemblage 1	Calcite	126	-3.7	6.0	Primary
				Calcite	126	-1.8	3.0	
				Calcite	125	-3.8	6.1	
			Assemblage 2	Calcite	164	-1.9	3.2	Primary
				Calcite	149	-1.9	3.2	
			Assemblage 3	Calcite	115	-21.0	22.8	Primary
				Calcite	118	-19.0	21.7	
				Calcite		-19.0	21.7	
				Calcite		-15.4	19.0	
				Calcite	127			
			Assemblage 4	Calcite	173	-17.5	20.6	Primary
				Calcite	168	-15.4	19.0	
			Assemblage 5	Calcite	86	-23.0	24.3	Primary
			Assemblage 6	Calcite	122	-23.0	24.3	
				Calcite	126	-21.2	23.1	
			Assemblage 7	Calcite	135	-2.1	3.5	Primary
			Assemblage 8	Quartz	126	-21.6	23.4	Primary
				Quartz	130	-21.6	23.4	
				Quartz	101	-21.6	23.4	
				Quartz	130	-21.6	23.4	

			Assemblage 9	Quartz	83	-19.6	22.1	Primary
				Quartz	87	-19.6	22.1	
				Quartz	98	-22.3	23.9	
				Quartz	98	-18.6	21.4	
				Quartz	98	-17.8	20.8	
				Quartz	98	-18.5	21.3	
			Assemblage 10	Quartz	122	-2.0	3.4	Primary
				Quartz	123	-2.9	4.8	
				Quartz	119	-1.4	2.4	
				Quartz	113	-1.4	2.4	
			Assemblage 11	Quartz	102	-2.3	3.9	Primary
				Quartz	102	-2.0	3.4	
				Quartz	108	-2.3	3.9	
				Quartz	108	-0.4	0.7	
SMD-2216	Payne Co., OK (#2)	Vertical	Assemblage 1	Calcite	80			
			Assemblage 2	Calcite	74	-8.9	12.7	Primary
			Assemblage 3	Calcite	74	-21.1	23.2	Primary
				Calcite	78	-21.1	23.1	
			Assemblage 4	Calcite	122	0.7		Primary
				Calcite	111	1.1		
			Assemblage 5	Calcite	89	-2.1	3.5	Primary
SMD-2217	Payne Co., OK (#3)	Vertical/ptygmatic	Assemblage 1	Calcite	83			Primary

				Calcite	83			
				Calcite	83			
				Calcite	83			
				Calcite	83			
				Calcite	83			
				Calcite	83			
			Assemblage 2	Calcite	156			Primary
			Assemblage 3	Calcite	119			Primary
SMD-2208	Payne Co., OK (#1)	Solution/vertical	Assemblage1	Calcite	96	1.4		Primary?
				Calcite	128	1.4		
			Assemblage 2	Calcite	77			Primary?
				Calcite	77			
			Assemblage 3	Calcite	100	1.0		Primary?
				Calcite	88			
				Calcite	90	2.5		
				Calcite	90	2.5		
				Calcite	90	2.5		
				Calcite	90	2.5		
				Calcite	90	2.5		
				Calcite	90	2.5		
				Calcite	90	2.5		

		Calcite	90	2.5		
		Calcite	90	2.5		
		Calcite	90	2.5		
		Calcite	90	2.5		
		Calcite	90	2.5		
		Calcite	90	2.5		
		Calcite	90	2.5		
		Calcite	90	2.5		
	Assemblage 4	Calcite	98	-0.3	0.5	Primary?
		Calcite	98	-0.3	0.5	
		Calcite	98	-0.3	0.5	
		Calcite	98	-0.3	0.5	
		Calcite	98	-0.3	0.5	
		Calcite	98	-0.3	0.5	
		Calcite	98	-0.3	0.5	
		Calcite	98	-0.3	0.5	
		Calcite	98	-0.3	0.5	
		Calcite	98	-0.3	0.5	
		Calcite	98	-0.3	0.5	
		Calcite	98	-0.3	0.5	
		Calcite	98	-0.3	0.5	
		Calcite	98	-0.3	0.5	

		Calcite	98	-0.3	0.5	
		Calcite	98	-0.3	0.5	
		Calcite	98	-0.3	0.5	
		Calcite	98	-0.3	0.5	
		Calcite	98	-0.3	0.5	
		Calcite	98	-0.3	0.5	
		Calcite	98	-0.3	0.5	
		Calcite	96	0.4		
	Assemblage 5	Calcite	90	1.8		Primary?
		Calcite	100	1.8		
		Calcite	101	1.3		
		Calcite	101	1.3		
		Calcite	101	1.3		
		Calcite	101	1.3		
		Calcite	101	1.3		
		Calcite	101	1.3		
		Calcite	101	1.3		
		Calcite	101	1.3		
		Calcite	101	1.3		
		Calcite	101	1.3		
		Calcite	101	1.3		
		Calcite	101	1.3		

		Calcite	101	1.3	
		Calcite	101	1.3	
		Calcite	101	1.3	
		Calcite	101	1.3	
		Calcite	101	1.3	
		Calcite	101	1.3	
		Calcite	101	1.3	
		Calcite	101	1.3	
		Calcite	101	1.3	
		Calcite	97	1.3	
		Calcite	103	1.3	
		Calcite	103	1.3	
	Assemblage 6	Calcite	92		Primary?
		Calcite	92		
		Calcite	92		
		Calcite	92		
		Calcite	92		
		Calcite	92		
		Calcite	92		
		Calcite	92		
		Calcite	92		
		Calcite	92		

		Calcite	92		
		Calcite	92		
		Calcite	92		
		Calcite	92		
		Calcite	92		
		Calcite	92		
		Calcite	92		
		Calcite	92		
		Calcite	92		
		Calcite	92		
		Calcite	92		
	Assemblage 7	Calcite	86		Primary
		Calcite	80	1.9	
		Calcite	80	1.9	
		Calcite	80	2.3	

Table 2. Stable isotope data for calcite cements and host rocks. Clay-sized calcite referred to calcite mud. (Calcite #1 is earlier than #2, but both are late calcite cements), (Vertical = vertical fracture, Breccia = breccia fracture, shear = Shear zone, solution = solution-enlarged fracture, ptygmatic = ptygmatic fracture). *R shows data from Wang et al. (in editorial review). TE shows data from Mohammadi et al. (in editorial review).

Sample	**Locality**	**Open space type**	**Mineralogy**	**$\delta^{13}C$‰ (VPDB)**	**$\delta^{18}O$‰ (VPDB)**	**$\delta^{18}O$‰ (VSMOW)**
GS-9699-A	Blaine Co., OK	Breccia	Calcite cement	-0.78	-6.40	24.32
GS-9699-B			Pelletic micrite	-3.45	-1.31	29.57
GS-9834-A		Vertical	Calcite cement #1	-0.50	-5.79	24.95
GS-9834-B		Vertical	Calcite cement #2	-0.18	-7.30	23.39
GS-9834-C			Pelletic micrite	-0.96	-1.07	29.82
GS-9698-A		Breccia	Calcite cement	0.36	-2.41	28.44
GS-9698-B			Pelletic micrite	-3.38	-2.53	28.31
GS-9696-A		Vertical	Calcite cement	0.64	-6.21	24.52
GS-9696-B			Pelletic micrite	-1.62	-1.64	29.23
CA-1-99336-A-A	Canadian Co., OK	Vertical/shear	Calcite cement #1	-1.16	-7.25	23.45
CA-1-99336-A-B		Vertical/shear	Calcite cement #2	-1.05	-6.96	23.74
CA-1-99336-A-C			Pelletic micrite	-0.02	-3.64	27.17

CA-1-10071.11		Ptygmatic	Calcite cement	1.15	-7.42	23.27
CA-1-9985.9		Vertical	Calcite cement	-1.22	-6.55	24.17
CA-1-10174.6			Brachiopod	0.41	-2.64	28.20
CA-1-10208		Vertical	Calcite cement	0.99	-7.64	23.04
AM-8371-A	Kingfisher Co., OK	Ptygmatic	Calcite cement	1.82	-7.34	23.35
AM-8371-B			Calcite mud	2.31	-3.24	27.58
AM-8312-A		Ptygmatic	Calcite cement	1.92	-7.19	23.51
AM-8312-B			Calcite mud	2.07	-4.93	25.84
SMD-2222-A	Logan Co., OK (#1)	Solution/vertical	Calcite cement	1.30	-5.32	25.43
SMD-2222-B			Pelletic micrite	1.65	-3.48	27.33
SMD-2223-A		Solution/vertical	Calcite cement	1.45	-5.37	25.39
SMD-2223-B			Pelletic micrite	-0.47	-3.11	27.71
TE15	Logan Co., OK (#2)	-	Skeletal debris	1.55	-2.51	28.33
TE15.D		-	Replacive dolomite	1.58	-1.73	29.14
TE16		-	Skeletal debris	2.22	-3.58	27.23
TE17		-	Skeletal debris	2.02	-3.22	27.60
TE18		-	Skeletal debris	2.16	-4.54	26.24
TE19		-	Skeletal debris	2.35	-4.07	26.72

TE20		-	Skeletal debris	2.28	-2.61	28.23
TE21		-	Skeletal debris	2.66	-3.64	27.17
TE22		-	Skeletal debris	2.17	-4.19	26.60
TE23		-	Skeletal debris	2.33	-2.88	27.95
TE24		-	Skeletal debris	1.93	-3.33	27.49
TE25		-	Skeletal debris	0.44	-4.34	26.45
TE26		-	Skeletal debris	-0.45	-3.19	27.63
SMD-2100	Osage Co., Ok	Ptygmatic	Calcite Cement	2.58	-4.04	26.76
SMD-2102		Solution/vertical	Calcite Cement	-2.58	-6.21	24.52
SMD-2103		Breccia	Calcite Cement	0.90	-7.06	23.64
*R-6738	Osage Co., Ok	Ptygmatic	Calcite Cement	2.54	-6.44	24.28
*R-6742		Ptygmatic	Calcite Cement	2.58	-6.12	24.61
*R-6740		Ptygmatic	Calcite Cement	1.19	-6.83	23.88
*R-6744		Ptygmatic	Calcite Cement	0.45	-6.23	24.50
*R-6741		Ptygmatic	Calcite Cement	-4.46	-6.37	24.35
*R-6746		Ptygmatic	Calcite Cement	-4.21	-6.14	24.59
*R-6739		Ptygmatic	Calcite Cement	2.24	-9.21	21.43
*R-6743		Ptygmatic	Calcite Cement	2.51	-8.27	22.39
*R-6745		Ptygmatic	Calcite Cement	-3.40	-6.65	24.06
SMD-2206-A	Payne Co., OK (#1)	Vertical/ptygmatic/shear	Calcite cement	2.05	-4.98	25.78
SMD-2206-B			Pelletic micrite	1.89	-7.58	23.11

SMD-2208-A		Solution/vertical	Calcite cement	1.02	-6.02	24.71
SMD-2208-B			Pelletic micrite	1.21	-5.18	25.58
SMD-2211-A		Vertical/ptygmatic	Calcite cement	-2.25	-4.89	25.88
SMD-2211-B			Pelletic micrite	1.30	-3.23	27.59
SMD-2213-A	Payne Co., OK (#2)	Vertical	Calcite cement	1.46	-5.72	25.02
SMD-2213-B			Pelletic micrite	1.45	-3.95	26.85
SMD-2216-A		Vertical	Calcite cement	-1.18	-4.45	26.34
SMD-2216-B			Pelletic micrite	1.21	-3.85	26.95
SMD-2217		Vertical/ptygmatic	Calcite cement	-4.88	-6.01	24.73
TE1	Wood Co., OK	-	Skeletal debris	-3.45	-1.48	29.39
TE2		-	Skeletal debris	-0.71	-5.23	25.53
TE3		-	Skeletal debris	0.13	-5.35	25.40
TE4		-	Skeletal debris	0.20	-5.13	25.63
TE5		-	Skeletal debris	1.97	-3.07	27.76
TE5.D		-	Replacive dolomite	2.87	0.51	31.45
TE6		-	Skeletal debris	2.54	-0.02	30.90
TE7		-	Skeletal debris	2.09	-3.74	27.06
TE7.D		-	Replacive dolomite	2.87	0.02	30.94
TE8		-	Skeletal debris	2.28	-3.18	27.64

TE9	-	Skeletal debris	2.14	-3.64	27.17
TE9.D	-	Replacive dolomite	2.77	-0.44	30.47
TE10	-	Skeletal debris	2.09	-3.51	27.30
TE11	-	Skeletal debris	1.91	-3.97	26.83
TE12	-	Skeletal debris	2.05	-3.32	27.50
TE13	-	Skeletal debris	2.08	-3.98	26.82
TE14	-	Skeletal debris	2.32	-2.99	27.84

Table 3. Sr and oxygen isotope data (‰) for carbonate components in rocks of the study area. (Vertical = vertical fracture, Breccia = breccia fracture, shear = shear zone, Solution = solution-enlarged fracture, Ptygmatic = ptygmatic fracture). Bann shows data from Mohammadi et al. (in editorial review).

Sample	**Location**	**Open space type**	**lithology**	**$^{87}Sr/^{86}Sr$**	**$\delta^{18}O$ (VPDB)**	**$\delta^{13}C$ (VPDB)**
GS-9699	Blaine Co., OK	Breccia	Calcite cement	0.707812	-6.40	-0.78
CA-1-99336-A	Canadian Co., OK	Vertical/shear	Calcite cement	0.707868	-6.96	-1.05
AM-8371	Kingfisher Co., OK	Ptygmatic	Calcite cement	0.707898	-7.34	1.82
AM-8371			Calcite mud	0.708210	-3.24	2.31
SMD-2222	Logan Co., OK	Solution/vertical	Calcite cement	0.707801	-5.32	1.30
SMD-2222			Pelletic micrite	0.707785	-3.48	1.65
SMD-2102	Osage Co., OK	Solution/vertical	Calcite cement	0.711238	-6.21	-2.58
BB-3170	Osage Co., OK	Ptygmatic	Calcite cement	0.710229	-6.12	-2.58
BB-3406		Ptygmatic	Calcite cement	0.711198	-6.14	-4.21
BB-3407		Ptygmatic	Calcite cement	0.711080	-6.65	-3.4
SMD-2211	Payne Co., OK (#1)	Vertical/ptygmatic	Calcite cement	0.708203	-4.89	-2.25
SMD-2216	Payne Co., OK (#2)	Vertical	Calcite cement	0.708055	-4.45	-1.18
SMD-2216			Pelletic micrite	0.707981	-3.85	1.21
Bann-5274	Wood Co., OK	-	Replacive dolomite	0.707820	0.51	2.87

Table 4. T_h values of fluid inclusions, $\delta^{18}O$ values of carbonate cements and calculated $\delta^{18}O$ values of calculated waters in equilibrium with these cements and their host rocks at the temperatures shown. The fractionation equation used for calcite is O'Neil, et al. (1969). The mean $\delta^{18}O$ values (VSMOW) for the host limestone in the study area is 27.4‰. (Vertical = vertical fracture, Breccia = breccia fracture, shear = Shear zone, Solution = solution-enlarged fracture, Ptygmatic = ptygmatic fracture).

Sample	**Location and Host Cement**	**Open space type**	**T_h °C**	**$\delta^{18}O_{calcite}$‰ VSMOW**	**$\delta^{18}O_{cement\text{-}depositing\ water}$‰ VSMOW**	**$\delta^{18}O_{water\ for\ Limestone}$‰ VSMOW**
GS-9699	Blaine Co., OK, Calcite	Breccia	131 to 142	24.3	10.12 to 11.32	13.2 to 14.4
GS-9698	Blaine Co., OK, Calcite	Breccia	87 to 117	28.4	9.94 to 12.94	8.9 to 11.9
CA-1-99336-B	Canadian Co., OK, Calcite	Vertical/shear	47, 104 to 147	23.7	-0.26, 7.24 to 10.74	3.4, 10.9 to 14.4
AM-8371	Kingfisher Co., OK, Calcite	Ptygmatic	130	23.3	8.85	12.9
SMD-2222	Logan Co., OK, Calcite	Solution/vertical	140	25.4	11.9	13.9
SMD2100	Osage Co., OK #1, Calcite	Ptygmatic	80 to 120	26.8	7.3 to 11.8	8.7 to 13.1
SMD2102	Osage Co., OK #2, Calcite	Solution/vertical	115, 135, 149, 173	24.5	9.0 to 11.0, 11.9 to 13.5	12.6 to 14.6, 15.5 to 17.1
SMD-2216	Payne Co., OK #1, Calcite	Vertical	74 to 122	26.3	6.84 to 11.54	7.9 to 12.6
SMD-2217	Payne Co., OK #1, Calcite	Vertical/ptygmatic	83	24.7	6.23	8.9
SMD-2208	Payne Co., OK #2, Calcite	Solution/vertical	77 to 112	24.7	4.71 to 8.71	7.4 to 11.4

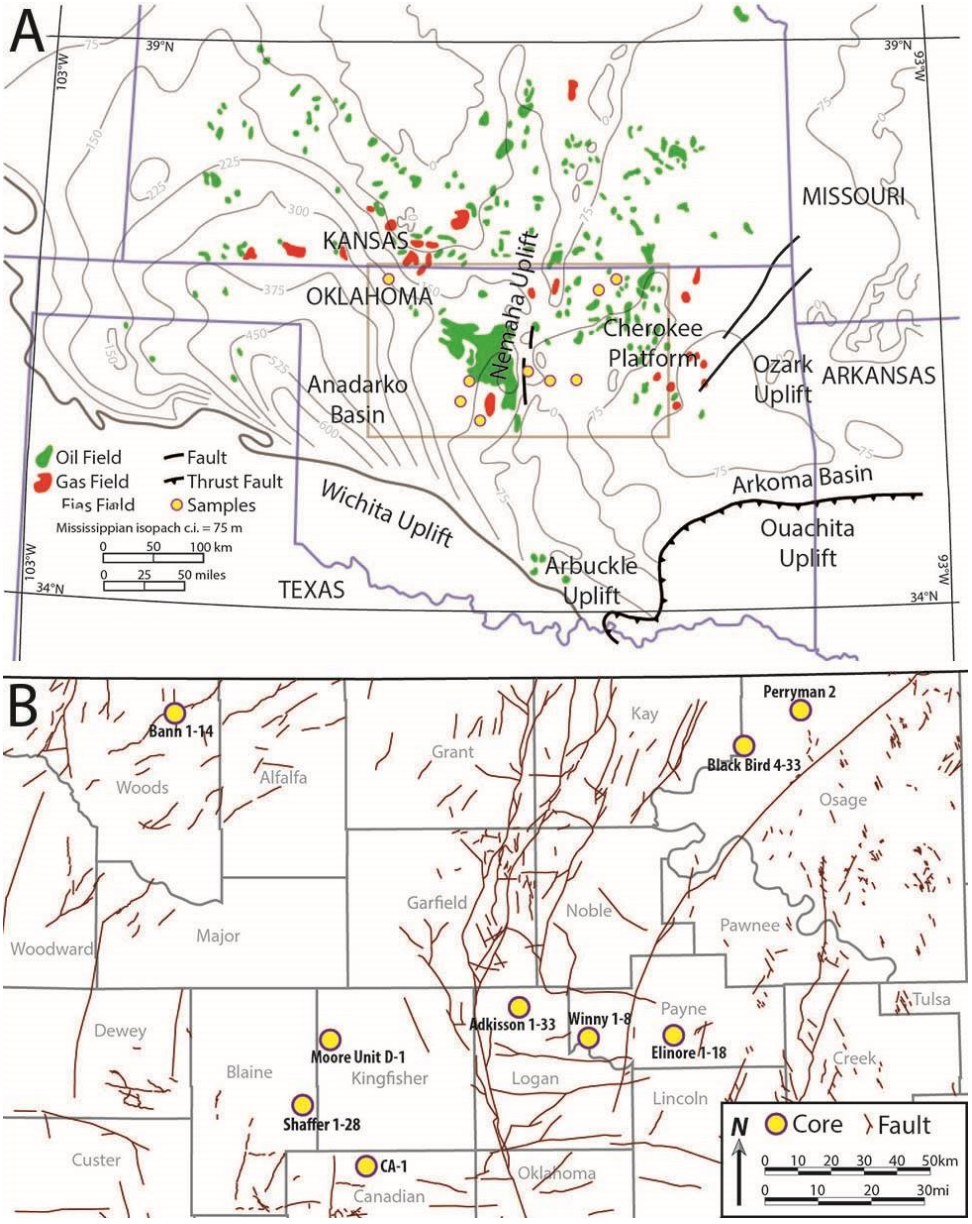

Figure 1. A) Map of Oklahoma and neighboring states showing the study area (tan rectangle) and sample localities. Isopach of Mississippian strata is shown and conventional petroleum production is shown in green (oil) and red (gas). Modified from Harris (1987). B) Structural map for the study area showing cores studied relative to faults penetrating the basement. Modified from Gay (2003) and Darold & Holland (2015).

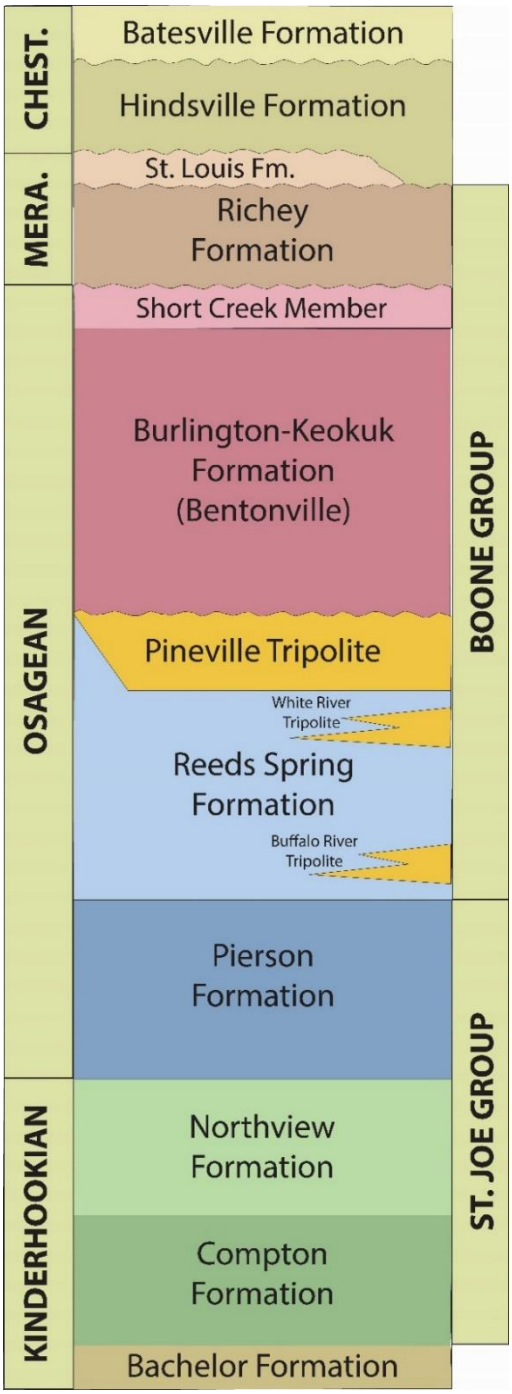

Figure 2. Stratigraphic section for the study area (MERA = Meramecian; CHEST = Chesterian). Modified from Mazzullo et al. (2013).

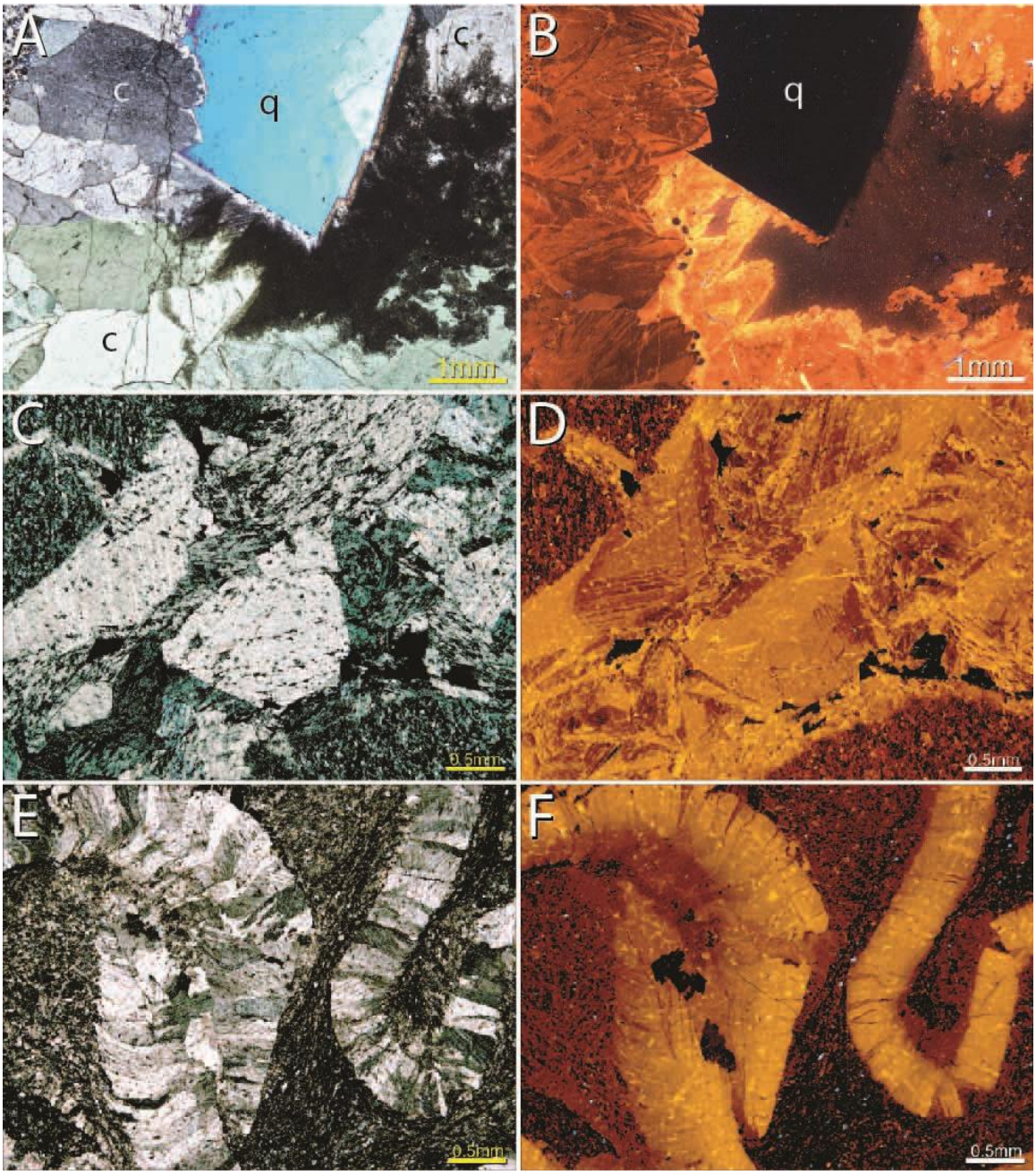

Figure 3. A) Breccia filled by calcite and quartz cement from Blaine County, OK. Parageneticaly, calcite cement is followed by large quartz crystals (compare to quartz cement in Figure 4D) and finally a fine-grained opaque filling (bitumen?). Crossed polarized light. B) CL photomicrograph of (A) showing faint and irregular compositional zoning in calcite cement. Authigenic quartz displays no CL response. C) Cherty mudstone with solution-enlarged vertical (channel) porosity from Kingfisher County, OK filled by calcite cement. Crossed polarized light. D) CL photomicrograph of (A). Note that calcite displays faint, irregular compositional zonation. E) Ptygmatic fracture in cherty, partly dolomitized mudstone from Kingfisher County, OK filled by calcite cement. Note the strong type II and III twinning (Burkhard, 1993) in the calcite. Cross polarized light. F) CL photomicrograph of (E) showing yellow-orange calcite cement filling ptygmatic fracture. Note the small (red under CL) dolomite crystals partly replacing the mudstone matrix.

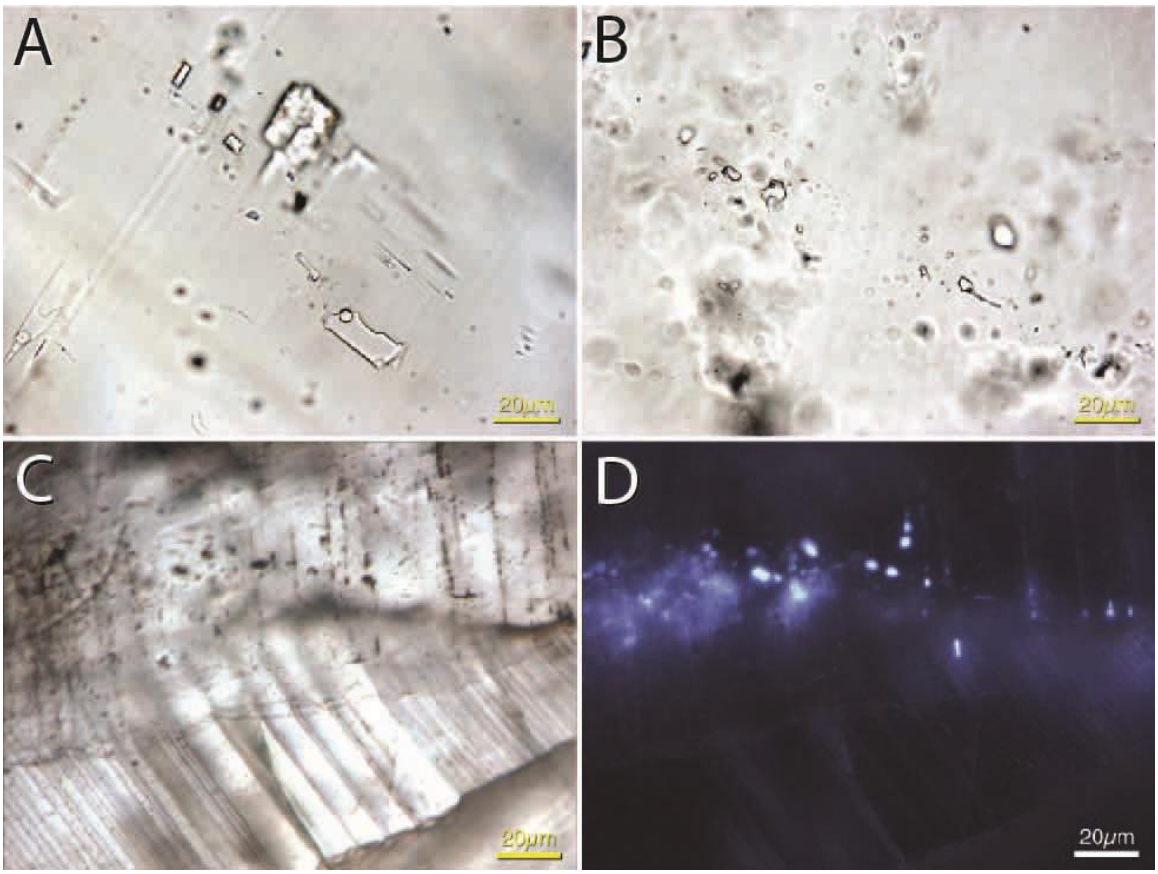

Figure 4. A) An assemblage of primary two-phase fluid inclusions in a breccia-filling calcite cement (Figure 3A). Plane polarized light. B) An assemblage of primary two phase fluid inclusions in a breccia filling quartz cement (Figure 3A). Plane polarized light. C) Assemblage of primary petroleum-bearing inclusions in calcite cement filling a ptygmatic fracture from Kingfisher County, OK. Note the type II twinning (Burkhard, 1993) in the calcite crystals. Plane polarized light. D) Ultraviolet photomicrograph of (C) displaying light blue to cream color fluorescence of petroleum-bearing fluid inclusions.

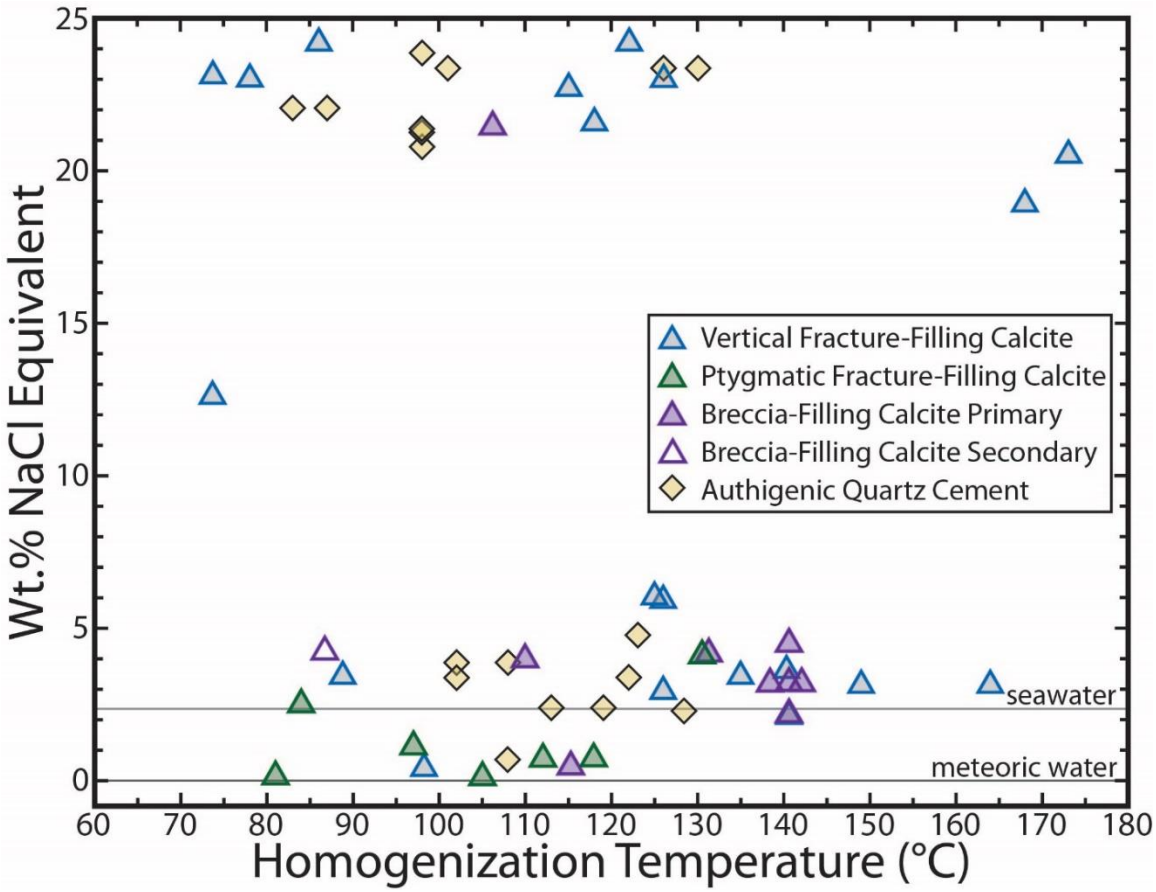

Figure 5. Plot of fluid inclusion homogenization temperature (T_h) versus calculated salinities Note that the data cluster into two distinct salinity populations.

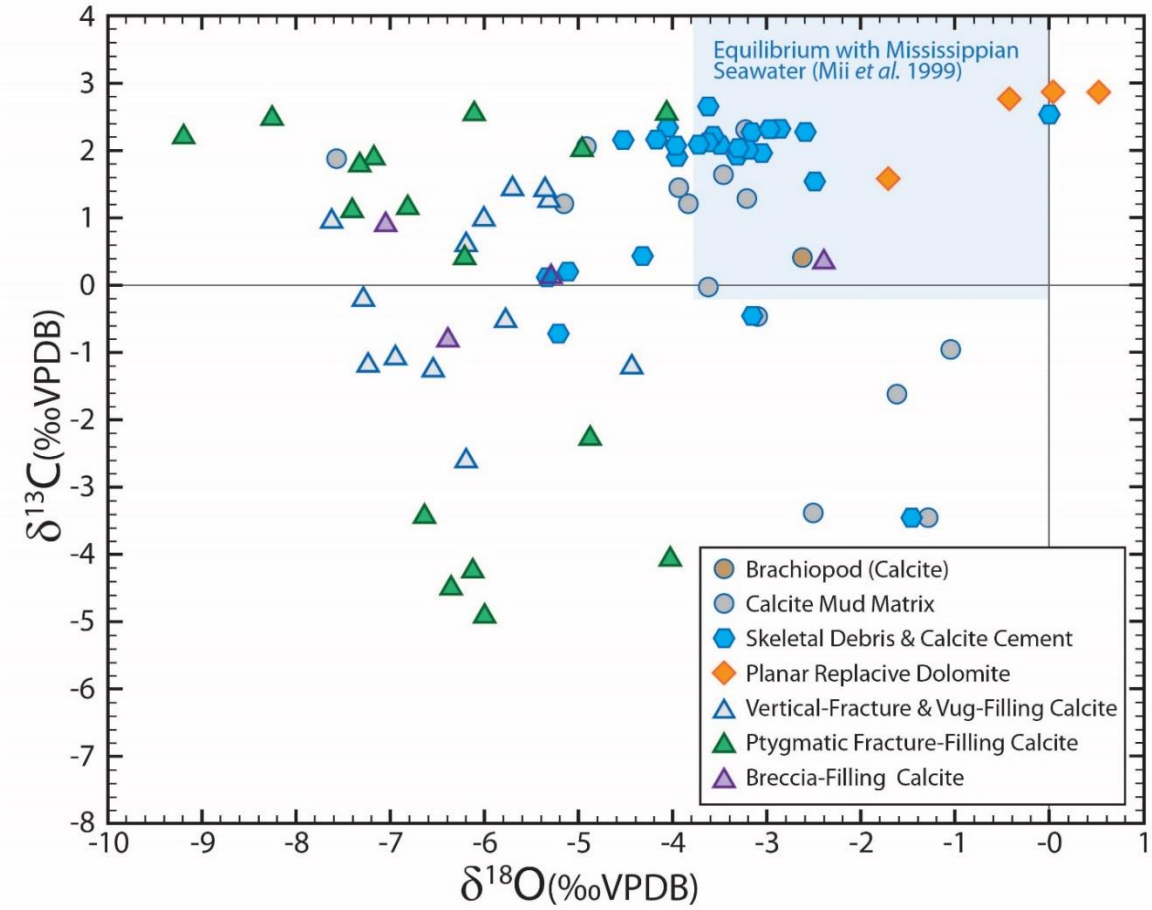

Figure 6. Values of $\delta^{18}O$ and $\delta^{13}C$ (per mil VPDB) for calcite and dolomite in Mississippian rocks of the north-central Oklahoma study area. Data for brachiopod, calcite mud matrix, skeletal debris and calcite cement, and dolomite are from Mohammadi et al. (in editorial review).

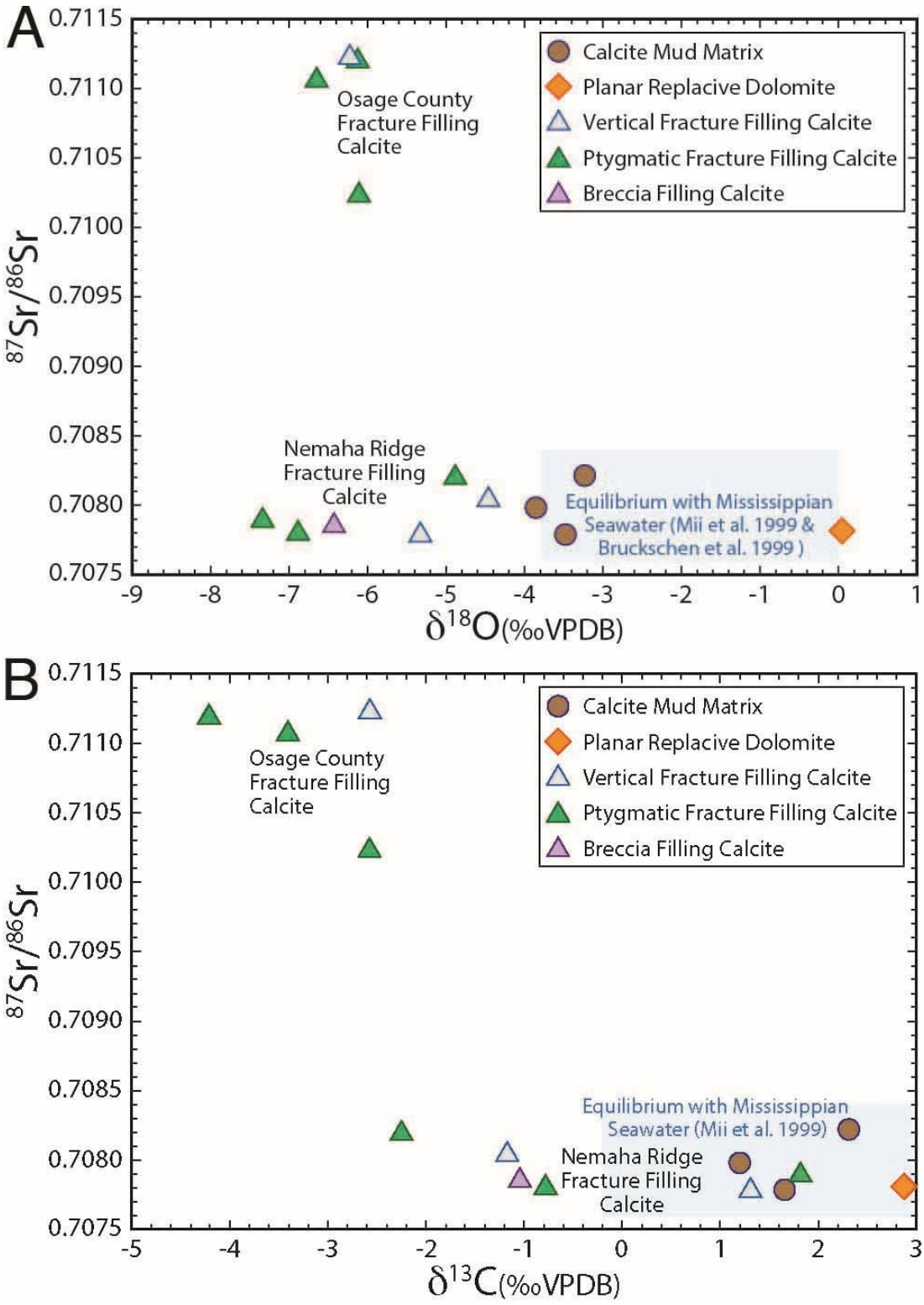

Figure 7. A) Plot of $^{87}Sr/^{86}Sr$ versus $\delta^{18}O$ values for calcite samples of the study area. B) Plot of $^{87}Sr/^{86}Sr$ versus $\delta^{13}C$ values for calcite samples of the study area. Values for calcite cement filling ptygmatic fractures in Osage County are courtesy of G. M. Grammer. Data for brachiopod, calcite mud matrix, skeletal debris and calcite cement, and dolomite are from Mohammadi et al. (in editorial review).

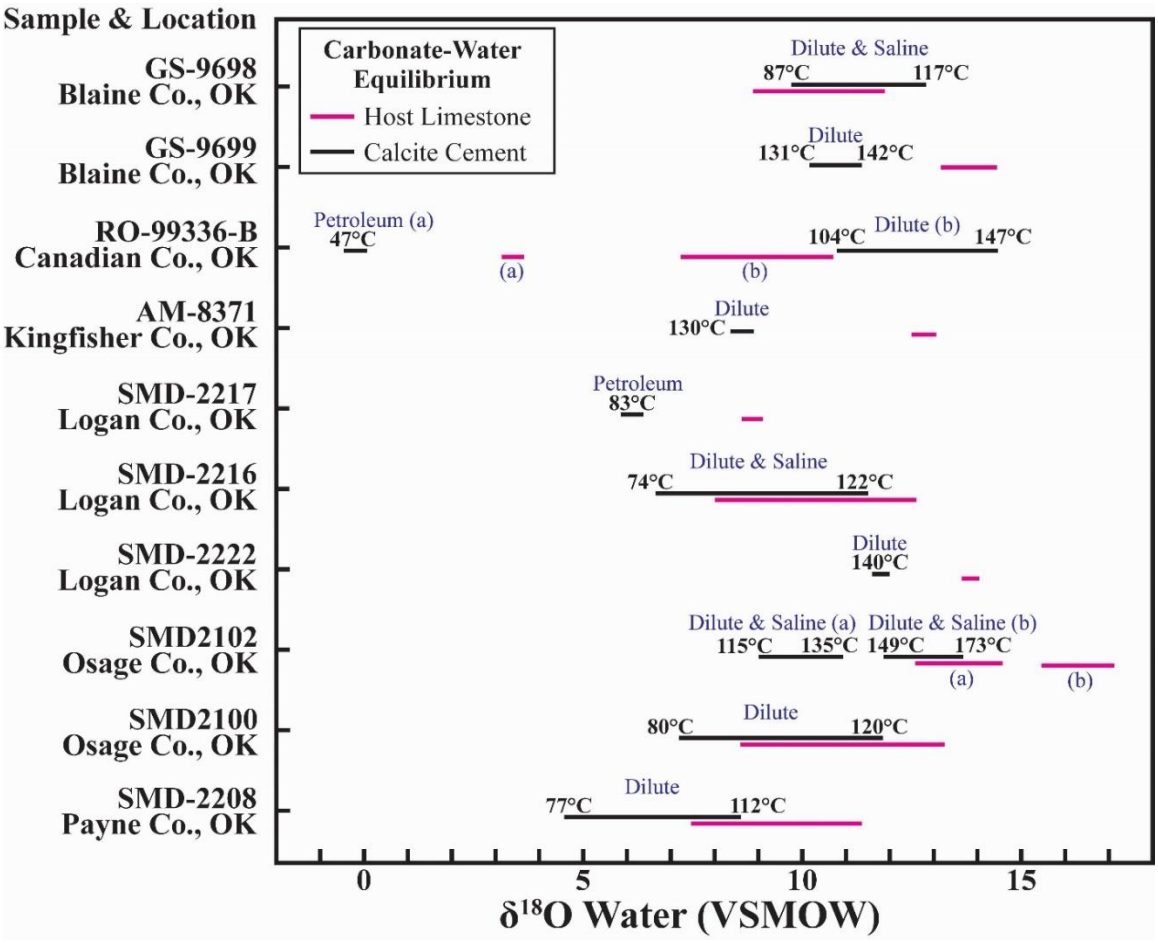

Figure 8. Calculated $\delta^{18}O_{water}$ values in equilibrium with calcite and host limestone using temperature ranges determined from fluid inclusions T_h values. Fractionation equations employed are from O'Neil et al. (1969).

PAPER III

Comparison of fluid inclusion data in Mississippian carbonates and vitrinite reflectance data in underlying Devonian Woodford Shale, Oklahoma, USA

4.0. INTRODUCTION

To better understand the timing of oil generation and migration into the Mississippian carbonate rocks in Oklahoma, vitrinite reflectance data from the underlying Woodford Shale (Upper Devonian-Lower Mississippian) (Cardott, 1989; 2012) were evaluated and compared with fluid inclusion homogenization data gathered for this study from the overlying Mississippian carbonate section (Figure 1). The Woodford Shale is one of the main hydrocarbon source rocks in Oklahoma and likely contributed the hydrocarbons in the Mississippian reservoirs (Comer and Hinch, 1987; Cardott, 1989; Johnson and Cardott, 1992). Since the Woodford Shale was deposited prior to the Ouachita orogeny (late Pennsylvanian to Permian), it should display the thermal history of that period (Cardott, 1989).

Porosity and permeability in Mississippian limestone reservoirs likely was affected by fluids moving upward along faults and fractures (Golestein and King, 2014; Mohammadi et al., in press; Mohammadi et al., in editorial review) (Figure 2). This faulting is associated with the Nemaha uplift and originates in the basement (Gay, 2003a, 2003b).

The activity of these faults likely is related to Late Mississippian or Early Pennsylvanian tectonics associated with the Ouachita and Appalachian orogenies (Gay 1999; Gay, 2003 a; b; Mohammadi et al., in editorial review).

Hood et al. (1975) defined 4 stages of petroleum generation: (1) formation and preservation of organic-rich sediments sourced from photosynthetic organisms, (2) thermal degradation of the organic matter during burial, (3) expulsion and migration of hydrocarbons, and (4) alteration of the petroleum due to continued burial and/or biological activity. The level of thermal maturity defines whether source rocks have been buried for a long enough time and exposed to temperatures that would allow them to generate hydrocarbons. Also indicated is which kind of hydrocarbons they may have generated (Figure 3).

Thermal history and level of hydrocarbon maturation can be determined by several methods including: (1) Fluid inclusion analysis (Tobin and Claxton, 2000), (2) vitrinite reflectance (R_o) (Ritter, 1984), (3) conodont color alteration index (Harris, 1979), and (4) spor and kerogen color alteration (Hood et al., 1975; Peters et al. 1977; Heroux et al., 1979) (Figure 3). In evaluating the thermal maturity of the Woodford Shale in Oklahoma, Cardott (1989; 2012) used vitrinite reflectance. Vitrinite is a component of coal that is comprised of cell wall material of woody tissue of plants. Vitrinite reflectance ($\%R_o$) is determined by the percentage of incident light reflected by vitrinite particles in sedimentary rocks at 500X magnification under oil immersion (Cardott, 2012). Higher R_o values indicate higher temperatures and/or longer periods of burial and also indicate increasing coal rank. Increasing R_o corresponds to physical and chemical changes in organic matter that occur over time with increasing burial and temperature and thus can

be used to assess the thermal maturity of a source rock, such as an organic rich shale (Cardott, 2012).

Fluid inclusion microthermometry differs from vitrinite reflectance in that it determines the minimum temperature of the fluids at the time of trapping of the inclusion and is not dependent on the length of time that the host mineral is held at this temperature (Tobin and Claxton, 2000). By analyzing homogenization temperatures (T_h), the minimum temperature of the fluids that precipitated the hosting mineral, such as open space filling calcite, dolomite, or quartz, can be estimated. In this study, the thermal maturity of the underlying Devonian Woodford Shale, as determined using vitrinite reflectance, is compared to late diagenetic fluid temperatures in the overlying Mississippian limestones, as determined by fluid inclusion microthermometry.

4.1. RESULTS AND DISCUSSION

Vitrinite reflectance (R_o) data for the Woodford Shale in Oklahoma (Cardott, 1989; 2012) are plotted and contoured in Figure 4. Basement faults have been identified throughout the region (Gay, 2003; Darold and Holland, 2015). R_o values in north-central Oklahoma fall largely in the range of >0.5 to 1.0, which corresponds to immature to mature levels of organic maturity (zone of oil generation) (Figure 3). Maturity increases to the southwest and to the southeast into the Anadarko and the Arkoma Basins respectively, as is expected to happen with increasing burial depth of the Woodford Shale. Within the immature to moderate maturity (Ro ≥1.0) zone in northern Oklahoma, however, there are several anomalously high R_o values (≤1.0) in southern Osage, western Payne, and eastern Garfield Counties, most of which appear to be associated with

basement faults. The reason for these anomalous increases in R_o values is not clear although high-temperature (≥140°C) fluid influx along faults, in principle, could be the cause.

T_h values for aqueous fluid inclusions range from 40° to 180°C with most of the T_h values clustered between 80° and 150°C (Figure 5). These temperatures, without pressure corrections, represent minimum temperatures at which the calcite and quartz cements that contain them were precipitated (Goldstein and Reynolds, 1994). Some of the higher temperatures, such as those obtained in Mayes and Ottawa counties can be regarded as outliers and may reflect stretching and/or necking of the inclusions. In any case, the maximum T_h values indicate anomalously high temperatures in the Mississippian section relative to the maximum burial temperatures calculated from R_o values obtained for the underlying Woodford Shale.

The R_o values measured by Cardott (1989; 2012) in northern Oklahoma range from <0.5% to 1.0%. Given these reflectance values the maximum paleo-temperatures expected in this region should range from 60º to 115ºC (Kantsler et al., 1978). But, the T_h values for fluid inclusions in cements of the overlying Mississippian carbonate rocks show much higher maximum temperature values (≥140ºC) (Figure 3 and 4).

Salinities of these included fluids range from 0.0 to 25 Wt.% NaCl equivalent. The higher salinity hydrothermal fluids most likely emanated from deeper Ordovician and/or basement strata and invaded the Mississippian limestone interval. The observation of petroleum-rich inclusions in many of the carbonate cement samples indicates that hydrocarbons, likely sourced in the Woodford Shale, followed the same pathways. The fluids likely moved upward along faults (Figure 2 and 4), which are connected with the

underlying strata (Figure 1), and mixed with less saline resident fluids in the Mississippian strata.

4.2. CONCLUSIONS

Vitrinite reflectance (R_o) data from the Devonian Woodford Shale in northern Oklahoma indicate immature to mature hydrocarbon maturity and correspond to palaeotemperatures between 60° and 115°C. However, in overlying Mississippian rocks, T_h values obtained for fluid inclusions in open space filling carbonate and quartz cements indicate much higher temperatures (≥140°C), suggesting that the fluid event(s) represent short-lived thermal anomalies compared to burial thermal conditions. The basinal fluids that precipitated these cements likely emanated from underlying Cambrian and Ordovician strata and migrated upward along the faults. The presence of petroleum-rich inclusions indicate that this fluid migration likely occurred during the period of petroleum generation and that petroleum generated in the underlying Woodford Shale also moved upward along the faults accompanying the deeper sourced saline basinal fluids. These hot fluids likely are associated with basinal fluid flow movement during Ouachita and Appalachian orogenies.

4.3. REFERENCES

Cardott, B. J., 1989, Thermal maturation of Woodford Shale in the Anadarko Basin: Oklahoma Geological Survey, Circular, 90, p. 32-47.

Cardott, B. J., 2012, Thermal maturity of Woodford Shale gas and oil plays, Oklahoma, USA: International Journal of Coal Geology, v. 103, p. 109-119.

Comer, J. B., and H. H. Hinch, 1987, Recognizing and quantifying expulsion of oil from the Woodford Formation and age-equivalent rocks in Oklahoma and Arkansas: American Association of Petroleum Geologists Bulletin, v. 71, p. 844-858.

Cooper, B. S., S. H. Coleman, P. C. Barnard, and J. S. Butterworth, 1975, Palaeotemperatures in the northern North Sea Basin: in Woodland, A. W. (Ed), Petroluem and continental shelf of Northwest Europe, Applied Science Publishers, London, p. 487-492.

Darold, A. P., and A. A. Holland, 2015, Preliminary Oklahoma optimal fault orientations: Oklahoma Geological Survey Open-File Report, OF4-2015.

Gay, S. P. Jr., 1999, Strike-slip, compressional thrust-fold nature of the Nemaha System in eastern Kansas and Oklahoma: American Association of Petroleum Geologists (AAPG) Midcontinent Section Meeting, p.39-49.

Gay, S. P. Jr., 2003a, The Nemaha Trend – A system of compressional thrust-fold, strike-slip structural features in Kansas and Oklahoma, Part 1: Shale Shaker: v. 54, p. 9-17.

Gay, S. P. Jr., 2003b, The Nemaha Trend – A system of compressional thrust-fold, strike-slip structural features in Kansas and Oklahoma, Part 2: Shale Shaker, v. 54, p. 39-49.

Goldstein, R. H., and T. J. Reynolds, 1994, Systematics of fluid inclusions in diagenetic minerals: Society for Sedimentary Geology (SEPM) short course 31, 199 p.

Goldstein, R. H., and B. D. King, 2014, Impact of hydrothermal fluid flow on Mississippian reservoir properties, southern Midcontinent: Unconventional

Resources Technology Conference (URTeC), 8 P. DOI 10.15530/urtec-2014-1934915.

Gradstein, F. M., J. G. Ogg, M. D. Schmitz, and G. M. Ogg, 2012, The Geologic Time Scale 2012 (Eds.): Elsevier, v. 1, p. 1-435.

Harris, A. G., 1979, Conodont color alteration, an organo-mineral metamorphic index, and Its application to Appalachian Basin geology: Society for Sedimentary Geology (SEPM) Special Publication, no. 26, p. 3-16.

Heroux, Y., A. Chagnon, and R. Bertrand, 1979, Compilation and correlation of major thermal maturation indicators: American Association of Petroleum Geologists Bulletin, no. 12, v. 63, p. 2128-2144.

Hood, A., C. C. M. Gutjahr, and R. L. Heacock, 1975, Organic metamorphism and the generation of petroleum: American Association of Petroleum Geologists Bulletin, no. 6, v. 59, p. 986-996.

Johnson, K.S., and B. J. Cardott, 1992, Geologic framework and hydrocarbon source rocks of Oklahoma: *in* Johnson, K.S., Cardott, B.J. (Eds.), Source Rocks in the Southern Midcontinent, 1990 Symposium: Oklahoma Geological Survey Circular, 93, p. 21–37.

Kantsler, A. J., A. C. Cook, and G. C. Smith, 1978, Organic maturation indices: Oil and Gas Journal, p. 196-205.

Mohammadi, S., J. M. Gregg, K. L. Shelton, M. S. Appold, and J. O. Puckette, (in press), Influence of late diagenetic fluids on Mississippian carbonate rocks on the Cherokee – Ozark Platform, NE Oklahoma, NW Arkansas, SW Missouri, and SE Kansas: *in* Grammer, G. M., Gregg J. M., Puckette, J. O., Jaiswal, P., Pranter, M.,

Mazzullo, S. J., and Goldstein, R. H., eds., Mississippian reservoirs of the mid-continent, U.S.A: American Association of Petroleum Geologists Memoir.

Mohammadi, S., T. A. Ewald, J. M. Gregg, and K. L. Shelton, (in editorial review), Diagenesis of Mississippian carbonate rocks in north-central Oklahoma, USA: *in* Grammer, G. M., Gregg J. M., Puckette, J. O., Jaiswal, P., Pranter, M., Mazzullo, S. J., and Goldstein, R. H., eds., Mississippian reservoirs of the mid-continent, U.S.A: American Association of Petroleum Geologists Memoir.

Peters, K. E., R. Ishiwatari, and I. R. Kaplan, 1977, Color of kerogen as index of organic maturity: American Association of Petroleum Geologists Bulletin, no. 4, v. 61, p. 504-510.

Ritter, U., 1984, The influence of time and temperature on vitrinite reflectance: Org. Geochem. V. 6, p. 473-480.

Shelton, J. W., and L. D. Gerken, 1995, Recognizing sequence surfaces in Mid-continent siliciclastic strata, *in* N. J. Hyne, ed., Sequence stratigraphy of the mid-continent: Tulsa Geological Society Special Publication, no. 4, p. 31-48.

Tissot, B., B. Durand, J. Espitalie, and A. Combaz, 1974, Influence of nature and diagenesis of organic matter in formation of petroleum: American Association of Petroleum Geologists Bulletin, no. 3, v. 58, p. 499-506.

Tobin, R. C., and B. L. Claxton, 2000, Multidisciplinary thermal maturity studies using vitrinite reflectance and fluid inclusion microthermometry: A new calibration of old techniques: American Association of Petroleum Geologists Bulletin, no. 10, v. 84, p. 1647-1665.

Vassoyevich, N. B., Yu. I. Korchagina, N. V. Lopatin, and V. V. Chernyshev, 1970, Principal phase of oil formation: International Geology Review, v. 12, p. 1276-1296.

Vassoyevich, N.B., A.N. Guseva, and Y.M. Zaslavskiy, 1974, K izucheniyu organicheskogo veshchestva sedimentitov (kriticheskiye zamechaniya). V kn.: Organicheskoye veshchestvo sovremennykh i iskopayemykh osadkov i tnetody yego izucheniya [Research on Organic Matter in Sedimentites (Critical Comments). In: Organic Matter in Recent and Ancient Sediments and Methods of Examining It].

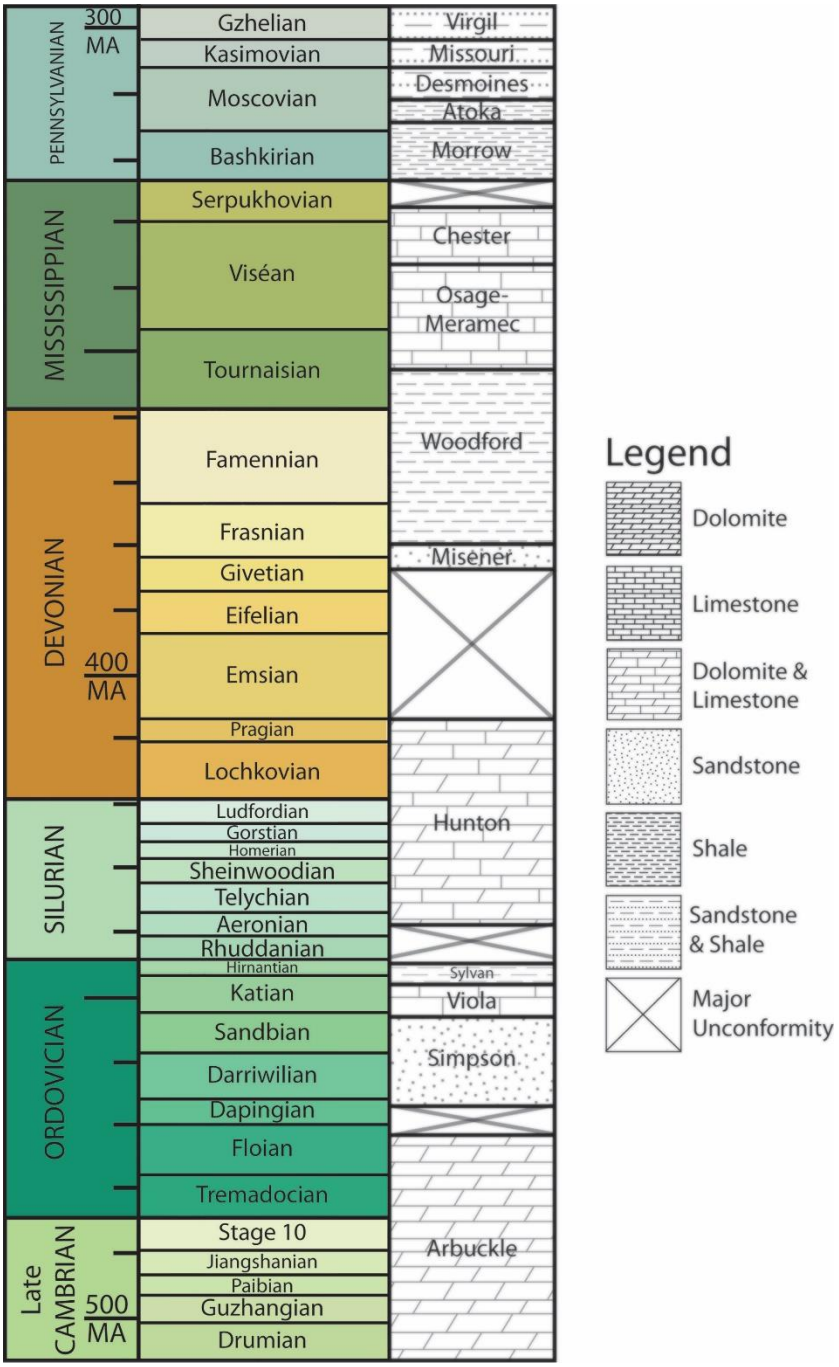

Figure 1. Stratigraphic column for Oklahoma modified from Shelton and Gerken (1995) and Gradstein, et al. (2012). Lithologies are generalized and representative of the section in north-central Oklahoma.

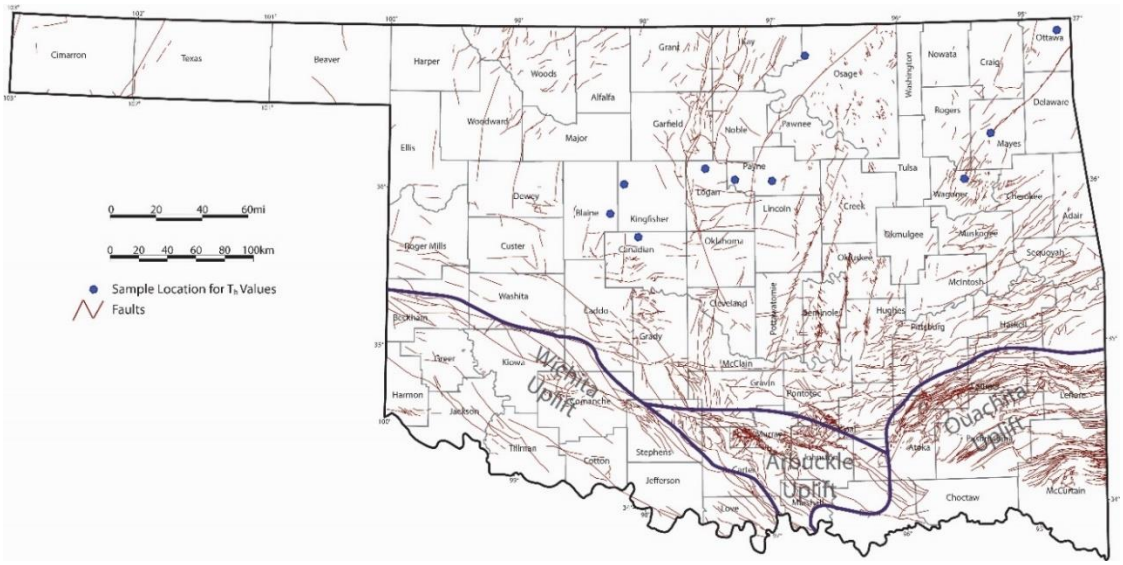

Figure 2. Structural map for Oklahoma showing cores studied relative to faults penetrating the basement. Modified from Gay (2003) and Darold & Holland (2015).

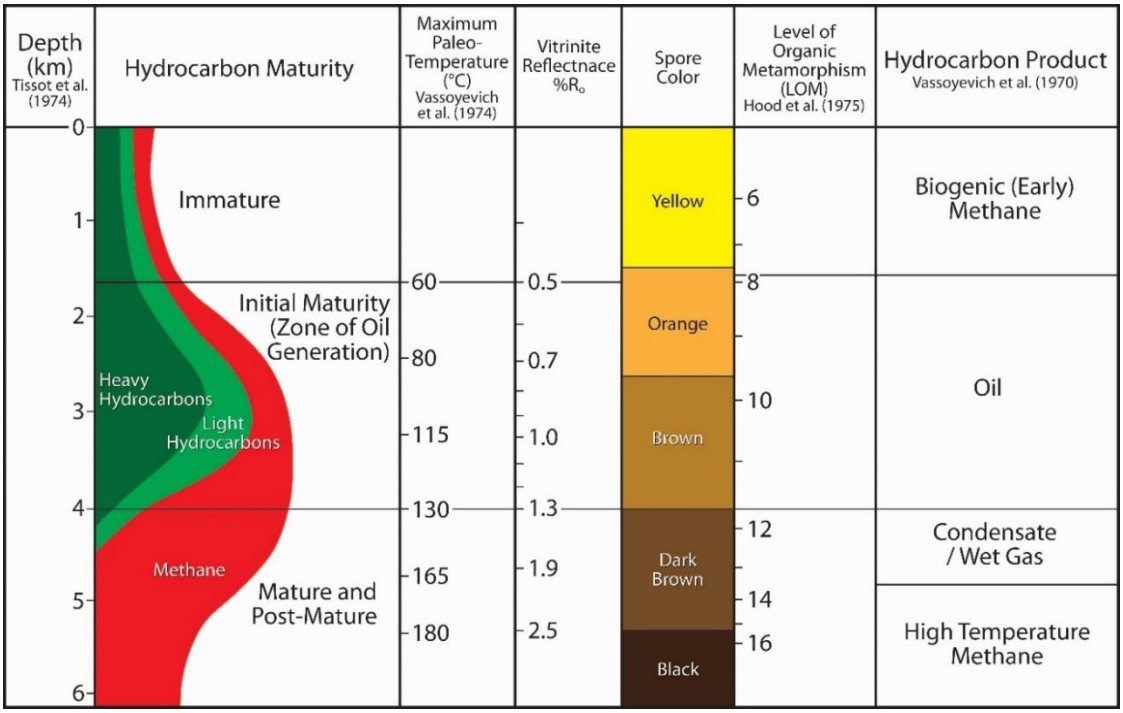

Figure 3. Hydrocarbon generation related to depth of burial and correlated to several organic maturation indices, modified from; Tissot et al. (1974); Cooper et al. (1975); and Kantsler et al. (1978).

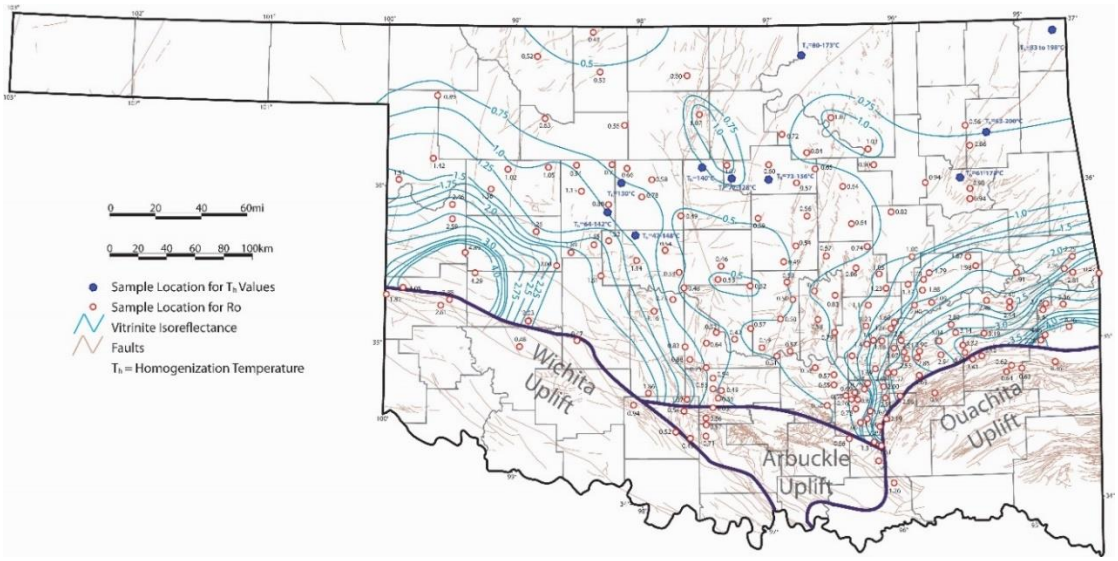

Figure 4. Vitrinite reflectance contour map of Devonian Woodford Shale modified from Cardott (1989; 2012). Range of fluid inclusion T_h values for the overlying Mississippian quartz and carbonate cements also are shown.

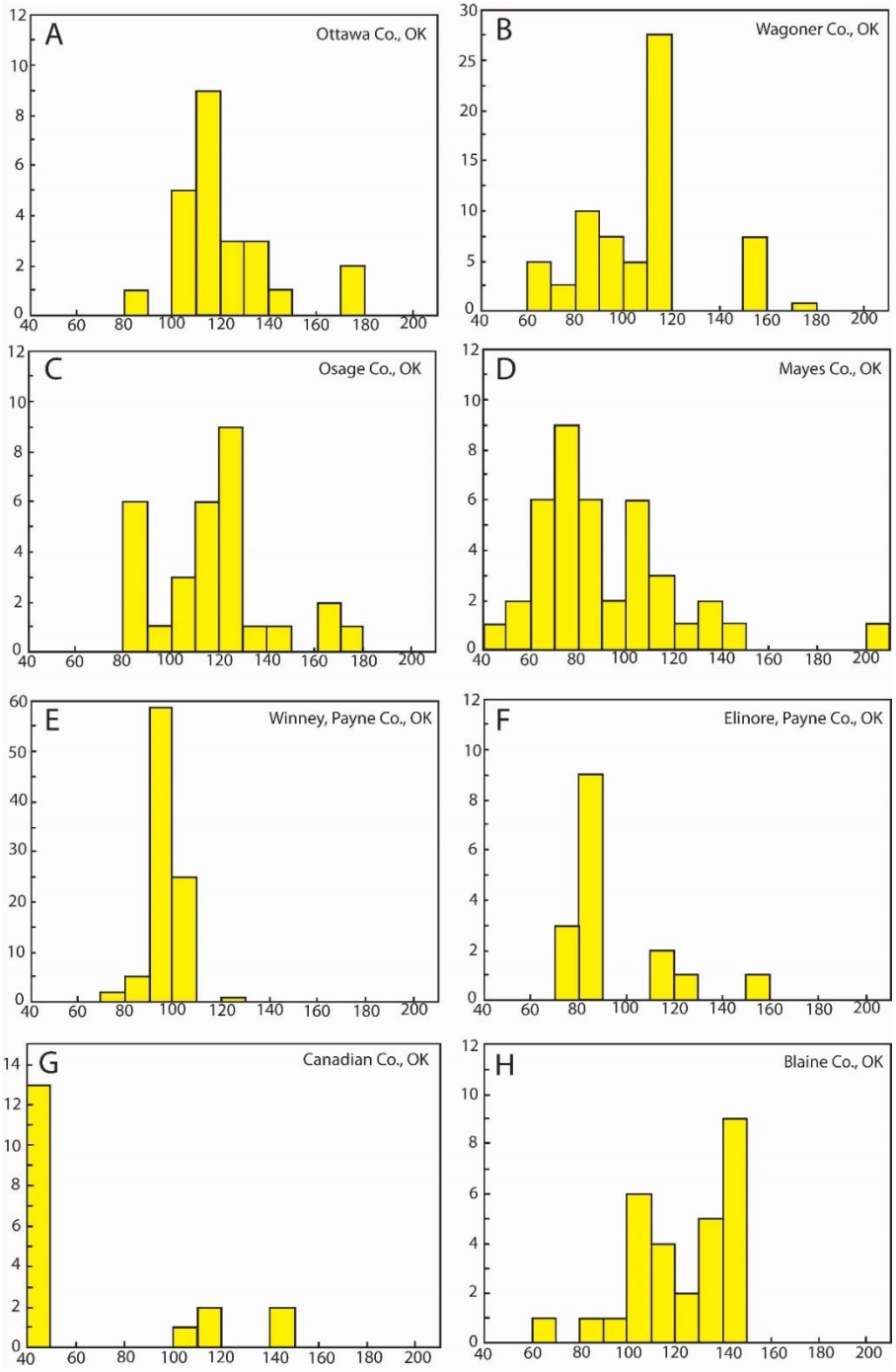

Figure 5. Histograms of fluid inclusion homogenization temperatures (T_h) for Mississippian quartz and carbonate cements for northern Oklahoma counties in the study area.

CONCLUSIONS

Mississippian carbonate rocks in the Cherokee and Ozark platform region were cemented by seawater followed by mixed seawater and meteoric waters during early diagenesis as indicated by petrographic fabrics and carbon, oxygen, and strontium isotope geochemistry. This early cementation partially filled primary intragrain, intergrain, and vug porosity. Remaining primary porosity, as well as late diagenetic fracture and breccia porosity was filled by calcite, dolomite and quartz cements that were precipitated by evolved basinal fluids as indicated by isotope geochemistry and fluid inclusion microthermometry. In the Mississippian limestones in north-central Oklahoma, early calcite cements were precipitated by marine water soon after deposition and by mixed marine and meteoric water during shallow phreatic diagenesis. Late diagenetic calcite and quartz cement was observed filling fractures, breccias, and vugs (FBV).

Two-phase fluid inclusions display T_h values of 50º to 175ºC and salinities of 0 to 25 equivalent wt.% NaCl in Mississippian limestones throughout the southern Mid-continent. Analysis of fluid inclusion data indicate that two distinct fluids were present in the study area during late diagenesis: a dilute fluid having salinities ranging from 0 to 10 wt.% NaCl equivalent and a saline fluid with salinities ranging from 15 to 25 wt.% NaCl equivalent.

Migration of late diagenetic fluids through the Cherokee and Ozark Platform portion of the study area likely corresponded with the emplacement of sulfides in the Tri-State

MVT district, which is related to regional fluid flow events instigated by the Ouachita Orogeny. The basinal fluids were accompanied by petroleum migration as indicated by the presence of petroleum inclusions in some of these cements. The regional flow of warm basinal fluids likely increased the geothermal gradient in the region, affecting the thermal maturity of the rocks. Porosity and permeability of the Mississippian carbonate rocks likely remained relatively high prior to and during migration of these fluids.

High T_h values (70° to 175°C) of fluid inclusions and lower $\delta^{18}O$ values (-9.2 to -4.0‰) of calcite cements in the north-central Oklahoma portion of the study area indicate that they were precipitated by warm basinal fluids during later stages of diagenesis. Low $\delta^{13}C$ values of some calcite cements indicate a component of oxidized organic carbon, possibly concomitant with sulfate reduction associated with petroleum migration. Fluid inclusion microthermometry of FBV-filling calcite and quartz cements indicates two distinct end-members fluid based on salinity, a dilute to moderately saline (0 to 6 Wt.% NaCl) fluid and a high salinity fluid (18 to 25 Wt.% NaCl). Similar results of high T_h values for fluid inclusions and lower $\delta^{18}O$ values for carbonate cements were observed for the Cherokee and Ozark platform region of the study area.

Formation of fractures in the Mississippian carbonate rocks in north-central Oklahoma likely is related to fault movement along the Nemaha Ridge instigated by Ouachita tectonism during the Pennsylvanian and extending into the Permian. This timing corresponds with regional flow of saline basinal fluids associated with the orogenic activity. These fluids ascended along faults and contributed to precipitation of FBV-filling cements. Calculated $\delta^{18}O_{water}$ values indicate that fluids precipitating fracture- and breccia-filling cements in some areas approached isotopic equilibrium with

the host carbonate rocks. In other areas, however, cement-depositing fluids have oxygen isotope signatures that reflect non-resident fluids whose flow was restricted to fault/fracture pathways, which did not permit isotopic equilibration with the host limestone. In particular, fracture-filling calcite veins from Osage County, with high $^{87}Sr/^{86}Sr$ (> 0.710) and low $\delta^{13}C$ values (-2.3 to -4.1‰), reflect fluids that retained isotopic characteristics that were derived through interaction with subjacent shale source rocks.

Vitrinite reflectance (R_o) data from the Devonian Woodford Shale in northern Oklahoma indicate immature to mature hydrocarbon maturity and correspond to palaeotemperatures of 60° and 115°C. However, in overlying Mississippian rocks, T_h values obtained for fluid inclusions in open space filling carbonate and quartz cements indicate much higher maximum temperatures (≥140°C), suggesting that these fluids were short-lived thermal anomalies compared to burial thermal conditions. The basinal fluids that precipitated these cements likely emanated from underlying Cambrian and Ordovician strata and migrated upward along the faults. The presence of petroleum-rich inclusions indicate that this fluid migration likely occurred during the period of petroleum generation and that petroleum generated in the underlying Woodford Shale also moved upward along the faults accompanying the deeper sourced saline basinal fluids. These hot fluids likely are associated with the basinal fluid flow movement during Ouachita and Appalachian orogenies.

VITA

Sahar Mohammadi Dehcheshmehi

Candidate for the Degree of

Doctor of Philosophy

Thesis: **REGIONAL DIAGENESIS OF MISSISSIPPIAN STRATA OF THE SOUTHERN MID-CONTINENT, USA**

Major Field: GEOLOGY

Biographical:

Education:

Completed the requirements for the Doctor of Philosophy in Geology at Oklahoma State University, Stillwater, Oklahoma in December, 2016.

Completed the requirements for the Master of Science in Geology at Azad University, Science and Research Branch-Tehran, Iran, in 2009.

Completed the requirements for the Bachelor of Science in Geology at Azad University, Khorasgan Branch-Isfahan, Iran, in 2002.

Experience: Teaching and Research Assistant, Boone Pickens School of Geology August 2011-December 2016. Project Engineer at Mines & Industries Organization, Iran, October 2005-July 2006. Vice Chairman of Board of Directors and Project Geologist at Zamin Pazhohan Zagros Consultant Engineers Co. Iran, November 2004-August 2005.

Professional Memberships:
American Association of Petroleum Geologists (AAPG), Tulsa Geological Society (TGS), Society of Exploration Geophysicists (SEG), Society for Sedimentary Geology (SEPM), Geological Society of America (GSA), Association for Women Geoscientists (AWG), and member of Sigma Xi